Published in final edited form as:
Chem Erde. 2017 May ; 77(2): 227–256. doi:10.1016/j.chemer.2017.01.007.

The nature, origin and modification of insoluble organic matter in chondrites, the possibly interstellar source of Earth's C and N

C.M.O'D. Alexander[1], **G.D. Cody**[2], **B.T. De Gregorio**[1], **L.R. Nittler**[1], and **R.M. Stroud**[3]

[1]Dept. Terrestrial Magnetism, Carnegie Institution of Washington, 5241 Broad Branch Road, Washington, DC 20015, USA.

[2]Geophysical Laboratory, Carnegie Institution of Washington, 5251 Broad Branch Road, Washington, DC 20015, USA.

[3]Materials Science and Technology Division, U.S. Naval Research Laboratory, Washington, DC, USA.

Abstract

All chondrites accreted ~3.5 wt.% C in their matrices, the bulk of which was in a macromolecular solvent and acid insoluble organic material (IOM). Similar material to IOM is found in interplanetary dust particles (IDPs) and comets. The IOM accounts for almost all of the C and N in chondrites, and a significant fraction of the H. Chondrites and, to a lesser extent, comets were probably the major sources of volatiles for the Earth and the other terrestrial planets. Hence, IOM was both the major source of Earth's volatiles and a potential source of complex prebiotic molecules.

Large enrichments in D and ^{15}N, relative to the bulk solar isotopic compositions, suggest that IOM or its precursors formed in very cold, radiation-rich environments. Whether these environments were in the interstellar medium (ISM) or the outer Solar System is unresolved. Nevertheless, the elemental and isotopic compositions and functional group chemistry of IOM provide important clues to the origin(s) of organic matter in protoplanetary disks. IOM is modified relatively easily by thermal and aqueous processes, so that it can also be used to constrain the conditions in the solar nebula prior to chondrite accretion and the conditions in the chondrite parent bodies after accretion.

Here we review what is known about the abundances, compositions and physical nature of IOM in the most primitive chondrites. We also discuss how the IOM has been modified by thermal metamorphism and aqueous alteration in the chondrite parent bodies, and how these changes may be used both as petrologic indicators of the intensity of parent body processing and as tools for classification. Finally, we critically assess the various proposed mechanisms for the formation of IOM in the ISM or Solar System.

1. Introduction

The study of the organic material in chondritic meteorites aims to establish where and how it formed - either the interstellar medium (ISM) or the solar protoplanetary disk (nebula) - and to determine how it was subsequently modified by nebular and parent body processes. Here we focus on the dominant organic component, the so-called insoluble organic material

(IOM), that is the major carrier of C, N and noble gases in chondrites, and second only to water/OH as a carrier of H. How and where the organic material formed will have even wider significance if, as some have speculated, it played a role in the origin of life on Earth (e.g., Ehrenfreund and Charnley, 2000). At the very least, the IOM was probably the ultimate source of most of the C, N and noble gases, as well as much of the H, accreted by the terrestrial planets (e.g., Alexander et al., 2012; Marty, 2012). Because the organics are low temperature materials, they can also provide information about dust evolution in the solar nebula, and presumably disks around other low mass stars. This complements what can be inferred about high temperature processing and dust transport from the abundance and properties of crystalline silicates (e.g., Ciesla, 2009; Watson et al., 2009).

There have been a number of fairly recent reviews of the organic matter in meteorites (Botta and Bada, 2002; Sephton, 2002; Gilmour, 2003; Sephton, 2005; Pizzarello et al., 2006). However, with the renewed interest in the subject, the introduction of new techniques, and the availability of new samples from Antarctica and Comet 81P/Wild 2, the field is evolving rapidly. Traditionally, studies of the organic and inorganic components of chondrites have been treated as essentially separate disciplines, with little attempt to use the one to inform the other. Recently, it has become increasingly apparent that the organic material has great utility as a petrologic tool, both for classification purposes (Quirico et al., 2003; Bonal et al., 2006; Bonal et al., 2007) and for thermometry (Busemann et al., 2007a; Cody et al., 2008c). Here we try to link the organic chemistry with the petrology of the chondrites to show how the organic material can provide important constraints on the origin and evolution of chondrites, comets and, ultimately, our Solar System.

The three basic types of extraterrestrial material that are accreted by the Earth and survive atmospheric entry are classified in order of increasing size into: interplanetary dust particles (IDPs), micrometeorites and meteorites. Micrometeorites are generally severely heated on atmospheric entry and, except in rare cases (e.g., Duprat et al., 2010), retain little unmodified organic material, so they are not considered in detail here. With a few exceptions, those that come from the Moon and Mars, meteorites are fragments of main-belt asteroids (2–4 AU), with a strong bias towards inner belt asteroidal sources (Morbidelli et al., 2002). While there is an overall radial gradient of spectral classes amongst the larger objects in the asteroid belt (Gradie et al., 1989), there has been considerable radial mixing of smaller bodies that are largely collisional fragments (DeMeo and Carry, 2014). As a result, it is likely that the meteorite collection has sampled many asteroid types that formed over a wide range of radial distances (Burbine et al., 2002). Only the most primitive types of meteorite, the chondrites, contain abundant indigenous organic material. This is because non-chondrites come from parent bodies that experienced extensive melting, and even wholesale differentiation into silicate mantles and iron cores.

IDPs almost certainly come from the Zodiacal Cloud and have both cometary and asteroidal sources. The proportions of cometary and asteroidal particles accreted by the Earth is a matter of debate (Dermott et al., 2002; Nesvorný et al., 2010), but recent dynamical arguments suggest that most come from Jupiter family comets that probably formed at about the same distance from the Sun as Neptune (Nesvorný et al., 2010).

The presence of organic material in chondrites, along with presolar circumstellar grains (Nittler, 2003; Clayton and Nittler, 2004; Alexander, 2009), demonstrates that they contain a primitive, low temperature component. The organic materials in primitive chondrites often have large D and ^{15}N enrichments, relative to bulk Solar System H and N isotopic compositions, including extreme enrichments in so-called hotspots (Busemann et al., 2006c; Nakamura-Messenger et al., 2006). The large isotopic anomalies in bulk and in hotspots point to formation of the IOM or its precursors in cold, radiation-rich environments, most likely the outer Solar System and/or the ISM (Charnley and Rodgers, 2008). Very similar hotspots are seen in IDPs (Messenger, 2000; Floss et al., 2006). Since at least some IDPs come from comets (Nesvorný et al., 2010; Bradley, 2014), the similarities in their isotopic properties suggests that there is a genetic relationship between chondritic and IDP/cometary organic matter. This is supported by the similar elemental compositions of the most primitive (most aliphatic and isotopically anomalous) chondritic IOM, $C_{100}H_{75–79}O_{11–17}N_{3–4}S_{1–3}$ (Alexander et al., 2007b) and comet Halley CHON particles, $\sim C_{100}H_{80}O_{20}N_4S_2$ (Kissel and Krueger, 1987).

Despite the likely genetic relationship between IOM in chondrites and IDPs, here we focus primarily on chondritic IOM for practical reasons – the considerably larger mass of material afforded by chondrites means that a much more varied array of techniques have been applied to them. First, we review what is known about the petrology, and physical and chemical properties of the IOM in the most primitive chondrites. This is followed by a discussion of how aqueous alteration and thermal metamorphism in the meteorite parent bodies has modified the IOM. Finally, we explore whether the differences in the IOM within and between extraterrestrial bodies (sources of chondrites, IDPs and comets) reflect parent body processes or differences produced in the solar nebula, and whether the IOM formed in the Solar System or the ISM.

2. Classification of chondritic meteorites and IDPs

Historically, the chondrites have been divided into three classes based on their compositions and mineralogies (ordinary, carbonaceous and enstatite). These in turn have been subdivided (Krot et al., 2014) into a number of groups: ordinary chondrites into H, L and LL, carbonaceous chondrites into CI, CM, CR, CV, CO, CB, CH and CK, and enstatite chondrites into EH and EL. The name carbonaceous chondrite is a historical one and is a bit misleading since some ordinary and enstatite chondrites contain more C than some carbonaceous chondrites. The chondrite classification scheme is still evolving as more meteorites are found - two new classes (R and K chondrites) have been recognized, and a number of individual meteorites do not belong to any recognized group. While there are variations, the bulk compositions of the chondrites are remarkably similar to that of the solar photosphere (excluding H, He, etc.). In terms of bulk composition, the most solar-like of the chondrites are the CIs (Lodders, 2003).

Chondrites are comprised of three main components: refractory inclusions, chondrules and fine-grained matrix. Refractory inclusions and chondrules are high temperature (1400–1800°C) objects that formed in the solar nebula. Given their high formation temperatures, organics would not have survived refractory inclusion or chondrule formation, although it

may have been responsible for the reduction many chondrules experienced (Connolly et al., 1994). Consequently, at the time when the chondrite parent bodies formed it was only in the matrix that organic matter would have been present.

After formation, the chondrites experienced secondary modification (thermal metamorphism and aqueous alteration) due to the internal heating of their parent bodies by the decay of short-lived (now extinct) radionuclides and shock heating associated with impacts. A petrographic classification scheme for secondary processes divides the chondrites into 6 types - types 3 to 6 reflect increasing extent of thermal metamorphism, and types 3 to 1 reflect increasing degrees of aqueous alteration. By convention, the chemical classification is followed by the petrologic one (e.g., CI1, CM2, CV3).

Chondritic IDPs, those with roughly chondritic bulk compositions, can be divided into two broad categories (Bradley, 2014): compact hydrated particles, and porous nominally anhydrous particles that are often referred to as chondritic porous (CP) IDPs. The hydrated particles share many mineralogical similarities with the CM and CI chondrites. The anhydrous particles do not seem to have a clear affinity to any known meteorite group. Based on their very fine grain size, disequilibrium assemblage of minerals and amorphous silicates, and abundant presolar materials, the CP-IDPs are thought to be the most primitive Solar System objects found to date.

3. The inventory of chondritic organics

The organic matter is normally divided into solvent soluble (SOM) and insoluble (IOM) fractions (Gilmour, 2003). Both the IOM and the SOM can have large D and ^{15}N enrichments that are usually interpreted to indicate that they or their precursors formed at very low temperatures in the presolar molecular cloud or in the early Solar System. The IOM shows tremendous variation in its elemental and isotopic compositions both within and between chondrite groups (Fig. 1). These variations are due, at least in part, to parent body processes, but may also reflect variations in the material accreted by the different chondrite groups (Section 6). In the chondrites that appear to have experienced the most benign parent body conditions (CIs, CMs and CRs), the bulk compositions of their IOM, normalized to 100 Cs, are in the range ~$C_{100}H_{70–80}O_{15–20}N_{3–4}S_{1–4}$. While not the focus of this paper, the SOM has an estimated bulk composition, at least in Murchison, of ~$C_{100}H_{155}O_{20}N_3S_3$ (Schmitt-Kopplin et al., 2010) that except for its H/C resembles the bulk composition of IOM. However, the abundances of the different compounds in the SOM vary considerably within and between chondrite groups (Table 1). Again, the variations in SOM, at least within a group, appear to be largely determined by parent body processes (e.g., Martins et al., 2007; Aponte et al., 2011; Glavin et al., 2011; Hilts et al., 2014), with some fraction of the SOM possibly being the product of alteration of IOM by parent body processes (e.g., Sephton et al., 2003; Huang et al., 2007).

As can be seen from Table 1, the vast majority of the reported organic C in carbonaceous chondrites is in the IOM. There are significant differences in the IOM C contents between the chondrite groups. However, because organic matter would not have survived chondrule and refractory inclusion formation, organic contents in chondrites are best compared when

they have been corrected (normalized) for the abundance of matrix. After normalization for their respective matrix abundances, the IOM contents of CI, CM and CR chondrites are quite similar. The same is also true for the most primitive ordinary and enstatite chondrites. However, as first noticed by Smith and Kaplan (1970), only ~45–80% of the C in bulk carbonaceous and ordinary chondrites can be accounted for by the reported IOM, SOM and carbonate abundances (Alexander et al., 2015a). The missing C seems to be lost during isolation of the IOM. The nature of this missing C is at present unknown, but it has similar N/C ratios and N isotopic compositions to IOM and may either be in very small IOM particles that are lost during IOM isolation or in acid hydrolysable functional groups on the IOM (Alexander et al., 2015a).

4. Where are the organics?

Relatively little work has been done to determine where in the matrix the organic material is. This is in spite of the fact that its physical distribution may provide clues to its origin. In addition, if the organic matter predates chondrite accretion it is a useful tracer of primitive regions of the matrix.

Remarkably, IOM survives the polishing process and can be found at the surfaces of thin sections. Two techniques for locating IOM grains in thin sections that are relatively benign are UV fluorescence (e.g., Alpern and Benkheiri, 1973) and Raman (Christophe Michel-Levy and Lautie, 1981) imaging. Contamination from polishing materials, epoxy, old C coat and even bacteria remain a problem, but they often can be distinguished spectroscopically or morphologically from the indigenous IOM. For the most primitive meteorites, the distribution of carbonaceous materials larger than ~100 nm and their H, C and N isotopic compositions can be mapped by secondary ion mass spectrometry (SIMS) (Fig. 2) (e.g., Messenger, 2000; Aléon et al., 2003; Busemann et al., 2006c; Zega et al., 2007; Floss et al., 2014). Once located, IOM grains can then be examined with high spatial resolution by scanning electron microscope (SEM) for potential mineralogical associations (Fig. 2a). Organic-rich areas can also be extracted from the section using focused ion beam (FIB) techniques for further micro-analysis, for example (Fig. 3) by transmission electron microscopy (TEM) examination and scanning transmission X-ray microscopy (STXM) and X-ray absorption near-edge spectroscopy (XANES).

Multi-meteorite, multi-technique in situ studies of organic matter have recently been conducted by Le Guillou and collaborators (Floss et al., 2014; Le Guillou et al., 2014; Le Guillou and Brearley, 2014). These studies have found a diversity of grain morphologies, sizes (mostly < 1μm) and isotopic compositions, including micron- to nanometer-sized veins, as well as a diffuse component that may be dominated by SOM. No simple relationship between minerals and IOM is evident. Figures 2 and 3 show many of the features described by Le Guillou and colleagues. There is a wide range in the sizes (~0.1–5 μm across), morphologies and isotopic compositions of the C-rich regions. The size distribution of C-rich areas in Figure 2 reflects, at least in part, random sectioning and the spatial resolution of the NanoSIMS instrument (typically ~0.1–0.2 μm) used to locate them. In general, the IOM does not seem to rim mineral grains, and the IOM is largely free of

mineral inclusions, at least at the spatial resolution of the instruments used (see also Remusat et al., 2010).

The absence of a clear mineralogical association between the IOM and any inorganic minerals, including presolar circumstellar grains that at best have only 10–20 nm thick coatings (Bernatowicz et al., 2003; Stroud and Bernatowicz, 2005; Croat et al., 2009), suggests that it did not form on catalytic or refractory mineral substrates, as predicted by Fischer-Tropsch-type (FTT) synthesis or the classical Greenberg model for interstellar grains (e.g., Greenberg et al., 2000). Messenger et al. (2005) found ^{15}N-rich organic material spatially associated with a supernova silicate grain in an IDP, but this seems to be the exception rather than the rule and, therefore, may be coincidental. While there is no obviously consistent spatial association between IOM and presolar grains (e.g., Fig. 2), this does not exclude a presolar origin for the IOM since the presolar grains themselves are not associated with one another.

One intriguing feature of Figure 2a is the proximity to the IOM of what appears to be a section through an enstatite needle or plate. Similarly shaped enstatite grains have been reported in the matrices of other chondrites (e.g., Hutchison et al., 1987; Leroux et al., 2015), and are one of the characteristic features of sections of primitive IDPs (Bradley, 2014). TEM analysis of the large IOM inclusion in Figure 2 shows it to be an aggregate or vein of so-called nanoglobules (Fig. 3). Nanoglobules are typically roughly spherical objects that are often hollow and range in size from 10s of nanometers to several microns (Nakamura et al., 2002; Garvie and Buseck, 2004). The enstatite needles, nanoglobules and other mineralogical features (e.g., Klöck et al., 1989) suggest that there is a direct link between IDPs and a major component of chondrite matrices.

In an *in situ* study of carbonaceous chondrites using an Os labeling technique, Pearson et al. (2002; 2007) only found IOM in matrix, and reported an apparent association between organic material and phyllosilicates. Kebukawa et al. (2010) reported a similar apparent association based on near-field IR spectroscopy. Phyllosilicates are generally thought to be the products of aqueous alteration in the meteorite parent bodies (Section 6.1). Based on their observations, Pearson et al. suggested that phyllosilicates may have acted as traps or even catalysts enabling simpler precursor compounds to be transformed in the meteorite parent bodies into the complex IOM now present. Zega et al. (2010) also observed phyllosilicates in close association with ^{15}N-rich amorphous organic carbon in Tagish Lake (C2) matrix. An even more intimate association was reported by Garvie and Buseck (2005) who found structurally bound carbonaceous material in Orgueil (CI1) phyllosilicates. It is not clear what fraction of the organic C in Orgueil and Tagish Lake is in this form. However, the occurrence of IOM in minimally altered chondrites (e.g., Figs. 2 and 3), as well as IOM-like material in anhydrous IDPs (e.g., Thomas et al., 1993; Messenger and Walker, 1997; Flynn et al., 2003; Keller et al., 2004; Busemann et al., 2009) and in aqueously unaltered comet Wild 2 samples (Sandford et al., 2006; Cody et al., 2008a; Matrajt et al., 2008; De Gregorio et al., 2011) rules out phyllosilicates playing a dominant role in the formation of the IOM. Nevertheless, it seems likely that phyllosilicates played a role in the modification of primordial organic material, particularly SOM, that was present in the fluids that were responsible for the aqueous alteration. For instance, Le Guillou and Brearley (2014) suggest

that: (1) the organic material was accreted in ices; (2) on melting of the ices, there was some redistribution of the organics, including the IOM, along cracks and into pores; (3) the SOM would have been distributed more widely than the IOM; and (4) as the fluid was consumed the SOM was trapped in growing phyllosilicates, adsorbed onto grain surfaces, or underwent polymerization to form a second generation of IOM.

5. The nature of the most primitive IOM in meteorites

In this section, we seek to summarize what is known about the structure and composition of the IOM in the most primitive chondrites that have been studied. We do not designate the IOM from any one chondrite or chondrite group as being the most primitive because this would assume that all IOM has a common origin, which has yet to be definitively established.

The most primitive chondrites were selected on the basis of petrologic evidence for little or no heating, and low degrees of aqueous alteration. The CR Elephant Moraine (EET) 92042 is one of the least altered CRs (Abreu and Brearley, 2004). Other CRs (Graves Nunataks (GRA) 95229, Queen Alexandra Range (QUE) 99177 and Meteorite Hills (MET) 00426) are equally or perhaps even less altered than EET 92042 (Abreu and Brearley, 2010; Alexander et al., 2013; Harju et al., 2014; Le Guillou and Brearley, 2014; Howard et al., 2015), but their IOM has yet to be studied in as much detail. QUE 97990 is one of the less altered CMs (Rubin et al., 2007; Alexander et al., 2013; Howard et al., 2015). In terms of its isotopic composition, Bells IOM appears to be more primitive than any other CM (Alexander et al., 2007b), although there is some disagreement over the extent of alteration Bells as a whole experienced (Alexander et al., 2013; Beck et al., 2014; Quirico et al., 2014; Howard et al., 2015) and the style of alteration Bells experienced is distinct from other CMs (Brearley, 1995). While it is one of the less altered CMs, Murchison is more altered than QUE 97990 (Rubin et al., 2007; Alexander et al., 2013; Howard et al., 2015). Nevertheless, so much work has been conducted on Murchison organics that it is included in this section. For similar reasons, the CI Orgueil is included here despite the fact that it has experienced almost complete aqueous alteration of its primary minerals. Meteorites from other chondrite classes that are generally considered primitive (e.g., Acfer 094 - C3.0, Alan Hills (ALH) 77307 - CO3.0, Kaba - CV3.1, Semarkona - LL3.0 and Tagish Lake – ungrouped C2) are not discussed in this section because the IOM in all these meteorites has been affected by parent body processes, and in the case of Acfer 094 by terrestrial weathering (Alexander et al., 2007b).

5.1 The physical nature of the IOM

Based on TEM observations of carbonaceous chondrite acid residues, there are at least two morphologically distinct components of the IOM (e.g., Garvie and Buseck, 2006) - the major component has a fluffy texture, while the minor component occurs as solid or hollow globules/nanoglobules (also sometimes referred to as nanospheres) (Fig. 4). Garvie and Buseck (2006) concluded that the fluffy material in Orgueil IOM is largely amorphous, but they found some regions that had fringe spacings of 0.21 nm and 0.34–0.39 nm, roughly corresponding to the (100) and (002) d-spacings of graphite, respectively. The (002) d-

spacing of pure graphite is 0.335 nm, but significant concentrations of heteroatoms can cause it to increase. They also observed 2–3 nm nanodiamonds in the IOM, identifiable by their strong 0.206 nm (111) lattice fringes and characteristic electron energy-loss spectroscopy (EELS) C-K edge shape. Derenne et al. (2005) and Le Guillou et al. (2012) found fringes to be much more ubiquitous in their images of Orgueil and Murchison IOM residues. Derenne et al. (2005) interpreted the fringes as being local regions of order due to stacking of 2–3 of layers PAHs that are typically 2–3 rings across (i.e., ~4–9 rings/layer). The range of interlayer spacings (d-spacings) reported by the two studies was 0.35–0.65 nm, with an average of ~0.44–0.48 nm, considerably larger than for pure graphite. Derenne et al. (2005) suggested that heteroatoms and high degrees of substitution for Hs on the peripheries of the PAHs might account for this. None of the TEM studies were able to estimate the fraction of IOM that is in ordered domains.

There are a number of uncertainties associated with the quantitative interpretation of the sub-nm-range order reported in the fluffy material because: (i) fringe contrast in general is not uniquely interpretable, as multiple atomic arrangements can give rise to similar image contrast, and in particular the fringe contrast from such small domains is highly dependent on sample thickness that could only be estimated in the studies discussed above, (ii) the size and ordering of PAH domains can be rapidly altered due to electron irradiation damage, including rapid loss of H and N, at the 200 kV energies used in all three studies, and (iii) extensive Fourier processing of images can impose periodicities not present in a raw image. It should be noted that Vollmer et al. (2014) conducted high resolution scanning TEM (STEM) imaging of organic grains in two CRs and two IDPs at an accelerating voltage of 60 kV, well below the knock-on damage threshold of ~80 kV for C=C bonds (Meyer et al., 2012), and found them all to be amorphous. Vollmer et al. (2014) also showed that under “gentle STEM” conditions the irradiation-induced loss of N was eliminated. However, significant H loss from organic samples is inevitable in any TEM studies, unless a cryogenic stage is used (Egerton, 2014).

Nanoglobules in carbonaceous chondrites range in size from 10 nm to >1 μm (e.g., Nakamura et al., 2002; Garvie and Buseck, 2004; Garvie and Buseck, 2006; Nakamura-Messenger et al., 2006) and, unlike the fluffy material, they contain no ordered domains (Garvie and Buseck, 2006). It should be pointed out that few nanoglobules are truly spherical, and rare forms even have vermiform or tubular shapes (Garvie and Buseck, 2006; Garvie et al., 2008). The great majority of nanoglobules do not appear to contain any mineral grains in their interiors (e.g., Matsumoto et al., 2013), but recently Hashiguchi et al. (2013) reported silicate and oxide grains inside a few of what they termed ring globules in a CR2. Nanoglobules are a common component of chondritic IOM (e.g., Garvie and Buseck, 2004; Nakamura-Messenger et al., 2006), and have also been found in micrometeorites (Dobrică et al., 2009), IDPs (Busemann et al., 2009), and comet Wild 2 samples (De Gregorio et al., 2010). The size distributions, morphologies, and abundances of nanoglobules appear to vary from meteorite to meteorite (De Gregorio et al., 2013). At present, it is not clear whether these variations reflect systematic inter- and/or intra-group differences. If systematic variations do emerge, they will provide important clues to the origin(s) of these enigmatic objects.

5.2 Elemental and isotopic compositions

For most studies of IOM it is necessary to isolate it from the mineral matrix. Demineralization of meteorites is generally carried out using either HF-HCl (e.g., Robert and Epstein, 1982) or CsF (e.g., Cody et al., 2002). The HF-HCl protocols used often involve elevated temperatures (50–80 °C) in one or more steps, but the CsF approach is conducted entirely at room temperature. Despite their significant differences, the two IOM isolation techniques produce similar yields and bulk isotopic compositions (Alexander et al., 2007b, Electronic Annex). Nevertheless, there is always the concern that the IOM is modified during its isolation, particularly since so much of the bulk C cannot be accounted for (Section 3). Using isotopically labeled acids, Kerridge et al. (1988) estimated that at most there is 3–5 % H isotopic exchange during isolation of Murchison IOM using the HF-HCl technique. In a more extensive set of experiments, Halbout et al. (1990) inferred higher proportions of H and O exchangeable material in Orgueil IOM, but this may have been at least in part be because their residues were relatively impure (Alexander et al., 2007b, Electronic Annex). Thus, while some modification and isotopic exchange during preparation of IOM residues is inevitable, the fact that two quite distinct isolation techniques give similar results suggests that what is isolated is relatively robust.

On average, the nanoglobules and the fluffy material have relatively similar elemental compositions (determined in the TEM by electron energy loss spectroscopy or EELS), although the nanoglobules tend to be more variable and have higher N/C ratios (Garvie and Buseck, 2004, 2006). In terms of their N/C and S/C ratios, the nanoglobule compositions are similar to that of the bulk IOM from their respective meteorites (Alexander et al., 2007b). This is to be expected given that the fluffy material and the nanoglobules are the major IOM components. However, the O/C ratios determined by EELS for both materials are significantly lower than the bulk values. The cause of this difference is unclear. It is not possible to determine H/C ratios by conventional EELS. As the dominant component, the average H/C ratio of the fluffy material must be close to those of the bulk IOM for each meteorite, but the H/C ratios of the less abundant globules remains unknown.

The bulk elemental compositions of the IOM in CI, CM and CR chondrites are similar to one another, but there are some dramatic differences in their bulk isotopic compositions (Fig. 1). Whether these differences are primary or secondary in origin will be explored further in Section 6. As mentioned in the introduction, the bulk elemental compositions of the IOM in these meteorites, but particularly the CRs, closely resemble the estimated average composition of the Halley CHON particles.

Stepped combustion and pyrolysis experiments have shown that IOM in primitive chondrites is not a monolithic material, but clearly has components with very different isotopic compositions (e.g., Robert and Epstein, 1982; Kerridge, 1983; Yang and Epstein, 1983; Kerridge et al., 1987; Alexander et al., 1998; Sephton et al., 2003). For instance, the $\delta^{15}N$ varies by up to 50–100 ‰ during high-resolution stepped combustion/pyrolysis of some IOM, requiring that it contain at least two to three isotopically distinct N-bearing components. The isotopic complexity of the IOM is even more apparent in SIMS measurements of both extracted IOM and *in situ* in chondrite matrices (e.g., Fig. 2). These show that in the primitive chondrites the majority of the material has H- and N-isotopic

ratios clustering near average values for a given sample, but a small fraction of grains have much higher D and/or ^{15}N enrichments ("hotspots") with δD values of up to ~40,000 ‰ and δ^{15}N values of up to 2000–3000 ‰ (Busemann et al., 2006c; Busemann et al., 2007b; Floss et al., 2014; Hashiguchi et al., 2015). Some but not all hotspots are associated with nanoglobules (Nakamura-Messenger et al., 2006; De Gregorio et al., 2013; Floss et al., 2014; Hashiguchi et al., 2015). In IDPs the most extreme D hotspot that has been reported had a δD≈50,000 ‰ (Messenger, 2000). The sizes of the hotspots vary from ~1.5–2 μm across down to the spatial resolution of the SIMS measurements (~0.1–0.5 μm depending on the instrument).

The apparent abundances of hotspots in IOM depend on the spatial resolution and the analytical precision of the SIMS measurements, as well as the criteria used to define them - at present there is no widely accepted definition. Busemann et al. (2006c) estimated D hotspot abundances of roughly 2.4 area% for EET 92042 IOM, and 4.3 area% for Murchison IOM. Remusat et al. (2009) using somewhat less stringent criteria report much higher abundances of D hotspots in the IOM of the CI Orgueil (15–38 area%). Clearly it is important to resolve why there are such large differences in the hotspot abundance estimates. The hotspots in both studies were defined relative to the bulk IOM compositions. The bulk H isotopic compositions of Murchison IOM (δD≈800 ‰) and Orgueil (δD≈1000 ‰) IOM are much lower than that of EET 92042 IOM (δD≈3000 ‰). Consequently, the Murchison and Orgueil hotspots generally have much lower D enrichments than those in EET 92042 IOM. Whether the differences in hotspot compositions between EET 92042, and Murchison and Orgueil (as well as in their bulk IOM compositions) are primary or have been modified by aqueous alteration will be addressed further in Section 6.1.2. If the IOM in Orgueil and Murchison has been altered, it is possible that many of their hotspots are less altered regions of the original EET 92042-like IOM, explaining their higher abundance.

In terms of H/C and N/C ratios, there is no apparent difference between hotspots and bulk IOM, at least at the precision of the SIMS measurements (Busemann et al., 2006c). Nor is there a simple relationship between the D and ^{15}N hotspots. The D hotspots are not associated with any C isotopic anomalies. On the other hand, ^{15}N hotspots can be associated with modest ^{13}C depletions (δ^{13}C down to −250 ‰), and more rarely modest ^{13}C enrichments (δ^{13}C≈100–160 ‰), in the CR chondrites EET 92042, MET 00426 and QUE 99177 (Busemann et al., 2006b; Floss and Stadermann, 2009; Floss et al., 2014). The one ^{15}N-rich and ^{13}C-depleted region that has been examined in the TEM (from a FIB section of an EET 92042 IOM separate) proved to be monolithic, amorphous C that was quite distinct from the highly porous IOM in which it was embedded (Busemann et al., 2006a). Only one of the regions in the CR chondrites with isotopically anomalous C appears to be a nanoglobule (Floss and Stadermann, 2009; Floss et al., 2014).

Similarly D and ^{15}N enriched hot spots and isotopically C anomalous regions have also been observed in IDPs (Messenger, 2000; Floss et al., 2004; Floss et al., 2006; Busemann et al., 2009), strengthening the case for a genetic link between the IOM in IDPs and chondrites.

5.3 Functional Group Chemistry

5.3.1 Chemical degradation—Hayatsu et al. (1977; 1980) applied a number degradative chemical techniques originally developed for studying coals to try to break the IOM down into its constituent parts. The two apparently most successful methods were oxidation reactions with aqueous $Na_2Cr_2O_7$ and alkaline CuO. $Na_2Cr_2O_7$ is thought to preferentially attack aliphatic side groups on aromatic molecules, replacing them with carboxylic groups (-COOH). CuO is understood to preferentially cleave aryl-ether (AR-O-C, where AR = aromatic ring) linkages, i.e., replacing aryl-aliphatic ethers with carboxylic groups and aryl-phenols (AR-OH).

Applying aqueous $Na_2Cr_2O_7$ oxidation chemistry to Murchison IOM, Hayatsu et al. (1977) identified 17 basic molecular units in the reaction products, 15 of which were small aromatic molecules with several containing N, O and S heteroatoms. These neoformed aromatic molecules were composed of up to four aromatic rings (polyaromatic hydrocarbons or PAHs), but the majority of them contained only one or two rings. The reported yield of the neoformed molecules was 58 wt.% of the initial IOM sample. As is standard practice in coal studies, Hayatsu et al. assumed that the number of carboxylic groups attached to these aromatic molecules (e.g., benzene with 2–6 AR-COOH groups) reflects the degree of cross-linking in the IOM macromolecule, although not all side groups need form cross-links. Typically, the most abundant products had 2–4 carboxylic groups. Given the small sizes of the PAHs, Hayatsu et al. inferred that they must be highly substituted by short aliphatic chains, and this in turn implied a considerable degree of cross-linking between PAHs.

Oxidation with CuO (Hayatsu et al., 1980) also only released small PAHs and these PAHs had at least two or three substitutions. The abundance of phenolic groups and the absence of systems containing the relatively stable aryl-methoxy (e.g., AR-O-CH_3) groups in the oxidation products led to the conclusion that aryl-ethers (Ar-O-Ar) form direct cross-links between aromatic moieties in the IOM. Quirico et al. (2014) arrived at a similar conclusion based on a correlation between Raman spectral features and bulk IOM O/C ratio.

More recently, Remusat et al. (2005a) and Huang et al. (2007) have used RuO_4 oxidation to investigate the aliphatic side groups and linkages in the IOM of Orgueil and Murchison. RuO_4 destroys the aromatic rings converting the aromatic C to which the aliphatic moieties are attached into a carboxylic group. As a result, non-crosslinking aliphatic side groups are converted to monocarboxylic acids, and aliphatic linkages will have two or more carboxylic groups.

Remusat et al. (2005a) reported that dicarboxylic acids were the most abundant products in their study, followed by mono- and tricarboxylic acids. The di- and tri-acids are almost certainly aliphatic linkages between aromatic units. Of the diacids, butanedioc (COOH-CH_2-CH_2-COOH) and methylbutanedioc acids were the most abundant products, followed by pentanedioic acid and the two isomers of methylpentanedioic acid. Diacids with up to nine carbons were observed, with the abundance decreasing with increasing C number, and for a given C number the abundances of the different isomers being similar. This pattern of complete structural diversity and decreasing abundance with increasing C number is a common property of meteoritic organics.

Since the two end C atoms (carboxylic groups) of diacids are inherited from the aromatic ring, the abundances of butanedioic and pentanedioic acids, as well as their methylated homologues, indicate that the aliphatic linkages are short and highly branched. Hydrogen isotopic measurements of selected diacids (dD=801–1270 ‰; Remusat et al., 2006) from Orgueil (Fig. 5) scatter around the bulk IOM composition (δD=972 ‰; Alexander et al., 2007b). Remusat et al. (2005a) only found $\geq C_{14}$ monocarboxylic acids and concluded that all were contaminants. Based on the sensitivity of their technique, they argued that side groups in the IOM must be composed of three carbons or less. The yield of the study was only ~1% of the C in the IOM, compared to the ~25 % aliphatic C (~10 % with no O functionality) in Orgueil (Cody and Alexander, 2005). Hence, it is not clear how representative this study is of the bulk IOM, and only qualitative abundances for individual compounds were reported. Nevertheless, it is the best picture we have of the aliphatic linkages in IOM.

Concentrating exclusively on the monoacid products of RuO_4 oxidation of Murchison IOM, Huang et al. (2007) report monoacids with up to 10 C atoms, again with an overall decline in abundance with increasing C number. In general, except for acetic acid and the $\geq C_7$ straight chain monoacids, the H isotopic compositions of the monoacids (straight chain $<C_7$ δD=391–657 ‰, branched δD=723–1283 ‰; See Fig. 5) demonstrated that they were indigenous and similar to the compositions of the solvent extractable acids (straight chain $<C_9$ δD=100–823 ‰, branched δD=965–2024 ‰) from Murchison (Huang et al., 2005; Aponte et al., 2011; Aponte et al., 2014b). The acetic acid (δD=8 ‰) and $\geq C_7$ straight chain monoacids produced by the oxidation are not D enriched (δD= −129 to 15 ‰), suggesting the possibility of severe terrestrial contamination. A similar behavior is seen in the solvent extractable acids. The C isotopic compositions of the solvent extractable monoacids tend to be heavier than the oxidation products, particularly the branched moieties, which Huang et al. (2007) attributed to formation of the solvent soluble acids by hydrothermal alteration of the IOM. Huang et al. (2007) estimated that the monoacids they detected represent ~5 % of the aliphatic C in Murchison IOM. Whether this is because only ~5 % of the aliphatic C is in non-crosslinking side groups or because of low yields from the oxidation is unknown. The Huang et al. (2007) results are also at odds with the earlier Remusat et al. (2005a) study that reported diacids to be more abundant than monoacids as well as significantly lower yields.

The degradative studies point to the IOM being composed of small PAHs that are highly substituted and cross linked by short, highly branched aliphatics and esters. The side groups have D enrichments that are comparable to the bulk IOM compositions, but the branched moieties tend to be more enriched than the straight chain ones. However, because of the low yields and lack of quantitative abundances for individual compounds, it is not clear how representative of the bulk IOM the degradative results are and they cannot be used to build a quantitative picture of the IOM structure.

5.3.2 Pyrolysis

5.3.2.1 Molecular building blocks: A number of pyrolytic techniques, coupled with gas chromatography mass spectrometry (GC-MS), have been employed to study the molecular building blocks of IOM. In GC-MS, molecules liberated from the IOM are swept into the

GC in a He flow. The time it takes different molecules to pass through the column depends on how strongly they interact with the column's lining. From the GC, the pyrolysates flow onto a hot filament and fragment. The masses of the fragments are determined by the mass spectrometer. The identities of the individual molecules are determined from both their retention times in the column and their fragmentation patterns in the mass spectrometer.

The most common pyrolytic technique involves flash heating (pyrolysis), typically at 600–650°C, in an inert He atmosphere. As a result, bonds in the IOM are cleaved thermally. How the resulting radicals are subsequently stabilized is uncertain, but the potential for modification of the fragments in the vapor plume is high. Also yields of identifiable organic species tend to be low. For instance, total weight losses from the IOM of only 25–30 % are typical, with the most abundant species being CO, CO_2, H_2O, and H_2S (e.g., Komiya et al., 1993; Remusat et al., 2005b; Okumura and Mimura, 2011) and a significant fraction of the remaining signal being in a very broad release (so-called humpane or unresolved organic matter) that underlies the identifiable peaks (Fig. 6). Finally, the absolute or relative yields of identifiable species are rarely reported in pyrolysis studies.

Despite these potential drawbacks, pyrolysis GC-MS (pyr-GC-MS) is a useful forensic tool, particularly for comparing the more thermally labile components in IOM from different meteorites. Komiya and Shimoyama (1996) identified over 130 organic compounds in pyrolysates from Murchison IOM. The major identifiable peaks in most studies are dominated by 1–3 ring aromatic molecules, many with one or more short aliphatic side chains (Fig. 6) (Komiya et al., 1993; Komiya and Shimoyama, 1996; Remusat et al., 2005b; Wang et al., 2005). The substituted moieties include all possible isomers. This is broadly consistent with the chemical degradation results described above (Section 5.3.1) and the NMR results described below (Section 5.3.3), although the degree of substitution of the aromatic moieties is lower in the major pyrolysates. Aliphatic and alicyclic compounds tend to be relatively uncommon, as do heteroatom-bearing (O, N and S) compounds. The low abundance of aliphatic material amongst the pyrolysates is inconsistent with the NMR results (and the inferences of the chemical degradation studies) that show that 40–60 % of the C in IOM is aliphatic (Section 5.3.3). In the most quantitative pyrolysis study to date, Okumura and Mimura (2011) reported approximate yields of major compound types, but not individual species, released during stepped pyrolysis of Murchison IOM. They obtained roughly comparable yields of aliphatic (peaking at C_4) and aromatic compounds, along with lower abundances of heteroatom-bearing compounds. Nevertheless, total yields of organic compounds only represented a small fraction of the C in the IOM, and it is clear from the progressively decreasing H/C of the char with increasing pyrolysis temperature that the pyrolysates are not representative of the bulk IOM.

Pyrolysis with the sample intimately mixed with tetramethylammonium hydroxide (TMAH) to increase yields (though not quantified) revealed the presence of ester and ether linkages between the aromatic units (Remusat et al., 2005b), as had also been inferred from chemical degradation studies (Section 5.3.1). The low relative abundances of N-containing compounds in the pyrolysates and the relatively high N contents of residual chars (unlike H, O and S) have been interpreted as due to the bulk of the N in IOM being in refractory heterocycles (Remusat et al., 2005b; Okumura and Mimura, 2011).

To overcome some of the potential problems associated with reactions in the plasma during conventional pyrolysis, heating of samples has been carried out in the presence of water (hydrous pyrolysis) and high pressure H_2 (hydropyrolysis). With these approaches, the hope is that when a bond cleaves the radical immediately reacts with H from the water or H_2, thereby preventing further structural and/or chemical modification. Hydrous pyrolysis also approximates the pressures and temperatures of relatively high temperature hydrothermal alteration.

Hydrous pyrolysis studies of IOM from Orgueil, Murchison and the more altered CM2 Cold Bokkeveld were first carried out by Sephton and coworkers (Sephton et al., 1998, 2000; Sephton and Gilmour, 2001). They reported the same range of compounds in all three meteorites, but differences in their relative abundances apparently correlated with the degree of parent body alteration. For instance, with increasing alteration the relative abundances of phenols decreased and single ring aromatics increased in the pyrolysates. Sephton et al. suggested that the phenols formed during hydrous pyrolysis by cleaving of ether linkages in the IOM. The abundances of these linkages appear to decrease with increasing alteration. However, there are no systematic variations in bulk IOM H/C or O/C with degree of alteration (Alexander et al., 2007b). Yabuta et al. (2007) conducted hydrous pyrolysis analysis of Murray (CM2) IOM, and reported a wider range of products than the previous studies, including more heteroatom-bearing compounds. As with the pyrolysis studies, hydrous pyrolysis only releases a small fraction of the C in the IOM, ~15–26 % (Sephton et al., 2004; Yabuta et al., 2007), the total yield of C in the identified individual products may be even lower (≥1.36 %; Sephton et al., 1998), and the yields of individual compounds have not been quantitatively determined.

Hydropyrolysis experiments have also been carried out by Sephton et al. (2004; 2005; Sephton et al., 2015). In the initial experiments, pyrolysates were recovered from the H_2 flowing through the reactor bed using a CO_2 ice cold trap. The loss of C from the IOM samples was ~44 % and the pyrolysates were found to be dominated by 3–6 ring PAHs with few side chains (Sephton et al., 2004). These PAHs are much larger than is typically seen in either the pyrolysis or hydrous pyrolysis experiments. However, trapping of more volatile species was very inefficient. Later experiments utilizing a liquid N_2 trap greatly increased the abundance of smaller more volatile species, but again there was little substitution on the PAHs, few heteroatom-bearing compounds, and it is not clear what fraction of the C is in the larger PAHs because absolute yields were not determined (Sephton et al., 2005; Sephton et al., 2015). Sephton et al. (2004) speculated that the ~56 % of IOM C that is not released even by hydropyrolysis is composed of ≥5–6 ring PAHs bridged by small aliphatic units, much like an anthracite coal. However, this is inconsistent with the NMR results (Section 5.3.3).

5.3.2.2 Isotopes of constituents: Several studies have measured the isotopic compositions of individual IOM pyrolitic products by compound specific GC isotope ratio mass spectrometry (GC-irMS). In GC-irMS, after passing through the GC the individual compounds are either combusted or pyrolysed depending of the system being studied, and the products are passed into a conventional mass spectrometer for measuring isotope ratios. Sephton and coworkers (Sephton et al., 1998, 2000; Sephton and Gilmour, 2001) analyzed

the C isotopic compositions of aromatic and polyaromatic compounds released from Orgueil, Murchison and Cold Bokkeveld IOM by hydrous pyrolysis. Murchison and Cold Bokkeveld extracts exhibit opposite trends of C isotopic composition vs. C number, while the Orgueil extracts shows no clear relationship. The lack of consistent trends makes interpretation of the data difficult.

Two studies have measured the isotopic compositions of individual compounds in conventional pyrolysates (Fig. 7). Remusat et al. (2006) measured the H isotopic compositions in a number of aromatic molecules in the pyrolysate of Orgueil IOM. They found a range of H isotopic compositions (unsubstituted, $\delta D \approx 600–773$ ‰; substituted, $\delta D \approx 795–1111$ ‰). Combining these with measurements of aliphatic linkages between aromatic groups released by RuO_4 (Section 5.3.1), they interpreted this range as being due to mixing of three types of C-H bonds each with different H isotopic compositions – benzylic C-H $\delta D = 1250$ ‰, aliphatic C-H $\delta D = 550$ ‰ and aromatic C-H $\delta D = 150$ ‰ (benzylic C is an aliphatic C that is bonded directly to an aromatic ring). In arriving at these component compositions, they assumed: (1) that there was no significant isotopic fractionation or isotopic exchange during pyrolysis, (2) that cleaved C-C bonds were replaced by C-H bonds with the H coming from the less stable benzylic moieties, (3) that the number of C-C bonds that had to be broken to release an aromatic molecule from the IOM (i.e., degree of substitution) could be estimated assuming that on average 70 % of the aromatic C in the bulk IOM is unhydrogenated (Gardinier et al., 2000), and (4) that H in methyl side groups has a benzylic isotopic composition. The isotopic composition of H released during pyrolysis of Orgueil IOM up to 600–650°C (Robert and Epstein, 1982; Robert et al., 1987) is on average much lighter than the benzylic composition above, and there is evidence for a component in the IOM with a δD of at least 1600 ‰ (Robert and Epstein, 1982) that is higher than the benzylic composition. Thus, the validity of assumption (2) is unclear, and the three components do not account for all the isotopic variability present in the thermally labile IOM material.

Nevertheless, if this variation in isotopic composition with bond type is correct, then seemingly the D enrichment is inversely correlated with bond energy. Remusat et al. (2006) interpreted their results as being due to decreasing exchange with H_3^+ with increasing C-H bond energy. The H_3^+ ion is very important in ion-molecule chemistry in molecular clouds and can become very D-rich at low temperatures. They estimated a formation temperature of ~100 K from the benzylic H isotopic composition, which is high for a molecular cloud prompting them to conclude that IOM formed in the Solar System (see Section 7.2 for further discussion).

However, Wang et al. (2005) measured the H isotopic compositions of individual pyrolysates from IOM from six meteorites, including Orgueil and the isotopically much more anomalous CR2 EET 92042. They reported a wider range of compositions for Orgueil aromatic pyrolysates than Remusat et al. (2006) ($\delta D = 549–1481$ ‰) and, in all but one case, for the same molecules the Wang et al. (2005) results are more D-rich (by up to 500 ‰). Nor is there a clear trend with degree of substitution amongst the aromatic moieties in the Wang et al. (2005) results (Fig. 7). Wang et al. (2005) also reported the isotopic compositions of aliphatic pyrolysates ($\delta D = 412–1362$ ‰) from Orgueil that exhibit a similar range to the

aromatic species. The three CMs they studied, including Murchison, produced a somewhat wider range of isotopic compositions (δD=207–1995 ‰) than Orgueil both within and between molecules, and the variations do not obviously correlate with degree of substitution or with the degree of alteration experienced by the meteorites. Perhaps not surprisingly, EET 92042 produced pyrolysates with both much more enriched and more variable isotopic compositions (δD≈2500–4500 ‰).

The compositions of the chars remaining after pyrolysis are rarely reported. Okumura and Mimura (2011) reported a ~80 ‰ decrease in the bulk δD value of the char produced in stepped pyrolysis of Murchison IOM to 800°C, with the biggest drop in the 450–550°C step by which time ~60 % of the initial H had been lost from the IOM. This is consistent with the more labile material being somewhat more D-rich than the bulk IOM. However, the peak in the release of aliphatic material occurred at ≤450°C when there was much less change (~20 ‰) in the bulk δD of the char, and the 80 ‰ decrease is less than would be expected if a D-rich aliphatic material had been completely driven off. Interestingly, Mimura et al. (2007) obtained significantly larger changes in δD values after shock heating of Murchison IOM to the same nominal peak temperatures and for the same H loss fractions as in the pyrolysis experiments of Okumura and Mimura (2011), but why this should be is not obvious.

The causes of the inconsistencies between the Wang et al. (2005) and Remusat et al. (2006) studies are unclear, but they need to be understood before the pyrolysis results can be used to infer mean H isotopic compositions for different components in IOM. More generally, the pyrolysis results cannot be used to develop a detailed picture of the functional group chemistry and structure of the bulk IOM because: (1) the fractions of the C in IOM released by the different pyrolytic techniques are low, and the fractions of C in identifiable compounds are even lower, (2) the H/C ratios of the pyrolysates are higher than the bulk IOM and there is generally a paucity of aliphatic compounds and heteroatom-bearing organic compounds in the pyrolysates, and (3) none of the studies provide quantitative yields for those individual molecules that have been identified in the pyrolysates.

5.3.3 NMR—Solid-state nuclear magnetic resonance (NMR) spectroscopy is a complex but powerful tool for identifying functional groups present in solids and for estimating their abundances (Duer, 2004). NMR spectroscopy has the added advantage of being nondestructive. However, the samples do need to be relatively pure, to increase sensitivity, and largely free of magnetic minerals. Common meteoritic minerals, such as Fe-metal and magnetite (Fe_3O_4), are easily removed during isolation of the IOM, but fine-grained paramagnetic chromite ($FeCr_2O_4$) is not. Chromite can make up 10 wt.% or more of an IOM separate and may contribute to line broadening of NMR spectra (Levin et al., 2007). Also, IOM is known to contain stable radicals (Section 5.3.4) and these will hide nuclei that are near to them from the NMR.

In NMR spectroscopy, a sample is placed at the center of a strong static magnetic field, where the spins of nuclei align themselves with and precess around the static field at characteristic (Larmor) frequencies. Not all isotopes possess the nuclear property of spin. For instance, ^{12}C has no spin, but ^{13}C is a spin ½ nucleus (as are ^{1}H and ^{15}N) and can be

used in NMR. Small variations in the local magnetic field around nuclei that are caused by their local bonding environments result in small changes in the precession frequencies, and it is these variations that are the basis of NMR spectroscopy. The variations in precession frequency are measured relative to a standard reference frequency and are usually expressed in units of parts per million (ppm).

To obtain NMR spectra, the nuclei are resonantly excited by short, powerful pulses of radio frequency (RF) radiation. The excited nuclei subsequently emit an RF signal as they relax, which can be converted into a spectrum that is characteristic of the chemistry of the system. In the case of solids, the samples must also be spun at high speeds at the so-called magic angle (54.7°) to average out anisotropy in the surrounding local magnetic environments of the nuclei and thereby reduce the severe line broadening that is inherent to solids. NMR spectroscopy is a relatively insensitive technique. For abundant nuclei in organic solids, like ^{1}H, this poses little problem and the nuclei can be excited directly (single pulse or SP experiments) without requiring excessive amounts of spectrometer time. For the less abundant ^{13}C, rather than exciting it directly one can use the more sensitive so-called cross polarization (CP) technique in which one directly excites ^{1}H and then transfers polarization to neighboring ^{13}C atoms. While it enhances the sensitivity, the dynamics of CP experiments are also more complex than SP experiments. In particular, the rates at which ^{13}C in different functional groups are excited in CP experiments, as well as the levels of excitation, depend sensitively on the time over which ^{1}H and ^{13}C are allowed to remain in ‘contact’. For instance, aromatic ^{13}C tends to be excited more rapidly than aliphatic ^{13}C. As a result, if the contact time is too short the relative abundances of aliphatic and aromatic moieties will not be representative. Another important feature of CP experiments is that the degree to which a ^{1}H can excite a ^{13}C falls off rapidly with distance, so that a ^{13}C that is more than a few bond lengths away from a ^{1}H can be invisible.

The first ^{13}C NMR spectra for IOM were reported by Cronin et al. (1987) for Murchison (CM2) and Orgueil (CI1) using CP. However, the first really detailed study was conducted by Gardinier et al. (2000), also for Murchison and Orgueil IOM, and again using CP. They were able to identify eight different types of C functional groups in the IOM – aliphatic-linked and aromatic-linked -CH_3, methylenes (-CH_2-), protonated and non-protonated aromatic C, aliphatic C linked to heteroatoms (O or N) by a single bond, carboxyl (R-COO-R; acid or ester) and carbonyl (R-CO-R; aldehyde or ketone).

Based on the relative abundances of aliphatic CH_2 and CH_3 groups, Gardinier et al. (2000) concluded that the aliphatic component must be made of relatively short and/or highly branched chains, which was consistent with their and earlier Fourier transform infrared (FTIR) measurements (see Section 5.3.6). However, when they combined the eight functional groups that they identified in their measured relative abundances, they arrived at a much higher bulk H/C ratio for IOM than measured directly by elemental analysis. This led them to conclude that large fractions of the aromatic C atoms (~20–30 % of the total C in Orgueil and ~40–60 % in Murchison) were too far from a H nucleus to be excited in CP experiments, either because they are in large, compact aromatic units or because the aromatic units are relatively small but heavily substituted.

Cody et al. (2002) and Cody and Alexander (2005) applied a broader suite of NMR experiments to Murchison, Orgueil and EET 92042 (CR2) IOM. First, they demonstrated that the 1 ms contact time used in most coal and kerogen CP studies is too short for IOM and results in the aromatic C signal being underrepresented. This would explain why other primitive IOM studies (Cronin et al., 1987; Gardinier et al., 2000; Yabuta et al., 2005) that employed the 1 ms contact time obtained significantly lower aromaticities. Contact times of 4.5 ms produce CP spectra (Fig. 8a) that most accurately represent the true functional group abundances. This was confirmed by comparing the H-^{13}C CP spectra with ^{13}C SP spectra for the same residues (Fig. 8). By detecting the ^{13}C directly, the SP spectra are not subject to the potential biases associated with CP, although they tend to suffer from lower signal/noise (Fig. 8b).

Based on their SP and longer contact time CP experiments, Cody et al. (2002) and Cody and Alexander (2005) concluded that there is little or no hidden C in the IOM – at most ~5 % of the C may be hidden. This means that there cannot be significant amounts of large, compact (pericondensed) aromatic units in the IOM, particularly if they are stacked on top of one another as suggested by Derenne et al. (2005). This and the high fraction of unprotonated aromatic C (~70 % for Murchison and Orgueil, and ~50 % for EET 92042), again suggests that the aromatic units are small and highly substituted. Based on the NMR results, it cannot be completely ruled out that there are large aromatic units composed of long chains of benzene rings (catacondensed) in the IOM, but no other techniques have found evidence for such structures. Like Gardinier et al. (2000), Cody et al. (2002) and Cody and Alexander (2005) inferred that the aliphatic component in all the meteorites that they studied must be composed of short, highly branched chains. However, Cody and Alexander (2005) found a range of aliphatic contents in the order EET 92042>Orgueil>Murchison. The range of bulk H/C ratios estimated from the measured relative abundances of the different functional groups for each of the IOM residues straddled the measured values. For Murchison at least, the NMR O/C ratio was too high and could only approach the measured value if: (i) all the carboxylate is linked to aromatic C via aromatic esters, (ii) the remaining aromatic O is linked to aliphatic C via alkyl aryl esters and (iii) the remaining aliphatic O is in aliphatic esters. However, more recently Cody et al. (2011) using a two dimensional solid-state H-^{13}C NMR technique showed that, contrary to expectations, furans (five-membered unsaturated cyclic ethers) are a significant component of Murchison IOM rather than O substituted aromatics (e.g., phenols).

No N or S functionality was unambiguously identified by Gardinier et al. (2000), Cody et al. (2002; 2011) or Cody and Alexander (2005). Remusat et al. (2005b) reported a low signal-to-noise H-^{15}N CP NMR spectrum for an Orgueil IOM residue that they interpreted as being due to the presence of pyrroles and indoles (N containing aliphatic and aromatic heterocycles, respectively), and possibly nitriles. However, they were unable to detect any N in Murchison even though the N/C ratios of Murchison and Orgueil IOM are very similar. After analyzing ~85 mg samples of Murchison, GRO 95577 and Tagish Lake IOM for four weeks each (Cody and Alexander, 2016) were unable to obtain signals that were above background. Given the N/C ratios of these IOM samples, the N functionality should have been detectable in the NMR experiments. The negative results are consistent with the N either always being far from H or always being close to radicals. The former could indicate

that most N is in the cores of large PAHs, but as discussed earlier there is no evidence for the NMR hidden C that this model would predict. Alternatively, the N could be hidden from the NMR by proximity to radicals. The latter would require ~10^{21} radicals/g to hide every N, assuming one radical per N. This number could be reduced somewhat if the Ns are clumped near radicals, but it is unlikely that clumping could reduce the required radical concentrations to the ~10^{18}-10^{19} radicals/g that have been measured in IOM (Section 5.3.4). Thus, at present our inability to obtain ^{15}N NMR spectra for IOM is an intriguing mystery.

5.3.4 EPR and related techniques—Electron paramagnetic resonance (EPR) is a nondestructive way to study the distribution and nature of free organic radicals (unpaired electrons) in materials such as coal and IOM. The most commonly measured EPR parameters are: (1) the concentration of unpaired electron spins (spins/g) associated with free radicals, and (2) the g-factor that depends on the structure of the radicals and their proximity to heteroatoms (i.e., N, O and S).

Binet et al. (2002) determined the bulk spin concentrations in Murchison and Orgueil IOM residues to be 1.8±0.3×10^{18} spins/g and 7.0±0.8×10^{18} spins/g, respectively, and based on their g-factors that these radicals are probably associated with O functional groups. The radical concentrations are similar to those observed in relatively immature coals, and much lower than the C concentrations (~3×10^{22} C/g) in IOM. After rejecting other possible explanations (such as the presence of paramagnetic minerals), Binet et al. (2002) also inferred from their relaxation behavior that the free radicals in the IOM must be concentrated in clusters with localized radical densities of 3–4×10^{19} spins/g, implying that these clusters make up ~4–6 % of Murchison IOM and 17–23 % of Orgueil IOM. Why the bulk of the IOM is essentially devoid of radicals was not explained.

While not accurately known, after isolation meteoritic nanodiamonds have spin densities of ~10^{19} spins/g and the radicals are probably associated with the ~1 at.% N in their structures (Braatz et al., 2000; Jeschke pers. comm.). Nanodiamonds make up ~3–4 % of the C in CM and CI IOM residues (Alexander et al., 1998), so they could be a significant component of the EPR spectra and their radicals would be clustered. Because proximity to radicals can hide a nucleus during NMR spectroscopy, the high radical densities in the nanodiamonds could also explain why NMR underestimates nanodiamonds abundances in IOM residues (e.g., 0.8–1.4 % of the C in Murchison and Orgueil; Cody and Alexander, 2005). However, while the g-factors of the nanodiamonds and IOM are very similar, the EPR spectra of the purified nanodiamonds have pronounced H-induced shoulders that are not seen in the IOM spectra. Thus, the nanodiamonds cannot be the major component of the IOM EPR spectra, unless the H-induced shoulders are artifacts of the harsh procedures used to isolate them.

Only monoradicals (S=1/2) are observed in terrestrial coals and kerogens, and they show no dependence of concentration with temperature (so-called Curie Law behavior). However, Orgueil, Murchison and Tagish Lake IOM all exhibit temperature-dependent spin concentrations, leading Binet et al. (2004a; 2004b) to infer that IOM contains a mix of 60–75 % monoradicals and 25–40 % temperature-dependent biradicaloids (S=0 in ground state, and increasingly S=1 above 100 K). Binet et al. (2004a; 2004b) also argued that the biradicaloids are attached to substituted aromatic moieties composed of 35–40 C atoms or

10–15 aromatic rings. A considerable fraction of the interior C of such large PAHs would almost certainly be hidden from H-^{13}C CP NMR measurements, even if the radicals themselves were unable to hide them completely. However, even if all radicals are associated with such structures and all the C in them is NMR invisible, for a radical concentration of 10^{18}-10^{19} spins/g and 40 C atoms/radical, this would account for ~0.1–1 % of the C in the samples, well below the upper limit of ~5 % of C that could be invisible to H-^{13}C CP NMR measurements (Section 5.3.3). Delpoux et al. (2011) have subsequently significantly revised the estimated relative abundances of the radical species in Orgueil IOM to be 61 % biradicaloids, 31 % biradicals (S=1) and only 8 % monoradicals. At present, there is no definitive explanation for why the radical speciation in IOM is so different from what is observed in terrestrial coals and kerogens.

Gourier et al. (2008) and Delpoux et al. (2008), using the two dimensional HYSCORE EPR technique, concluded that the radicals in Orgueil IOM are enormously enriched in D (δD≈96,000 ‰), with the D located at the benzylic positions of aliphatic side chains. While it depends on the assumed average number of Hs/radical, these results would imply that on the order of 20 % of the D in IOM is associated with radicals. The H isotopic compositions of side groups released by treatment of Murchison IOM with RuO_4 are not more D-rich than the bulk IOM (Huang et al., 2007), but perhaps the radicals are susceptible to isotopic exchange or destruction during this treatment. The fact that the radicals appear to be so D-rich and clustered prompted Gourier et al. (2008) to suggest that they are associated with the D-rich hotspots observed in IOM. They also suggested that the large D enrichments were the result of preferential exchange between the radicals and D-rich H_3^+ that formed at 40 K or less, significantly lower than the ~100 K initially proposed by Remusat et al. (2006).

Given the potentially very important implications of the EPR results, Alexander et al. (2015b) have measured the IOM from 18 carbonaceous chondrites that have a larger range of D enrichments than displayed by Murchison and Orgueil, including two very D-rich CR chondrites and the anomalous CM2 Bells. They found a generally lower and more restricted range of radical concentrations (roughly 5×10^{17} to 2×10^{18} spins/g). For instance, while the radical concentration for Murchison IOM is in agreement with the previous studies, those for Orgueil and Tagish Lake are roughly factors of 5 and 10 times lower, respectively. Nor did Alexander et al. (2015b) find any correlation between spin concentration and the bulk H isotopic compositions of the IOM, despite bulk IOM δD values that ranged from roughly ~500 ‰ to ~3500 ‰. Naively, such a correlation might have been expected if the radicals carry a significant fraction of the D in IOM. Hence, the relationship between radicals and D enrichments in IOM may be more complex than is apparent from studies of Murchison and Orgueil alone.

5.3.5 C, N, O and S XANES and EELS—Both the XANES and EELS techniques rely on the excitation of 1*s* core shell electrons in C, N, O, and S atoms to their lowest energy unoccupied molecular orbitals (π* or σ*). XANES spectra are generated by measuring the degree of absorption as the energy of a focused, monochromated beam (≥20–40 nm) of X-rays is scanned across an element's absorption edge. EELS, on the other hand, uses a monochromated primary beam of energetic electrons and a spectrometer to measure the energy spectrum of the electrons after they have been inelastically scattered as they passed

through the sample. Both techniques can induce beam damage in IOM samples, requiring some care to avoid producing analytical artifacts. For EELS, electron beam energies below ~80 kV appear to give the best results (e.g., Vollmer et al., 2014), particularly if combined with a cryogenic stage, while for XANES in addition to low X-ray doses analyzing the samples in an O-free atmosphere is essential.

Not only can XANES and EELS be used to obtain elemental ratios (Garvie and Buseck, 2004), but they also be used to identify a variety of functional groups that may be present (Fig. 9, Table 2). However, quantification of functional group abundances is complicated by the wide range in their absorption cross sections that means some abundant groups may be barely detectible while other minor groups produce distinct peaks. Sample thickness can also limit quantification of spectra. Specimens that are too thin give poor signal to noise, and sections that are too thick show saturation in XANES, and multiple scattering effects in EELS. In general, 100 nm to 150 nm sections are well suited to C XANES, and EELS at 200 kV, whereas 30 nm is better for EELS at 60 kV. For functional group identification, high energy resolution is needed and resolutions of 0.3 eV for EELS (e.g., Vollmer et al., 2014) and 0.1 eV for XANES (Kilcoyne et al., 2003) are now readily achievable.

As can be seen from Figure 9, the bulk IOM C XANES spectra are remarkably consistent for all type 1 and 2 chondrites, as well as type 3.0s. This also true for C EELS as well as N and O XANES/EELS spectra. The C absorption edge of primitive IOM (Fig. 9a) contains a number of near-edge peaks (e.g., Cody et al., 2008a; Vollmer et al., 2014). The most prominent of these peaks is at 285 eV and attributed to C=C double bonds in aromatic ring structures. Another peak at 288.5 eV is attributed to carboxyl (-COOH) functional groups. An additional peak is at 286.5–286.7 eV, an energy range where both nitrile (C≡N) groups and ene-ketones (aromatic C=O) can contribute, but is generally attributed to ketone groups. Oxygen substituted aromatic C (e.g., phenol) absorbs at 287.2 eV, aliphatic C occurs at roughly 287.8–288.0 eV, and alcohols and ethers at 289.5 eV. However, these transitions are relatively weak and as a result C-XANES/EELS spectra are dominated by unsaturated functional groups even if they are not always the most abundant.

The overall N abundance of IOM is low (N/C≈0.03). Nevertheless, there is enough N to obtain reasonably high signal/noise bulk spectra. The spectra are remarkably similar across chondrite groups and petrologic types, exhibiting near continuous absorption spanning the entire N-XANES region (i.e., up to the ionization edge) and only a few relatively small peaks (Fig. 9b). The 1s-π^* transitions in N-XANES tend to be very intense relative to the continuum absorption above the absorption edge (~405 eV). A distinct shoulder at 398–399 eV is consistent with a very small amount of imine (e.g., pyridinic N where N substitutes for a C in a benzene ring) and nitrile. The more prominent peak at 401.3 eV is consistent with pyrrolic N (N in aromatic heterocycles). The near continuous intensity above ~402 eV requires the presence of other N functional groups whose identities have yet to be established. The absence of strong peaks for pyrroles, indoles and nitriles is inconsistent with the ^{15}N NMR spectrum obtained for Orgueil by Remusat et al. (2005b).

As there are only two types of bonding environments for O (sp^2 and sp^3), one expects and observes a lower energy absorption for carbonyl (C=O) and a higher energy transition for O sigma bonded to C (C-O-R) as in the case of alcohols and ethers (Fig. 9c).

Speciation of S in chondritic carbonaceous matter has only been reported in a single ANES study of bulk IOM in a number of CIs and CMs, a CR and Tagish Lake (Orthous-Daunay et al., 2010). The authors divided the S functionality into three major groups with similar absorption energies: aliphatic S (disulfides, thioethers and thiols), S heteorcycles (thiophenes and thianthrenes) and oxidized S groups (sulfoxides, sulfones and sulfonates). The most intense absorption features in all the IOM spectra is due to aliphatic S, with much weaker heterocycle and oxidized S intensities. The relative abundances of these functional groups could not be determined more quantitatively. However, the relative heterocycle and oxidized S intensities are higher in CI chondrites and Cold Bokkeveld (CM2) compared to other CMs and Renazzo (CR2), suggesting that there was some modification of the S functionality during parent body alteration.

While bulk XANES/EELS spectra are relatively similar across all primitive chondrites, greater diversity becomes apparent when IOM is studied at smaller scales either in residues or in situ. Nanoglobules have come under particular scrutiny, and the earliest EELS investigations of IOM were initially motivated by the need to characterize their functional group chemistries (Garvie and Buseck, 2004). De Gregorio et al. (2013) targeted over 180 nanoglobules in IOM residues from seven primitive chondrites with XANES and found that most have similar functional group chemistries to the bulk IOM (i.e., aromatic C=C, ketones, and carboxyl), but with significantly sharper ketone and carboxyl peaks that indicate less chemical complexity. However, there is a subpopulation of “highly aromatic” nanoglobules, characterized by spectra with higher aromatic C=C intensities, lower carboxyl intensities, and almost no evidence for ketone groups. These highly aromatic nanoglobules appear to be more abundant in chondrites that have experienced less aqueous processing, although the sample sizes for individual meteorites remain limited. There appears to be no robust correlation between globule morphology, functional group chemistry, and isotopic composition. Very little is known about the N or O XANES/EELS spectroscopy of nanoglobules. Nitrogen XANES spectra of some ^{15}N-rich isotopic hotspots have a peak that has been attributed to the presence of nitriles (Busemann et al., 2007b; Peeters et al., 2012; Bose et al., 2014), although the presence of imines rather than nitriles should not be completely ruled out. To date, there have been no reports of unusual XANES/EELS spectra for D-rich hotspots.

XANES has also been used to search for variations in C functional group chemistry *in situ* within FIB-extracted sections of meteorite matrices. Although the typical IOM spectral features are present in all carbonaceous sub-grains (aromatic, ketone, and carboxyl), there is increased heterogeneity with increasing degree of alteration as well as an overall increase in aromaticity and carboxyl abundance (Le Guillou et al., 2014; Le Guillou and Brearley, 2014). In addition, diffuse, inter-grain carbonaceous matter (as opposed to discrete carbonaceous grains) contains a much lower abundance of aromatic functionality and additional peaks that may be due to abundant aliphatic carbon and organic CO_3

functionality. The abundance of this diffuse organic matter also appears to increase with increasing degree of alteration (Le Guillou et al., 2014; Le Guillou and Brearley, 2014).

5.3.6 FTIR—Much of the early Fourier transform infrared (FTIR) work was motivated by the striking similarity between spectra of IOM and diffuse ISM (DISM) carbonaceous dust in the aliphatic C-H stretch (3.2–3.6 μm, or 2800–3100 cm^{-1}) region (Wdowiak et al., 1988; Ehrenfreund et al., 1991; Pendleton et al., 1994). Other synthetic materials, such as irradiated CH_4 ice, some interstellar ice analogs and hydrogenated amorphous C (HAC), provide equally good fits to the DISM aliphatic C-H stretch region (Pendleton and Allamandola, 2002), perhaps pointing to the kinds of processes that may have produced the IOM.

The aliphatic C-H stretch region is dominated by multiple overlapping peaks associated with $-CH_3$ (methyl) and $-CH_2-$ (methylene) groups. Generally, FTIR is only used for comparing changes in functional group ratios in similar materials because the absorption cross sections depend sensitively on the nature of the functional group and its immediate environment. Obtaining quantitative estimates of CH_2/CH_3 ratios from IR spectra is sensitive to how the peaks and the baseline are fitted, as well as the absorption cross sections used. Neither the fitting routines nor the absorption cross sections are uniform across all studies. Nevertheless, typically the reported CH_2/CH_3 ratios for IOM from the least heated chondrites are ~2 (Pendleton et al., 1994; Orthous-Daunay et al., 2013; Alexander et al., 2014). Such a low ratio implies that on average aliphatic chains are short. Based on the DISM spectra, Sandford et al. (1991) also concluded that these aliphatic chains must be attached to electronegative groups, such as aromatic rings and -OH. The IOM C-H stretch region sits on an absorption feature due to –OH groups and adsorbed water. However, NMR measurements indicate that there is not enough O in the aliphatic material to account for all the electronegative groups, and that much of the aliphatic material must be side groups on aromatic units. If these aliphatic chains are a component of the cross linking between the aromatic units, the aliphatic component must be highly branched or the CH_2/CH_3 ratio would be much higher. An aliphatic component composed of short, highly branched chains is consistent with the NMR results (Section 5.3.3).

It should be noted that the Murchison spectrum used by Pendleton et al. (1994), as well as in subsequent reviews, was a 600°C sublimate of Murchison IOM. For the reasons discussed in Section 5.3.2, such a sublimate is not representative of the bulk IOM, yet this does not seem to have dramatically affected the aliphatic C-H stretch spectrum. Presumably this is because some fraction of the aliphatic material survives the pyrolysis more-or-less in tact, although why this would the case is not immediately obvious from the identified compounds in the pyrolysis experiments (Section 5.3.2). Even for heated CMs (probably shock heated) there is little or no change in CH_2/CH_2 ratio, but type 3 chondrites that were heated for prolonged periods do show changes in this ratio (Kebukawa et al., 2011; Orthous-Daunay et al., 2013; Alexander et al., 2014). These studies have also shown that the total aliphatic and C=O (carbonyl) stretch intensities tend to decrease in heated/metamorphosed chondrites relative to the aromatic C=C stretch intensity. Changes in the (CH_2+CH_3)/C=C and C=O/C=C intensity ratios have even been used to argue that CMs like Cold Bokkeveld that are

normally considered to be quite primitive may have been heated, probably by impacts (Orthous-Daunay et al., 2013; Quirico et al., 2014).

It was pointed out in the introduction that there are a number of reasons to believe that there is a genetic link between meteoritic IOM and the IOM in IDPs. However, IDPs tend to have higher CH_2/CH_3 ratios than meteoritic IOM (Flynn et al., 2003; Keller et al., 2004; Matrajt et al., 2005; Muñoz Caro et al., 2006; Brunetto et al., 2011). At present, it is unclear whether this reflects primary differences in their IOM, secondary modification of meteoritic IOM in the chondrite parent bodies, or modification of the IDP IOM (e.g., irradiation in interplanetary space, heating during atmospheric entry or 'weathering' during settling in the atmosphere).

5.4 Conclusions about the nature of bulk IOM in the most primitive chondrites

It will be apparent from the above discussion that while a number of techniques have been applied to the study of IOM, all of them have their shortcomings. The various degradative chemical and pyrolysis techniques suffer from low overall yields and generally a lack of quantitative yields for the individual molecular products. There is also considerable disproportionation during pyrolysis (i.e., the pyrolysates are not representative of the bulk). Whether this true for the chemical degradation studies is less clear, but it seems likely. It is also difficult to quantify the abundances of all functional groups in IOM using FTIR, XANES and EELS, and XANES and EELS can only be performed on relatively small volumes of material. At present, NMR provides the best quantitative picture of the bulk functional group chemistry of IOM, although it is still hampered by line broadening associated with the complex nature of IOM and with paramagnetic minerals in the residues.

Nevertheless, the degradative chemical and pyrolysis techniques both indicate that at least the chemically accessible and thermally labile components of IOM are composed of small aromatic units (typically 1–3 rings, although larger units are present) that have a high degree of substitution by aliphatic subgroups. The high degree of substitution and the macromolecular nature of IOM indicates that there must be considerable cross linking by the aliphatic material between the aromatic units that has generated a 3D network. This is consistent with the bulk IOM properties inferred by NMR and FTIR, which also indicate that the aliphatic material must be composed of short chains that are highly branched. Both the chemical degradation and Raman studies suggest that a significant fraction of the cross linking moieties involve O-bearing functional groups. Relatively little is known about S and N speciation in IOM. XANES shows that S occurs in a number of different functional groups with a range of oxidation states, but at present it is not possible to say anything more quantitative. The N XANES spectra are almost featureless, providing few clues to its speciation, and the difficulty of obtaining ^{15}N NMR spectra from IOM is a puzzle.

The nature of the radicals in IOM, as revealed by EPR, appear to be quite unique for natural materials. Identifying the processes responsible for them could very be revealing for understanding the processes and environments involved in IOM synthesis. This is particularly true if they are associated with highly deuterated functional groups (see Section 7.2). However, as often seems to be the case in IOM research, especially when a larger range of samples is examined, there are inconsistencies between studies that need to be resolved.

While all chondrites seem to have accreted IOM with many common features, the bulk elemental, isotopic and functional group chemistries of IOM vary significantly even amongst the nominally most primitive chondrites. It is also clear from high spatial resolution studies that the IOM in a particular meteorite is not a monolithic material, but a collection of micron to submicron grains with a range of properties. Nanoglobules and isotopic hotspots are particularly intriguing features of IOM. Whether these variations in IOM properties reflect accretion of different IOM by different chondrite groups or even within chondrite groups, or later modification of a common IOM precursor by parent body processes will discussed further in Section 6.

6. The effects of parent body alteration

All chondrite parent bodies were internally heated by the decay of short-lived radionuclides. The extent of heating experienced by a meteorite will have depended on when their parent bodies accreted, their sizes, their initial ice/rock ratios, and the depth within the bodies the meteorites came from. Thus, it is not surprising that all chondrites show evidence for having experienced thermal metamorphism (Huss et al., 2006) and/or aqueous alteration (Brearley, 2006) that often have had profound effects on their mineralogies and organic matter. Indeed, it was probably the lithification processes associated with metamorphism and alteration that enabled them to survive the impacts and atmospheric entry that delivered them to Earth. Generally, the chondrites have been predominantly affected by one or other parent body process, and so they are treated separately here.

6.1 Aqueous alteration

6.1.1 Source(s) of water, alteration processes and conditions—The conditions and results of aqueous alteration have been recently reviewed in detail (Brearley, 2006; Zolensky et al., 2008) and are only summarized briefly here. All textural evidence points to aqueous alteration having occurred in the chondrite parent bodies. The most likely sources of chondritic water were ices accreted together with the organic matter in the matrix. Therefore, the origins of the chondrite organics and water are inextricably linked. Carbonates are ubiquitous in aqueously altered chondrites, suggesting that either the accreted ices were rich in volatile C-bearing compounds (e.g., CO, CO_2 and CH_4) (Alexander et al., 2015a) or perhaps the organic matter was oxidized by peroxide produced by irradiation of the ices in space (Cody and Alexander, 2005) and/or during alteration (Foustoukos et al., 2011).

Metal and sulfides would have been amongst the first materials to alter, producing H_2, H_2S, and Fe oxides or hydroxides. The amount of H_2 generated could have been large. Consequently, as its pore pressures rose the H_2 must have begun to escape or the internal pressures would have led to catastrophic disruptions of asteroids. The loss of the H_2 will have produced increasingly oxidizing conditions. Also, as the silicates began to alter to phyllosilicates in a process akin to serpentinization on Earth, the release of alkalis, Mg, Ca, and Fe, into the aqueous solutions will have produced very alkaline conditions.

The presence of abundant Fe^{3+}-bearing minerals suggests that relatively oxidizing conditions existed during alteration of the CIs, CRs, and Tagish Lake. On the other hand, the

presence of tochilinite ($2Fe_{0.9}S*1.67Fe(OH)_2$), along with low magnetite contents, imply that most CM2s altered under more reducing conditions. Tochilinite is much less abundant in CM1s, either because temperatures approached its upper stability limit (~120°C) and/or because conditions were more oxidizing than in CM2s. It is interesting to note that Bells, the CM with the most isotopically anomalous IOM (Fig. 1), contains significant magnetite and no tochilinite, suggesting more oxidizing alteration conditions than other CM2s.

Alteration temperatures have been estimated in a number of ways and they range from 0–80°C for CMs, <50–150°C for CIs and ~100–150°C for CRs. What these temperatures actually mean (e.g., mineral formation temperatures, peak temperatures, closure temperatures, etc.) and how accurate they are is somewhat uncertain. The timescales for alteration are even less certain. Generally, the alteration is assumed to have been driven by internal radiogenic heating of the chondrite parent bodies, in which case the best estimates for timescales come from models. In detail the model predictions depend on many assumptions, but they all indicate that temperatures will have remained >0°C, at least in the more central regions of asteroids, for millions of years (e.g., Palguta et al., 2010; Fujiya et al., 2013). However, it has been suggested that impacts were responsible for the heating (Rubin, 2012; Quirico et al., 2014), in which case heating would be localized and brief. Simulations have shown that relatively low velocity impacts will induce compaction, as well as briefly and heterogeneously heating the matrix (Bland et al., 2014). One or more low velocity impacts were probably responsible for the development of the petrofabrics seen in some CMs that at least in a few cases has been shown to be contemporaneous with alteration (Hanna et al., 2015; Lindgren et al., 2015). However, the extent to which there was much heating during petrofabric formation is less clear. There are some strongly heated CIs, CMs and CRs (e.g., Abreu and Bullock, 2013; Alexander et al., 2013; Tonui et al., 2014), but there is some debate about whether these heating events were contemporaneous with or postdated the main phases of aqueous alteration in these parent bodies.

6.1.2 Effects of alteration on IOM—Whether there was modification of IOM during the alteration of CI, CM and CR chondrites is controversial, with the debate essentially being over the extent of IOM heterogeneity within and between chondrite groups at the time of their accretion. There is no systematic variation in bulk IOM elemental compositions or NMR spectra with petrologic type amongst either the CMs or CRs (Fig. 10). However, there appears to be a general relationship between IOM H isotopic composition and extent of hydration (petrologic type) - a somewhat curved trend between the least altered CRs (and the anomalous CM Bells) and the almost fully altered CMs and CIs (Fig. 11a). Such a trend would be consistent with increasing water-IOM H isotopic exchange or loss of a deuterated component with increasing extent of alteration from a common, probably CR-like, IOM precursor. Since the conditions and timescales of alteration would have varied within and between parent bodies, and the kinetics of aqueous alteration and water-IOM H isotope exchange are unlikely to have been identical, it is perhaps not surprising that some meteorites do not conform to this apparent trend. The two meteorites that most obviously fall off the trend are the highly altered CRs GRO 95577 and Al Rais, perhaps because in these meteorites conditions (e.g., low temperatures) did not favor modification of the IOM. The N isotopic compositions of the IOM exhibit a very similar behavior to the H isotopic

compositions (Fig. 11b), except that Bells IOM is significantly more ^{15}N-rich than the measured CRs.

The heterogeneous compositions of IOM particles in Orgueil, Murchison, and Renazzo, along with the absence of gradients in D/H ratios within the grains, led Remusat et al. (2010) to conclude that there was no interaction between water and IOM during alteration. However, these observations are equally consistent with IOM being composed of grains with diverse initial physical/chemical/isotopic properties, and isotopic exchange with water being dictated by the kinetics of the organic-water reaction(s) rather than diffusion of water into the grains. Indeed, such behavior is seen in experiments involving exchange between grains of formaldehyde polymer (an IOM analog) and water (Kebukawa et al., 2014).

Others have argued that the chondrite groups accreted IOM with different compositions, and that IOM modification during aqueous alteration was only a secondary influence (Quirico et al., 2011b; Orthous-Daunay et al., 2013). Given the generally limited overlap in petrologic types between the chondrite groups, this interpretation cannot be ruled out. The case for the heterogeneous IOM interpretation would be much stronger if it were shown that the anomalous Bells is not, in fact, a CM. Even if Bells is not a CM, the apparent general correlation between IOM isotopic composition and petrologic type, particularly within the CMs, would still have to be explained. Also, it is hard to reconcile a limited influence of aqueous alteration on IOM with direct observations that alteration apparently induced a diversification in the functional group chemistries of IOM grains (Le Guillou et al., 2014).

Perhaps the best evidence that parent body processes can produce the range of IOM properties seen amongst the C1/2 chondrites comes from Tagish Lake. The Tagish Lake fall is composed of multiple stones containing a range of lithologies. These lithologies experienced different intensities of alteration (Herd et al., 2011; Blinova et al., 2014) that are reflected in the properties of their IOM (Herd et al., 2011; Alexander et al., 2014). In terms of bulk H/C ratios and NMR spectra, the IOM from these different lithologies range from CR-like and aliphatic-rich, to CM-like, to resembling the aliphatic-poor IOM in the most primitive CO and OC chondrites (Fig. 12). The bulk H isotopic compositions of the IOM show dramatic variations that correlate with the elemental and structural changes (Figs. 1 and 13), indicating the loss of D-rich material and/or isotopic exchange with water. There is a parallel decrease in both the number of D-rich hotspots and their peak D/H values. By contrast, the N isotopic compositions of the IOM, including the abundances of ^{15}N hotspots, do not substantially change amongst the lithologies with the degree of alteration. Interestingly, the large changes in IOM aliphatic contents amongst the different lithologies was not accompanied by significant loss of C, suggesting that the aliphatic component was almost quantitatively converted to aromatic material (Alexander et al., 2014). The conversion of aliphatic to aromatic material involves the loss of H, and since it also involves the breaking of bonds it would also facilitate isotopic exchange. In addition, since linear side groups are unlikely to aromatize in such a facile and efficient manor, it seems more likely that most of the aliphatic material is in the form of cyclic linkages between the aromatic moieties.

This transformation of the Tagish Lake IOM was almost certainly thermally driven and probably occurred under hydrothermal conditions. Indeed, hydrothermal experiments (Yabuta et al., 2007; Oba and Naraoka, 2009) have produced similar compositional and structural changes in CM IOM (Fig. 13). However, there are differences between the experiments and the Tagish Lake samples – there was some loss of C and a change in bulk N isotopic composition in the experiment of Yabuta et al. (2007) that are not seen in Tagish Lake. It seems possible that this is because the hydrothermal activity in the Tagish Lake lithologies occurred at lower temperatures and for longer times than the experiments, and that the Tagish Lake fluids were NH_3-rich which effectively buffered the N isotopic compositions of the IOM, but this will have to be tested.

The elemental/structural changes in IOM that occur in response to heating are largely unidirectional and will mostly reflect the peak temperatures experienced. If correct, and if all IOM had a common precursor, the Tagish Lake results imply that: (1) the variations in aliphatic content seen amongst the C1/2 chondrites reflect peak alteration temperatures and not oxidation as proposed by Cody and Alexander (2005), and (2) the CMs and CIs all experienced similar peak temperatures that were significantly higher than experienced by the CRs (Alexander et al., 2014). The latter is contrary to mineralogical estimates of alteration temperatures (Section 6.1.1).

However, it must be pointed out that the changes in Tagish Lake IOM do not reproduce the variations in IOM elemental and isotopic compositions within and between the CI, CM and CR chondrites (Fig. 13). For instance, (a) the most CR-like Tagish Lake IOM (5b) is not as D-rich as the CRs, while the most CM-like lithology (11h) is more D-rich than any CM, except Bells, (b) in all the lithologies the N/C ratios of the Tagish Lake IOM are higher than in almost all CI, CM and CR chondrites, and (c) the modest ^{15}N enrichments do not vary significantly amongst the Tagish Lake samples despite differing considerably within and between the other chondrite groups. It is possible that the peak temperatures experienced by the various Tagish Lake lithologies were only sustained for relatively brief periods (Alexander et al., 2014; Quirico et al., 2014), which could explain some of the differences with other chondrites. In any event, if all IOM did have a common precursor one must appeal to differences in alteration conditions (e.g., Section 6.1.1) to explain the range of IOM compositions in the different chondrite groups. At least in principle, it should be possible to test this experimentally.

6.2 Thermal metamorphism

6.2.1 Conditions and processes—As is evident from Tagish Lake, dividing chondrites into either aqueously altered or thermally metamorphosed petrologic types is somewhat artificial. Water also had a role in the metamorphism of the OCs, Rs and CVs. However, even for these meteorites, the effects of thermal processes generally dominate their now largely anhydrous petrologies. Huss et al. (2006) reviewed in detail the effects and conditions of metamorphism in chondrites, and they are only briefly summarized here.

Metamorphism in the OCs is the best understood. The most primitive OC, Semarkona, experienced aqueous alteration, primarily of its matrix, at temperatures of ~200–260°C. The bulk of the OCs are now anhydrous despite evidence for some aqueous alteration prior to the

peak of metamorphism. The first petrologic evidence for metamorphism is seen in petrologic type 3.05 meteorites. As metamorphic grade increases, the matrix minerals coarsen and develop more homogeneous compositions. By type 3.6, peak metamorphic temperatures were ~600°C, the matrix olivines have relatively uniform compositions, even the coarser chondrule olivines exhibit clear evidence for having exchanged significantly with the matrix, the chondrule glasses have largely devitrified, and the organic material has all but been destroyed. The destruction of the IOM was presumably through oxidation by FeO – the IOM does not contain enough H or O to completely pyrolyse/autocombust on heating, witness the abundant char that is produced in pyrolysis experiments (Section 5.3.2).

The process of thermal metamorphism was more varied for the CVs. There are three CV subtypes (the more oxidized Bali and Allende types, and the more reduced type) identified based largely on their secondary features. The Bali-type CVs show clear evidence of aqueous alteration. The Allende-types show clear evidence for diffusion of halogens and Fe within chondrules and matrix, hinting at aqueous activity, but they were more heated than the Bali-type. The reduced types show little direct or indirect evidence for aqueous activity, but did experience thermal metamorphism. The COs seem to have experienced fairly similar metamorphic histories to the reduced CVs. The enstatite chondrites, on the other hand, experience metamorphism under extremely reducing conditions.

6.2.2 Effects on the IOM—The effect of metamorphism on the organic material is profound. In the very reduced ECs, there is progressive ‘graphitization’ of the IOM in the type 3s and into the type 4s (Busemann et al., 2007a; Quirico et al., 2011a; Piani et al., 2012). Here we use the term ‘graphitization’ to mean loss of heteroatoms and development of large aromatic domains. IOM is probably non-graphitizable on heating alone (Cody et al., 2008c; Quirico et al., 2009), and would have required some combination of water, pressure, shear, irradiation, etc. to promote true graphitization. Despite the metamorphism, vestiges of what may have originally been more CI-CM-CR-like IOM can be seen in ^{15}N-rich components revealed by stepped combustion (Alexander et al., 1998) and SIMS (Piani et al., 2012). A significant amount of C is present in type 5 and 6 ECs (Grady et al., 1986), some of which combusts at relatively low temperatures suggesting that it may be terrestrial contamination or material added after metamorphism (Remusat et al., 2012).

In the more oxidized OCs and CCs, there was competition between ‘graphitization’ and oxidation of the IOM. The IOM has all but disappeared from OCs by type 3.6–3.7 (Alexander et al., 1998; Alexander et al., 2007b), but persists, albeit in significantly reduced amounts, in the highest type COs and CVs (3.6–3.8) (Alexander et al., 2007b).

Despite the progressive destruction, the structural reorganization of the IOM during metamorphism, as measured by Raman spectroscopy, has proved to be a very useful classification tool for type 3 chondrites and has led to estimates of the peak temperatures during metamorphism that compliment mineralogical indicators. Raman spectra of coals and IOM have two major peaks, the graphite (G) and disorder (D) bands. The widths and relative intensities of the two bands are functions of thermal maturation (Quirico et al., 2005), and reflect increases in the sizes and number of stacked graphene layers, along with the removal of defects and heteroatoms. These processes are unidirectional, i.e., they will not be affected

by retrograde reactions, and are also likely to be most sensitive to the conditions during the peak of metamorphism.

The potential of Raman spectroscopy of IOM as a petrologic classification tool for type 3 chondrites was first demonstrated by Quirico et al. (2003) on the OCs, and has subsequently been extended to the CVs and COs (Bonal et al., 2006; Bonal et al., 2007) and the ECs (Quirico et al., 2011a). For the first time, it is possible to put the unequilibrated OCs, COs, CVs and ECs on the same petrologic scale. There are two implicit assumptions in this work: (1) that all four chondrite groups accreted similar IOM precursor material, and (2) that differences in metamorphic conditions had no influence on how the IOM responded. Based on a lack of correlation between H/C ratio and maturity as determined by Raman spectroscopy, Quirico et al. (2009) suggested that the accreted IOM in these chondrite groups were structurally similar but not identical. On the other hand, Busemann et al. (2007a) concluded that the trends in the Raman spectra amongst the OC, CO and CV chondrites are not identical due to differing parent body conditions. At present, it is unclear how to distinguish between these two explanations. Nevertheless, the new petrologic assignments given to the CVs, COs, and ECs are more comparable and realistic than previous ones.

Cody et al. (2008c) reported a novel feature, a 1s-σ* exciton, in XANES spectra of IOM that becomes increasingly pronounced with increasing petrologic type. Experiments showed that the development of the exciton is kinetically controlled. These experiments, along with an independent estimate of the peak metamorphic temperature for one of the meteorites, enabled Cody et al. (2008c) to estimate the peak metamorphic temperatures for 18 chondrites that are generally consistent with previous estimates and are not very sensitive to the assumed duration of heating. The increasing intensity of the exciton with metamorphic grade probably reflects the increasing sizes of graphene sheets and more ordered ‘graphitized’ domains in the IOM. This can also be seem in high resolution TEM images of the IOM, although the IOM microstructures at these scales can be quite heterogeneous (Le Guillou et al., 2012). It is worth noting that the heated CM Y 86720 has a very weak exciton despite mineralogical evidence for quite intense heating. The implication is that Y 86720 was heated only briefly, probably by an impact. IOM studies have implicated impact heating in producing other heated CMs as well (Yabuta et al., 2010; Orthous-Daunay et al., 2013; Quirico et al., 2014).

The IOM from all chondrites follow the same basic compositional trends with increasing petrologic type - decreasing overall abundance, and decreasing bulk H/C, N/C and O/C (Alexander et al., 2007b) – including heated CMs (Naraoka et al., 2004; Yabuta et al., 2005; Yabuta et al., 2010). These trends are consistent with their precursor IOM materials having compositions like that found in CI, CM and CR chondrites. However, the IOM trends are different to what is seen in coals as they mature, most obviously in the high O/C ratios of IOM, even as its abundances are decreasing, until relatively high petrologic grades (low H/C) are reached. Presumably these differences compared to coals reflect both differences in the starting materials (e.g., more stable O functionality in IOM, such as bridging groups) and the ‘rock’ dominated nature of the chondrites (i.e., more oxidizing, except in the ECs), as

well as the lower pressures and higher porosities that existed in the chondrite parent bodies (Quirico et al., 2009).

The isotopes also vary with the extent of metamorphism (Alexander et al., 2007b; Alexander et al., 2010). The most dramatic variations are seen in the δD values (Fig. 1). This is particularly true for the OCs whose IOM δD values increase with decreasing H/C ratios, with the most D-rich sample having a composition of almost δD=12,000‰. By contrast, in the COs, CVs and heated CMs there is up to a ~1000 ‰ increase in δD over a similar range of decreasing H/C to the OCs (Fig. 1), albeit with significant scatter that is probably due to the growing influence of terrestrial contamination at small H/C. The H isotopic variations in these carbonaceous chondrites are probably due to isotopic fractionation associated with the loss of H. However, this cannot be the explanation for the much larger isotopic variations in the OCs. Two possible explanations for this behavior are that the particular conditions in the OC parent body resulted in: (1) preferential preservation of a D-rich component, or (2) extreme isotopic fraction of H in a fluid phase that then exchanged with the IOM.

There is evidence that the most D-rich material in primitive IOM is aliphatic (Section 5.3.4), and during metamorphism aliphatic material is either lost through ‘cracking’ and/or oxidation, or converted to aromatic material. D-rich hotspots are also lost during metamorphism (Remusat et al., 2009; Alexander et al., 2010). Hence, it is hard to envisage how a D-rich signature carried by aliphatic material and/or hotspots would be preferentially preserved.

Alternatively, there is a very large equilibrium H isotopic fractionation between H_2 and H_2O below ~200°C. Progressive oxidation of metal by water at low temperatures and rapid loss of D-poor H_2 in a Rayleigh-type process would have left behind increasingly D-rich H_2O (Alexander et al., 2010). The low water/rock ratios in the OCs would have meant that most or all of the water was ultimately consumed by this process, and that towards the end the D enrichments in the water could have become very large. This would explain the D-rich water known to be present in some OCs (Deloule et al., 1998; Grossman et al., 2002; Alexander et al., 2012; Piani et al., 2015) that would otherwise require an interstellar source (Deloule et al., 1998). The experiments of Yabuta et al. (2007) and Oba and Naraoka (2009) have shown that the IOM undergoes extensive H isotopic exchange with water in days at temperatures ≥270°C. The water-IOM exchange did not necessarily have to have occurred at the low temperatures needed to generate the D-rich water. Nevertheless, it seems plausible that water-IOM H isotope exchange occurred on geologically short timescales at temperatures well below 270°C (Alexander et al., 2010). A similar mechanism may also explain the D-rich water found in R chondrites (McCanta et al., 2008).

Perhaps the most serious objection to this model is the fact that the CO and CV chondrites do not show the same behavior as the OCs. Since the COs exhibit very little evidence for water having been present, it is possible that what water they accreted was either wholly consumed by metal or was lost before much exchange with IOM had taken place. This is an unlikely explanation for the oxidized CVs, at least, with their abundant petrologic evidence for aqueous activity (Krot et al., 1998). For the oxidized CVs, perhaps the water/metal ratios

were high enough to prevent the water from becoming D-rich. However, neither of these explanations for the COs and CVs are entirely satisfactory.

To explain the OC IOM H isotopic variations, Remusat et al. (2016) proposed that they accreted a Murchison-like IOM that was intimately mixed with ≤1 % of very D-rich (but not ^{15}N-rich), very fine grained (less than a few 10s nm) and thermally more stable interstellar organic matter. They reached this conclusion based on the near absence of isotopic hotspots in OC IOM, and a pyrolysis experiment on IOM from GRO 95502 (L3.2) in which the δD increased from ~3250 ‰ to ~9000 ‰ upon flash heating to 600°C. By contrast, Murchison IOM does contain isotopic hotspots, and when heated not only do these hotspots disappear but its bulk δD decreases (Remusat et al., 2009). However, a significant fraction of interstellar carbonaceous dust is >100 nm across (e.g., Compiègne et al., 2011) and should be detectable as extreme H isotopic hotspots even in IOM from metamorphosed meteorites if it is more thermally stable than the bulk of the material. Based on its IOM Raman properties (Quirico et al., 2003; Busemann et al., 2007a; Quirico et al., 2009), XANES spectra (Cody et al., 2008c) and bulk H/C (Fig. 1), even Semarkona, the least metamorphosed OC, has been heated in the OC parent body to significantly higher temperatures than typical CMs. This metamorphism has almost certainly (i) aromatized much of the aliphatic material, thought to be the main carrier of D-rich material in primitive IOM, (ii) destroyed any CC-like isotopic hotspots that may have originally been present, and (iii) enabled isotopic exchange of aromatic H with any D-rich fluid that was present. As a result, metamorphism will have profoundly changed the response of OC IOM to thermal stress. An additional factor will also have contributed to the dramatic change in δD upon heating of the GRO 95502 IOM. Alexander et al. (2007b) reported δD values for IOM from GRO 95502 and its pair GRO 95504 of ~3200 ‰. However, after taking greater care to remove adsorbed atmospheric water (without heating), the δD of GRO 95504 increased to ~5900 ‰ (Alexander et al., 2010). Pyrolysis will tend to remove labile O functional groups, such as –COOH and –OH, that not only have relatively exchangeable Hs but also will promote adsorption of water. It seems possible, therefore, that the changes in δD reported by Remusat et al. (2016) for GRO 95502 IOM after pyrolysis reflected the loss of absorbed water and labile functional groups that had isotopically exchanged in the terrestrial environment. Thus, the evidence for OCs having accreted IOM that was distinct from other chondrites is far from definitive.

6.3 Was there a common IOM precursor?

Ultimately, whether there was a common precursor or a range of precursors will have important implications for where and how the IOM formed. For instance, a range of precursors would suggest that IOM formed in the solar nebula or at least was modified there. On the other hand, a common precursor would favor an interstellar origin and place limits on the thermal processing the most primitive components in matrix experienced in the nebula.

It will be apparent from the above discussion that parent body processes can profoundly modify the properties of IOM. The question that is the subject of vigorous debate is whether parent body processes can produce the entire range of IOM properties from a common precursor that CR IOM most closely resembles, or whether each chondrite group accreted

precursor IOM with similar but distinct properties. It is important to note that a common precursor does not necessarily mean that it was homogeneous at all scales, just that the same mix of materials/grains was accreted by all chondrites.

The range of IOM compositions found in the various Tagish Lake lithologies and after hydrothermal experiments reproduces much of the range of IOM elemental and functional group chemistries seen in CR, CI, CM and the most primitive COs, CVs and OCs. As more primitive members of each chondrite group are found, it does seem that the IOM becomes more aliphatic and isotopically anomalous. For instance, this appears to be the case for Paris (Vinogradoff et al., 2015), which petrologically is the most primitive CM yet found. However, to date no member of any other chondrite group has IOM that is identical to that found in the CRs. Also, while the Tagish Lake IOM and hydrothermal experiments can reproduce the range of elemental compositions and functional group chemistries amongst primitive chondrites, the agreement is not so good when the isotopic compositions are also considered (Figs. 1 and 13). The anomalous behavior of OC IOM is particularly striking. If there was a common precursor, then variations in alteration conditions must have produced the different isotopic behaviors. What these variations in conditions may have been remain poorly understood, but should be amenable to experimentation and would potentially be very revealing about chondrite parent body histories. On the other hand, in the absence of unprocessed members for each chondrite group, appealing to different IOM precursors for each group or even heterogeneous accretion of precursors within a group is a poorly constrained problem and, therefore, very hard to test.

For now, adopting and testing a common precursor hypothesis would seem to be the simplest and most appropriate approach. It does appear that all chondrite groups accreted IOM that was, at least, physically and chemically similar. A common precursor is also most consistent with the similar IOM to circumstellar grain ratios in the most primitive chondrites of each group. Finding more primitive members of each chondrite group and experiments to simulate hydrothermal/metamorphic modification of IOM will be essential for ultimately determining whether or not there was common precursor.

7. Where did the IOM form?

Because conditions in the ISM and the outer parts of the forming Solar System would have been quite similar in many ways, there is considerable debate over whether the IOM is primarily interstellar (e.g., Robert and Epstein, 1982; Kerridge, 1983; Yang and Epstein, 1983; Kerridge et al., 1987; Alexander et al., 1998; Alexander et al., 2007b) or solar (Remusat et al., 2006; Gourier et al., 2008) in origin. Ultimately, it may be difficult to ever definitively demonstrate whether the IOM is solar or interstellar. Certainly, at present the evidence for or against either origin is largely indirect. Consequently, in this section the pros and cons of various proposed interstellar and solar formation scenarios are explored below.

7.1 Some constraints.

There is incontrovertible evidence in the form of circumstellar grains (e.g., Nittler, 2003) that chondrites accreted presolar materials into their matrices. If matrix contains circumstellar grains, it must also contain interstellar grains and there is abundant

carbonaceous dust (≥50% of all C) in the ISM (e.g., Zubko et al., 2004; Draine, 2009; Compiègne et al., 2011). Chick and Cassen (1997) concluded that refractory interstellar organics would have survived infall from the molecular cloud onto the disk beyond 0.5–4 AU, depending on the conditions. Most chondrites seem to have formed at or beyond 2–4 AU at least 2 Ma after CAIs (e.g., Sugiura and Fujiya, 2014), by which time accretion onto the disk will have long since ended. Given that there would have been an overall flow of disk material onto the Sun, the primitive presolar-grain-bearing matrix probably includes material that fell onto the disk well beyond 2–3 AU. The elevated D/H ratios of chondritic water, relative to the solar D/H ratio, suggest that ~7–10% of it has an interstellar heritage, and the interstellar fractions in the even more D-rich comets must be higher still (Cleeves et al., 2014). An interstellar H isotopic signature in H_2O is probably less stable in the nebula than interstellar refractory organics.

On the other hand, unlike silicate dust in the ISM (Kemper et al., 2004; Kemper et al., 2005) much of the matrix in even the most primitive chondrites (as well as in IDPs) is crystalline. This crystalline material must ultimately be the product of thermal processing of ISM dust at temperatures (>1000 K) that would have severely modified or destroyed any carbonaceous interstellar dust. Efficient destruction of most interstellar carbonaceous dust is a prerequisite for a solar origin for IOM. Based on variations in the abundances of noble gas components carried by presolar grains and IOM, Huss et al. (2003) proposed that matrices in different chondrite groups contain variable amounts of material that was heated to ≥400–700°C in the nebula. Paradoxically, if correct the CRs would have the largest fraction of heated matrix despite containing arguably the most primitive IOM (see Section 5.4). If this is correct, then formation of the IOM in CRs, and probably all chondrites, must have postdated the nebular heating. However, there is evidence that the presolar SiC, at least, was partially degassed by parent body processes rather than destroyed in the nebula (Davidson et al., 2014). There are other possible ways of destroying organics in disks (e.g., Gail, 2002; Lee et al., 2010), but a solar origin for IOM requires that at some point all destructive mechanisms must be suppressed and an efficient means for producing carbonaceous dust emerge in the nebula.

The abundance of C in the CI-like matrix material also places constraints on the origin of the IOM (Alexander, 2005; Alexander et al., 2007a). Provided that there was no mechanism for concentrating C relative to silicates in the nebula or in parent bodies, the bulk C/Si ratios of Solar System objects cannot exceed the solar ratio (~8.3 (at.), Asplund et al., 2009). The IOM atomic C/Si ratio is ~0.47 in CIs, and increases to ~0.67 if the missing C is included (Section 3). Consequently, the process that formed the IOM from its precursor materials must have had a C conversion efficiency of at least 6 %, and closer to 8 % if the missing C is also IOM. In the most recent re-analysis of the PUMA measurements of Halley dust, the C/Si and C/Mg ratios are, respectively, 2 and 4 (Schulze et al., 1997) – the solar C/Si≈C/Mg. Thus, refractory C in Halley dust appears to be ~4–9 times more abundant than IOM in CI chondrites and its formation requires a C conversion efficiency of at least 25–55 %. Chondritic porous IDPs may be largely from comets and also have C contents that are on average several times CI (Schramm et al., 1989; Thomas et al., 1993), although there is potential for bias in the IDP population due to atmospheric entry. Nevertheless, the high abundance of refractory C in comets suggests that its abundance in the nebula increased with increasing radial distance from the Sun.

7.2 Solar?

If the IOM is solar, an efficient mechanism for making PAHs is required. Two nebular mechanisms that have been suggested are irradiation of condensed aliphatic material on dust grains (Strazzulla, 1997; Ciesla and Sandford, 2012) or direct formation from the solar gas at relatively high temperatures (Morgan et al., 1991; Kress and Tielens, 2001; Nuth et al., 2008).

While irradiation of ices containing simple molecules produces fairly refractory organic material it is not IOM-like (Nuevo et al., 2011), but further irradiation after sublimation of the ice may be able to produce more IOM-like material (Tachibana et al., 2015). Vertical transport in the disk could potentially cycle dust above and below the vertical H_2O snowline and into radiation-rich regions multiple times. It should be noted that cycling of dust between the dense and diffuse ISM may produce similar results. Implantation during irradiation by energetic particles could explain the association of IOM with Q/P1 noble gases (e.g., Huss et al., 1996; Busemann et al., 2000), but since the precursor material does not seem to be present in meteorites the process would have to have been very efficient. Nor is there any independent evidence for such an irradiation.

Direct formation of a large amount of PAHs at high temperature would take a significant fraction of a disk's lifetime (Morgan et al., 1991). Thus, one might expect to see a variation in IOM abundance with time of accretion. This does not seem to be the case (Alexander et al., 2007b). Nor does the model explain how a macromolecular material could form from these PAHs. Formation of PAHs in this way would also have to have occurred relatively close to the Sun, making it difficult to explain why refractory C abundances appear to be higher in outer Solar System objects than in chondrites.

Thermodynamic (Zolotov and Shock, 2001) and kinetic models (Kress and Tielens, 2001) suggest that FTT synthesis should have occurred in the nebula, albeit in a narrow region between about 2 AU and 4 AU. This could explain the presence of organics in chondrites, but it is not obvious why they would be more abundant in objects like comets that formed at much greater radial distances. Experiments by Sekine et al. (2006) showed that Kress and Tielens (2001) significantly overestimated the rate of FTT synthesis under nebular conditions. More problematic, given the high efficiency of IOM formation needed, is that in experiments using Fe-Ni metal catalysts under nebula-like conditions the products were volatile gases (Llorca and Casanova, 2000; Sekine et al., 2006). Some experiments have found that FTT-like processes can produce a condensed carbonaceous material that is autocatalytic (Nuth et al., 2008). However, the formation rates and yields of the coatings under nebular conditions are unknown, as are their compositions and molecular structures.

The one problem faced by all Solar System models is how to explain the very large D and ^{15}N enrichments found in the IOM from the most petrologically primitive meteorites (Section 5.2). Since the nebular H_2 D/H ratio was probably an order of magnitude lower than terrestrial values (Geiss and Gloeckler, 1998; Mahaffy et al., 1998), nebular materials produced at relatively high temperatures are likely to be strongly D depleted relative terrestrial materials, let alone primitive IOM.

One proposed mechanism for producing large D enrichments is through interaction of IOM grains with highly reactive H_3^+ (Remusat et al., 2006; Gourier et al., 2008) that can become very D-rich at low temperatures. The original estimate for the H_3^+ formation temperature was ~100 K (Remusat et al., 2006), which is high for a molecular cloud leading to the conclusion that the IOM formed in the solar nebula. That temperature estimate has since fallen to ≤40 K (Gourier et al., 2008) weakening the case for a solar origin. There are several potential problems that this model faces. At these low temperatures, grains are likely to be coated by ices that would inhibit interaction between the IOM and H_3^+. Models also suggest that, unlike in the ISM, the abundance of H_3^+ in disks is low and it does not become highly deuterated (Cleeves et al., 2014; Cleeves et al., 2015). On the other hand, CH_3^+ does become highly deuterated, but again its abundance is low. More problematic for any mechanism involving charged ions is that grains rapidly develop a negative surface charge, so that dissociative recombination reactions on the surface that involve no D transfer to the grain become dominant (Cleeves et al., 2015). Finally, at present there is no related explanation for the ^{15}N excesses in IOM. Nevertheless, this mechanism has yet to be ruled out, which means that large D enrichments alone cannot be taken as unequivocal evidence for an interstellar origin, as has often been done in the past.

A second possible mechanism is preferential cleavage of C-H bonds by electrons and/or UV, and subsequent loss of H (Laurent et al., 2015). Electron irradiation at room temperature has been shown to produce D enrichments in organic materials of up to ~1000 ‰ (De Gregorio et al., 2010; Le Guillou et al., 2013; Laurent et al., 2015). However, experiments conducted at 90 K, which is probably more relevant to dust temperatures in the nebula beyond 2–3 AU, show that this isotopic fractionation is suppressed at low temperatures (Le Guillou et al., 2013). Irradiation also generates radicals - initially monoradicals, but biradicals become increasingly important at higher radiation doses (Laurent et al., 2014; Laurent et al., 2015). This is the only proposed mechanism involved in IOM formation that has been shown to produce biradicals (whether biradicaloids are also created is not known). However, in both electron and UV irradiation experiments radical abundances appear to saturate at concentrations that are roughly four orders of magnitude lower than seen in IOM.

Electron irradiation would require exposure at the surface of the disk to the intense solar wind coming from the young Sun, almost certainly leading to grains being entrained in the wind and lost, as well as leading to sputtering and implantation of D-poor H^+ ions that could suppress any H loss and isotopic fractionation. Thus, if this mechanism is to work it probably requires UV irradiation in regions of the disk where dust temperatures were relatively high (to allow H loss and prevent formation of a protective ice layer). Whether such conditions occur in enough of a disk to make it relevant has yet to be determined. Even under optimal conditions, this mechanism cannot explain the full range of D/H ratios observed in bulk IOM from primitive chondrites ($\delta D \approx 700$ ‰ to 3500 ‰) with a single precursor, especially one that formed at high temperature, and so it would require that prior to irradiation the IOM precursor materials be variably enriched in D by an order of magnitude or more relative to the solar D/H ($\delta D \approx -860$ ‰). How these enrichments were achieved has not been satisfactorily explained. Finally, this mechanism cannot explain the ^{15}N enrichments of IOM (De Gregorio et al., 2010).

7.3 Interstellar?

The IR spectra of the IOM resemble in several ways the spectra of refractory organics in the diffuse ISM (Section 5.3.6). However, despite the similarities Pendleton and Allamandola (2002) ultimately concluded that the meteoritic IOM is not a good match to the diffuse ISM dust. For instance, the diffuse ISM dust does not seem to contain significant O, either as OH or carbonyl (C=O). There is considerable uncertainty about the nature of the C-rich dust in the diffuse ISM, as well as its origin (Mennella et al., 2002; Pendleton and Allamandola, 2002; Dartois et al., 2004). In perhaps the most widely accepted picture, the dust is a HAC composed of PAHs that are larger ($C_{20–200}$) and more abundant (~80 % of C) than in the most primitive IOM (Pendleton and Allamandola, 2002). If, as some suggest, this HAC formed in the outflows of C-stars (Pendleton and Allamandola, 2002; Kwok, 2004; Kwok and Zhang, 2011), this presents another serious objection to the interstellar origin of IOM. IOM has an essentially solar C isotopic composition and is enriched in D and ^{15}N. On the other hand, C-stars have very anomalous C isotopic compositions (Lambert et al., 1986), and their H and N isotopic compositions should be very light due to D-burning during the stars' earliest stages and mixing of the ^{14}N-rich ashes of core H-burning into the stellar envelopes, respectively (e.g., Iben and Renzini, 1983).

Others have argued that a HAC composed of highly substituted 1–2 ring PAHs produces a better fit to the diffuse ISM dust spectra (Jones et al., 1990; Dartois et al., 2005) and that it must form in the ISM (Jones et al., 1990; Serra Díaz-Cano and Jones, 2008). It is certainly possible to produce HAC with very IOM-like ^{13}C NMR spectra (Cho et al., 2008), and nanodiamonds may also form under ISM conditions (Stroud et al., 2011; Duley and Hu, 2012). On the other hand, the aliphatic C-H stretch features associated with the diffuse ISM dust are not seen in molecular clouds. This might be because in the diffuse ISM there is a balance between dehydrogenation driven by irradiation and hydrogenation by atomic H, but the latter is inhibited in molecular clouds by ice mantles (Mennella et al., 2001; Muñoz Caro et al., 2001; Vito, 2010) and the dominance of H_2 rather than the more reactive atomic H (Godard et al., 2011). Alexander et al. (2008) suggested that the O and N contents, the small sizes of the PAHs (if they were large initially), and the D and ^{15}N enrichments of IOM (particularly the aliphatic component) could all be the products of cosmic ray irradiation of diffuse ISM dust with icy mantles in the presolar molecular cloud. On warming during Solar System formation, the radiation-damaged regions of the C-rich grains would have reacted with molecules and radiation-produced radicals in the D- and ^{15}N-rich ices. Variable grain histories could potentially explain the isotopic hotspots. While speculative, this model should be amenable to testing experimentally.

Along similar lines, Nakamura-Messenger et al. (2006) suggested that nanoglobules formed by irradiation, probably in the ISM, of ices that were rich in simple organic molecules. The finite penetration depth of the radiation would explain why many globules are hollow. It remains to be seen whether irradiation of simple organics can produce globule-like material, and whether typical UV and/or cosmic ray penetration depths in ices in interstellar and/or disk environments can account for the observed range of globule wall thicknesses.

Finally, there is a hybrid interstellar/solar model in which IOM formed by polymerization of interstellar formaldehyde from aqueous solutions in planetesimals (Cody et al., 2008b; Cody

et al., 2011; Kebukawa et al., 2013; Kebukawa and Cody, 2015). One product of the initial experiments to simulate this process was abundant submicron spherules that in size and shape resemble nanoglobules. The NMR spectra of the initial polymer does not resemble that of IOM (too aliphatic and O-rich), but after heating to 250°C for 3 hrs the similarities while not perfect are quite striking. The kinetics of the transformation of the initial polymer are not yet known, but it is possible that heating for longer times at lower temperatures will achieve similar results.

To date, the formaldehyde polymer experiments have been the most successful ones at reproducing the microstructure and functional group chemistry of IOM. However, the formaldehyde model faces two major challenges. First, while formaldehyde is an important carbonaceous component of ISM (Gibb et al., 2004; Zasowski et al., 2009) and cometary ices (Mumma and Charnley, 2011) it is not the dominant one, and reaction yields are relatively low (≤20 %). Hence, it is not clear that there would have been enough formaldehyde present to produce the abundances of IOM in chondrites and IDPs (or CHON material in comets) without requiring super-solar ice/rock ratios. Also, there is little evidence for the ≥80 % of the formaldehyde that would not have become incorporated into the polymer. Second, there is abundant IOM in IDPs and meteorites that appear to have experienced little of no aqueous alteration, and the possibility of aqueous activity in comets is controversial (but see discussion in Kebukawa and Cody, 2015). Whether there are conditions under which polymerization from solution is much faster than rates of aqueous alteration of silicates and metal (e.g., by development of organic coatings on grains) has yet to be demonstrated, but alteration of IDP material can be rapid even at modest temperatures (Nakamura-Messenger et al., 2011).

8. Summary and conclusions

The IOM is the major identified carbonaceous component in chondrites. However, the IOM recovered in demineralized residues typically only accounts for ~60% of the bulk C. Only a small fraction of the unrecovered C can be accounted for by carbonate or solvent soluble organic material. The remainder is probably either in very fine-grained IOM that is hard to recover from the demineralizing solutions or is in acid hydrolysable functional groups that are attached to the IOM.

The IOM (or its precursor material) in chondrites was accreted in matrix – it would not have survived chondrule and refractory inclusion formation. The carbonaceous grains in matrix, which are presumably dominated by IOM, are free of mineral inclusions and exhibit no obvious spatial relationship with any minerals. The grains occur in a diversity of grain morphologies, sizes (mostly < 1μm) and isotopic compositions. These include isolated irregular grains and nanoglobules, as well as veins. The veins probably reflect a redistribution of material when ices that were also accreted in the matrix melted.

This diversity of grain morphologies and isotopic compositions is preserved in IOM residues and it is the residues that have been studied in the most detail. The bulk elemental composition of IOM from the CR chondrites, $C_{100}H_{75–79}O_{11–17}N_{3–4}S_{1–3}$, closely resembles the bulk elemental composition of comet Halley CHON particles, ~$C_{100}H_{80}O_{20}N_4S_2$. The

CRs appear to have experienced the most benign alteration conditions for IOM of any chondrite group. The IOM from all other chondrite groups tend to have lower H/C ratios that roughly reflect the intensity of the parent body processing their host meteorites experienced. The IOM in CR chondrites is also, with rare exceptions, the most isotopically anomalous, both in bulk and at micron to submicron scales. When analyzed at similar scales, the range of H and N isotopic compositions seen in the most primitive IOM is very similar to that seen in CP-IDPs that may come from comets.

Chemical degradation and pyrolysis studies point to the IOM being composed of small PAHs that are highly substituted and cross linked by short, highly branched aliphatics and esters. However, yields from both chemical degradation and pyrolysis studies are low, so it is not clear how representative of the bulk material their results are. In addition, the yields of individual compounds are rarely determined quantitatively. IR spectroscopy suggests that at least the aliphatic material in bulk IOM is indeed composed of short and highly branched units. But at present it is NMR that provides the best quantitative picture of the functional group chemistry of bulk IOM. It too requires that most of the PAHs in IOM be small (1–3 ring) and highly substituted, and that the aliphatic component be composed of short, highly branched units. While some of the line broadening that is evident in the NMR spectra could be due the presence of paramagnetic minerals like chromite, most of it almost certainly reflects the considerable chemical complexity in IOM. Such complexity is perhaps not too surprising given that the analyzed IOM samples are collections of morphologically and chemically heterogeneous grains.

The H isotopic compositions of individual pyrolysates (both aromatic and aliphatic) and aliphatic side groups on the PAHs released by RuO_4 are comparable to those of the bulk IOM compositions, albeit with significant scatter. It has been suggested that this scatter reflects variations in the average δD values of functional groups with different H-C bond energies. This interpretation is not consistent with all pyrolysis results. On the other hand, some EPR experiments suggest that radicals in IOM are associated with very D-rich benzylic positions on aliphatic side chains. The C-H bond energies of benzylic radicals would be amongst the lowest in the IOM. The EPR experiments also show that the radical speciation in IOM is quite unlike those of terrestrial coals and kerogens despite their superficial resemblance in terms of elemental and functional group chemistries.

Thermal metamorphism has profoundly modified the IOM due to the competing processes of ‘graphitization’ and oxidation. The progressive ‘graphitization’ has for the first time provided a means of classifying low petrologic grade meteorites across chemical groups. Whether aqueous alteration has modified the IOM is more controversial. The IOM extracted from Tagish Lake lithologies that experienced varying intensities of alteration, show that alteration can produce much of the range in elemental compositions and functional chemistries amongst type 1, type 2 and type 3.0 chondrites. However, the linear correlation between H/C and δD seen in the Tagish Lake IOM samples is not seen in the other chondrite groups. This could simply reflect differences in alteration conditions amongst the chondrite groups, but it cannot be ruled out at this stage that there were some differences in the properties of the IOM accreted by the chondrite groups.

Currently, there is no consensus about where and how the IOM formed. If the IOM formed in the solar nebula, there must first have been an efficient mechanism for destroying the abundant interstellar carbonaceous dust, and later a mechanism for remaking carbonaceous dust must have emerged. This Solar System mechanism must have been relatively efficient and also be able to explain why comets appear to contain higher abundances of refractory C than chondrites. FTT-like processes may have operated in parts of the warm inner disk, but any dust formed there would have had near solar D/H ratios. Reaction with deuterated H_3^+ is one possible mechanism for producing D-rich IOM compositions, but models suggest that the formation and deuteration of H_3^+ is not very efficient in disks.

UV irradiation of carbonaceous dust can cause H loss, but the resulting D enrichment is not large enough to explain the full range of IOM H isotopic compositions. Nor can this mechanism explain the ^{15}N enrichments in IOM. However, it is the only mechanism to date that can explain the unusual radical speciation in IOM, albeit not in their observed abundances. Irradiation of ices near the surface of the disk might also have been able to produce refractory carbonaceous material, but experiments have yet to show that material produced in this way is IOM-like.

In many ways, an interstellar origin for IOM is the simplest explanation, and would be consistent with the presence of presolar circumstellar grains in chondrites and the evidence that some interstellar water survived Solar System formation. Carbonaceous dust is abundant in the diffuse ISM. However, this diffuse ISM dust does not seem to have the high heteroatom abundances of IOM, may be composed of much larger PAHs than present in IOM, and it is not clear what happens to this dust in the molecular clouds where stars form. It is possible that irradiation of ice-coated carbonaceous dust in molecular clouds was responsible for both reducing the sizes of the PAHs and introducing the heteroatom content of IOM, but this has yet to be demonstrated experimentally. Alternatively, the IOM may have formed from interstellar formaldehyde and ammonia in the chondrites through formaldehyde polymerization. The formaldehyde and ammonia would have been accreted in the ices that were responsible for the aqueous alteration in chondrites. Experiments have shown that formaldehyde polymerization can produce a material that chemically resembles IOM in many ways, as well as produce nanoglobules. However, it is not clear that there would have been enough formaldehyde in the ices to explain IOM abundances.

9. References

Abreu NM, Brearley AJ, 2004 Characterisation of matrix in the EET92042 CR2 carbonaceous chondrite: Insights into textural and mineralogical heterogeneity. Meteor. Planet. Sci 39, A12 (abstr.).

Abreu NM, Brearley AJ, 2010 Early solar system processes recorded in the matrices of two highly pristine CR3 carbonaceous chondrites, MET 00426 and QUE 99177. Geochim. Cosmochim. Acta 74, 1146–1171.

Abreu NM, Bullock ES, 2013 Opaque assemblages in CR2 Graves Nunataks (GRA) 06100 as indicators of shock-driven hydrothermal alteration in the CR chondrite parent body. Meteor. Planet. Sci 48, 2406–2429.

Aléon J, Robert F, Chaussidon M, Marty B, 2003 Nitrogen isotopic composition of macromolecular organic matter in interplanetary dust particles. Geochim. Cosmochim. Acta 67, 3773–3783.

Alexander CMO'D, Russell SS, Arden JW, Ash RD, Grady MMPillinger CT, 1998 The origin of chondritic macromolecular organic matter: A carbon and nitrogen isotope study. Meteor. Planet. Sci 33, 603–622.

Alexander CMO'D, 2005 Re-examining the role of chondrules in producing the volatile element fractionations in chondrites. Meteor. Planet. Sci 40, 943–965.

Alexander CMO'D, Boss AP, Keller LD, Nuth I,JA, Weinberger A, 2007a Astronomical and meteoritic evidence for the nature of interstellar dust and its processing in protoplanetary disks, in: Reipurth B, Jewitt D, Keil K (Eds.), Protostars and Planets V. University of Arizona Press, Tucson, pp. 801–814.

Alexander CMO'D, Fogel M, Yabuta H, Cody GD, 2007b The origin and evolution of chondrites recorded in the elemental and isotopic compositions of their macromolecular organic matter. Geochim. Cosmochim. Acta 71, 4380–4403.

Alexander CMO'D, Cody GD, Fogel M, Yabuta H, 2008 Organics in meteorites - Solar or interstellar?, in: Kwok S, Sandford SA (Eds.), Organic Matter in Space. Cambridge University Press, Hong Kong, pp. 293–297.

Alexander CMO'D, 2009 Laboratory studies of circumstellar and interstellar materials, in: Boulanger F, Joblin C, Jones A, Madden S (Eds.), Interstellar dust from astronomical observations to fundamental studies. European Astronomical Society Publication Series, pp. 75–102.

Alexander CM, Newsome SN, Fogel ML, Nittler LR, Busemann H, Cody GD, 2010 Deuterium enrichments in chondritic macromolecular material – Implications for the origin and evolution of organics, water and asteroids. Geochim. Cosmochim. Acta 74, 4417–4437.

Alexander CMO'D, Bowden R, Fogel ML, Howard KT, Herd CDK, Nittler LR, 2012 The provenances of asteroids, and their contributions to the volatile inventories of the terrestrial planets. Science 337, 721–723. [PubMed: 22798405]

Alexander CMO'D, Howard K, Bowden R, Fogel ML, 2013 The classification of CM and CR chondrites using bulk H, C and N abundances and isotopic compositions. Geochim. Cosmochim. Acta 123, 244–260.

Alexander CMO'D, Cody GD, Kebukawa Y, Bowden R, Fogel ML, Kilcoyne ALD, Nittler LR, Herd CDK, 2014 Elemental, isotopic and structural changes in Tagish Lake insoluble organic matter produced by parent body processes. Meteor. Planet. Sci 49, 503–525.

Alexander CMO'D, Bowden R, Fogel ML, Howard KT, 2015a Carbonate abundances and isotopic compositions in chondrites. Meteor. Planet. Sci 50, 810–833.

Alexander CMO'D, Nilges MJ, Cody GD, Herd CDK, 2015b Are Radicals the Carriers of D in IOM?, Lunar and Planetary Science Conference, p. 2721.

Alpern B, Benkheiri Y, 1973 Distribution de la matière organique dans la météorite d'Orgueil par microscopie en fluorescence. Earth Planet. Sci. Lett 19, 422–428.

Aponte JC, Alexandre MR, Wang Y, Brearley AJ, Alexander CMO'D, Huang Y, 2011 Effects of secondary alteration on the composition of free and IOM-derived monocarboxylic acids in carbonaceous chondrites. Geochim. Cosmochim. Acta 75, 2309–2323.

Aponte JC, Dworkin JP, Elsila JE, 2014a Assessing the origins of aliphatic amines in the Murchison meteorite from their compound-specific carbon isotopic ratios and enantiomeric composition. Geochim. Cosmochim. Acta 141, 331–345.

Aponte JC, Tarozo R, Alexandre MR, Alexander CMO'D, Charnley SB, Hallmann C, Summons RE, Huang Y, 2014b Chirality of meteoritic free and IOM-derived monocarboxylic acids and implications for prebiotic organic synthesis. Geochim. Cosmochim. Acta 131, 1–12.

Aponte JC, Dworkin JP, Elsila JE, 2015 Indigenous aliphatic amines in the aqueously altered Orgueil meteorite. Meteor. Planet. Sci 50, 1733–1749.

Asplund M, Grevesse N, Sauval AJ, Scott P, 2009 The chemical composition of the Sun. Ann. Rev. Astron. Astrophys 47, 481–522.

Beck P, Garenne A, Quirico E, Bonal L, Montes-Hernandez G, Moynier F, Schmitt B, 2014 Transmission infrared spectra (2–25 μm) of carbonaceous chondrites (CI, CM, CV–CK, CR, C2 ungrouped): Mineralogy, water, and asteroidal processes. Icarus 229, 263–277.

Bernatowicz TJ, Messenger S, Pravdivtseva O, Swan P, Walker RM, 2003 Pristine presolar silicon carbide. Geochim. Cosmochim. Acta 67, 4679–4691.

Binet L, Gourier D, Derenne S, Robert F, 2002 Heterogeneous distribution of paramagnetic radicals in insoluble organic matter from the Orgueil and Murchison meteorites. Geochim. Cosmochim. Acta 66, 4177–4186.

Binet L, Gourier D, Derenne S, Pizzarello S, Becker L, 2004a Diradicaloids in the insoluble organic matter from the Tagish Lake meteorite: Comparison with the Orgueil and Murchison meteorites. Meteor. Planet. Sci 39, 1649–1654.

Binet L, Gourier D, Derenne S, Robert F, Ciofini I, 2004b Occurence of abundant diradicaloid moieties in the insoluble organic matter from the Orgueil and Murchison meteorites: a fingerprint of its extraterrestrial origin? Geochim. Cosmochim. Acta 68, 881–891.

Bland PA, Collins GS, Davison TM, Abreu NM, Ciesla FJ, Muxworthy AR, Moore J, 2014 Pressure–temperature evolution of primordial solar system solids during impact-induced compaction. Nat. Commun 5.

Blinova AI, Zega T, Herd CDK, Stroud R, 2014 Testing variations within the Tagish Lake meteorite - I: Mineralogy and petrology of pristine samples. Meteoritics Planet. Sci 49, 473–502.

Bonal L, Quirico E, Bourot-Denise M, Montagnac G, 2006 Determination of the petrologic type of CV3 chondrites by Raman spectroscopy of included organic matter. Geochim. Cosmochim. Acta 70, 1849–1863.

Bonal L, Bourot-Denise M, Quirico E, Montagnac G, Lewin E, 2007 Organic matter and metamorphic history of CO chondrites. Geochim. Cosmochim. Acta 71, 1605–1623.

Bose M, Zega TJ, Williams P, 2014 Assessment of alteration processes on circumstellar and interstellar grains in Queen Alexandra Range 97416. Earth Planet. Sci. Lett 399, 128–138.

Botta O, Bada JL, 2002 Extraterrestrial Organic Compounds in Meteorites. Surveys in Geophysics 23, 411–467.

Braatz A, Ott U, Henning T, Jäger C, Jeschke G, 2000 Infrared, ultraviolet and electron paramagnetic resonance measurements on presolar diamonds: Implications for optical features and origin. Meteor. Planet. Sci 35, 75–84.

Bradley JP, 2014 Early solar nebula grains – Interplanetary Dust Particles, in: Davis AM (Ed.), Treatise on Geochemistry (Second Edition). Elsevier, Oxford, pp. 287–308.

Brearley AJ, 1995 Aqueous alteration and brecciation in Bells, an unusual saponite-bearing, CM chondrite. Geochim. Cosmochim. Acta 59, 2291–2318.

Brearley AJ, 2006 The Action of Water, in: Lauretta DS, McSween HY Jr. (Eds.), Meteorites and the Early Solar System II. The University of Arizona Press, Tucson, pp. 584–624.

Brunetto R, Borg J, Dartois E, Rietmeijer FJM, Grossemy F, Sandt C, Le Sergeant d'Hendecourt L, Rotundi A, Dumas P, Djouadi Z, Jamme F, 2011 Mid-IR, Far-IR, Raman micro-spectroscopy, and FESEM-EDX study of IDP L2021C5: Clues to its origin. Icarus 212, 896–910.

Burbine TH, McCoy TJ, Meibom A, Gladman B, Kiel K, 2002 Meteoritic parent bodies: Their number and identification, in: Bottke WF Jr., Cellino A, Paolicchi P, Binzel RP (Eds.), Asteroids III. University of Arizona Press, Tuscon, pp. 653–667.

Busemann H, Baur H, Wieler R, 2000 Primordial noble gases in "Phase Q" in carbonaceous and ordinary chondrites studied by closed system stepped etching. Meteor. Planet. Sci 35, 949–973.

Busemann H, Alexander CMO'D, Nittler LR, Zega TJ, Stroud RM, Bajt S, Cody GD, Yabuta H, 2006a Correlated analyses of D- and ^{15}N-rich carbon grains from CR2 chondrite EET 92042. Meteoritics & Planetary Science Supplement 41, A34.

Busemann H, Alexander CMO'D, Nittler LR, Zega TJ, Stroud RM, Cody GD, Yabuta H, Hoppe P, 2006b Correlated microscale isotope and scanning transmission X-Ray analyses of isotopically anomalous organic matter from the CR2 chondrite EET 92042. Lunar Planet. Sci 37, #2005.

Busemann H, Young AF, Alexander CMO'D, Hoppe P, Mukhopadhyay S, Nittler LR, 2006c Interstellar chemistry recorded in organic matter from primitive meteorites. Science 312, 727–730. [PubMed: 16675696]

Busemann H, Alexander CMO'D, Nittler LR, 2007a Characterization of insoluble organic matter in primitive meteorites by microRaman spectroscopy. Meteor. Planet. Sci 42, 1387–1416.

Busemann H, Zega TJ, Alexander CMO'D, Cody GD, Kilcoyne ALD, Nittler LR, Stroud RM, Yabuta H, 2007b Secondary ion mass spectrometry and X-Ray absorption near-edge structure

spectroscopy of isotopically anomalous organic matter from CR1 chondrites GRO 95577. Lunar Planet. Sci 38, #1884.

Busemann H, Nguyen AN, Cody GD, Hoppe P, Kilcoyne ALD, Stroud RM, Zega TJ, Nittler LR, 2009 Ultra-primitive interplanetary dust particles from the comet 26P/Grigg-Skjellerup dust stream collection. Earth Planet. Sci. Lett 288, 44–57.

Charnley SB, Rodgers SD, 2008 Interstellar Reservoirs of Cometary Matter. Space Sci. Rev 138, 59–73.

Chick KM, Cassen P, 1997 Thermal processing of interstellar dust grains in the primitive solar environment. Astrophys. J 477, 398–409.

Cho G, Yen BK, Klug CA, 2008 Structural characterization of sputtered hydrogenated amorphous carbon films by solid state nuclear magnetic resonance. Journal of Applied Physics 104, 013531–013538.

Christophe Michel-Levy M, Lautie A, 1981 Microanalysis by Raman spectroscopy of carbon in the Tieschitz chondrite. Nature 292, 321–322.

Ciesla FJ, 2009 Two-dimensional transport of solids in viscous protoplanetary disks. Icarus 200, 655–671.

Ciesla FJ, Sandford SA, 2012 Organic synthesis via irradiation and warming of ice grains in the solar nebula. Science 336, 452–454. [PubMed: 22461502]

Clayton DD, Nittler LR, 2004 Astrophysics with presolar stardust. Ann. Rev. Astron. Astrophys 42, 39–78.

Cleeves LI, Bergin EA, Alexander CMO'D, Du F, Graninger D, Öberg KI, Harries TJ, 2014 The ancient heritage of water ice in the Solar System. Science 345, 1590–1593. [PubMed: 25258075]

Cleeves LI, Bergin EA, Alexander CMO'D, Du F, Graninger D, Öberg KI, Harries TJ, 2015 Deuterium enriched simple organics in the solar nebula. Astrophys. J. Lett, in revision.

Cody GD, Alexander CMO'D, Tera F, 2002 Solid state (1H and 13C) NMR spectroscopy of the insoluble organic residue in the Murchison meteorite: A self-consistent quantitative analysis. Geochim. Cosmochim. Acta 66, 1851–1865.

Cody GD, Alexander CMO'D, 2005 NMR studies of chemical structural variation of insoluble organic matter from different carbonaceous chondrite groups. Geochim. Cosmochim. Acta 69, 1085–1097.

Cody GD, Ade H, Alexander CMO'D, Araki T, Butterworth A, Fleckenstein H, Flynn GJ, Gilles MK, Jacobsen C, Kilcoyne ALD, Messenger K, Sandford SA, Tyliszczak T, Westphal AJ, Wirick S, Yabuta H, 2008a Quantitative organic and light element analysis of Comet 81P/Wild 2 particles using C-, N-, and O- μ-XANES. Meteor. Planet. Sci 43, 353–365.

Cody GD, Alexander CMO'D, Kilcoyne ALD, Yabuta H, 2008b Unraveling the chemical history of the Solar System as recorded in extraterrestrial organic matter, in: Kwok S, Sandford SA (Eds.), Organic matter in space. Cambridge University Press, Hong Kong, pp. 277–282.

Cody GD, Alexander CMO'D, Yabuta H, Kilcoyne ALD, Araki T, Ade H, Dera P, Fogel M, Militzer B, Mysen BO, 2008c Organic thermometry for chondritic parent bodies. Earth Planet. Sci. Lett 272, 446–455.

Cody GD, Fogel ML, Yabuta H, Alexander CMO'D, 2008d The peculiar relationship between meteoritic organic molecular structure and deuterium abundance. Lunar Planet. Sci 39, #1765.

Cody GD, Heying E, Alexander CMO'D, Nittler LR, Kilcoyne ALD, Sandford SA, Stroud RM, 2011 Establishing a molecular relationship between chondritic and cometary organic solids. Proc. Nat. Acad. Sci 108, 19171–19176. [PubMed: 21464292]

Cody GD, Alexander CMO'D, 2016 H, D and ^{15}N NMR spectroscopy of chondritic IOM. In Prep.

Compiègne M, Verstraete L, Jones A, Bernard J-P, Boulanger F, Flagey N, Le Bourlot J, Paradis D, Ysard N, 2011 The global dust SED: tracing the nature and evolution of dust with DustEM. Astronomy & Astrophysics 525, A103.

Connolly HC Jr., Hewins RH, Ash RD, Zanda B, Lofgren GE, Bourot-Denise M, 1994 Carbon and the formation of reduced chondrules. Nature 371, 136–139.

Cooper G, Kimmich N, Belisle W, Sarinana J, Brabham K, Garrel L, 2001 Carbonaceous meteorites as a source of sugar-related organic compounds for the early Earth. Nature 414, 879–883. [PubMed: 11780054]

Croat TK, Bernatowicz TJ, Stadermann FJ, 2009 Auger and NanoSIMS Investigations of Pristine Presolar SiC Surfaces. Lunar Planet. Sci. 40, #1887.

Cronin JR, Pizzarello S, Frye JS, 1987 ^{13}C NMR spectroscopy of the insoluble carbon of carbonaceous chondrites. Geochim. Cosmochim. Acta 51, 299–303. [PubMed: 11542083]

Dartois E, Muñoz Caro GM, Deboffle D, d'Hendecourt L, 2004 Diffuse interstellar medium organic polymers. Photoproduction of the 3.4, 6.85 and 7.25 mm features. Astron. Astrophys 423, L33–L36.

Dartois E, Muñoz Caro GM, Deboffle D, Montagnac G, D'Hendecourt L, 2005 Ultraviolet photoproduction of ISM dust. Laboratory characterisation and astrophysical relevance. Astron. Astrophys 432, 895–908.

Davidson J, Busemann H, Nittler LR, Alexander CMO'D, Orthous-Daunay F-R, Franchi IA, Hoppe P, 2014 Abundances of presolar silicon carbide grains in primitive meteorites determined by NanoSIMS. Geochim. Cosmochim. Acta 139, 248–266.

De Gregorio BT, Stroud RM, Nittler LR, Alexander CMO'D, Kilcoyne ALD, Zega TJ, 2010 Isotopic anomalies in organic nanoglobules from Comet 81P/Wild 2: Comparison to Murchison nanoglobules and isotopic anomalies induced in terrestrial organics by electron irradiation. Geochim. Cosmochim. Acta 74, 4454–4470.

De Gregorio BT, Stroud RM, Cody GD, Nittler LR, Kilcoyne ALD, Wirick S, 2011 Correlated microanalysis of cometary organic grains returned by Stardust. Meteor. Planet. Sci 46, 1376–1396.

De Gregorio BT, Stroud RM, Nittler LR, Alexander CMO'D, Bassim ND, Cody GD, Kilcoyne ALD, Sandford SA, Milam SN, Nuevo M, Zega TJ, 2013 Isotopic and chemical variation of organic nanoglobules in primitive meteorites. Meteor. Planet. Sci 48, 904–928.

Deloule E, Robert F, Doukhan JC, 1998 Interstellar hydroxyl in meteoritic chondrules: implications for the origin of water in the inner solar system. Geochim. Cosmochim. Acta 62, 3367–3378.

Delpoux O, Gourier D, Binet L, Verzin H, Derenne S, Robert F, 2008 CW- and pulsed-EPR of carbonaceous matter in primitive meteorites: Solving a lineshape paradox. Spectrochimica Acta Part A 69, 1301–1310.

Delpoux O, Gourier D, Vezin H, Binet L, Derenne S, Robert F, 2011 Biradical character of D-rich carriers in the insoluble organic matter of carbonaceous chondrites: A relic of the protoplanetary disk chemistry. Geochim. Cosmochim. Acta 75, 326–336.

DeMeo FE, Carry B, 2014 Solar System evolution from compositional mapping of the asteroids. Nature 505, 629–634. [PubMed: 24476886]

Derenne S, Rouzaud JN, Clinard C, Robert F, 2005 Size discontinuity between interstellar and chondritic aromatic structures: A high-resolution transmission electron microscopy study. Geochim. Cosmochim. Acta 69, 3911–3917.

Dermott SF, Durda DD, Grogan K, Kehoe TJJ, 2002 Asteroidal dust, in: Bottke WF Jr., Cellino A, Paolicchi P, Binzel RP (Eds.), Asteroids III. University of Arizona Press, Tucson, pp. 423–442.

Dobrică E, Engrand C, Duprat J, Gounelle M, Leroux H, Quirico E, Rouzaud JN, 2009 Connection between micrometeorites and Wild 2 particles: From Antarctic snow to cometary ices. Meteor. Planet. Sci 44, 1643–1661.

Draine BT, 2009 Interstellar dust models and evolutionary implications, in: Henning T, Grün E, Steinacker J (Eds.), Cosmic Dust - Near and Far, pp. 453–473.

Duer MJ, 2004 Introduction to solid-state NMR spectroscopy. Blackwell Publishing.

Duley WW, Hu A, 2012 The 217.5 nm band, infrared absorption, and infrared emission features in hydrogenated amorphous carbon nanoparticles. Astrophys. J 761, 115.

Duprat J, Dobrică E, Engrand C, Aléon J, Marrocchi Y, Mostefaoui S, Meibom A, Leroux H, Rouzaud JN, Gounelle M, Robert F, 2010 Extreme deuterium excesses in ultracarbonaceous micrometeorites from central Antarctic snow. Science 328, 742–745. [PubMed: 20448182]

Egerton RF, 2014 Choice of operating voltage for a transmission electron microscope. Ultramicroscopy 145, 85–93. [PubMed: 24679438]

Ehrenfreund P, Robert F, D'Hendencourt L, Behar F, 1991 Comparison of interstellar and meteoritic organic matter at 3.4 microns. Astron. Astrophys 252, 712–717.

Ehrenfreund P, Charnley SB, 2000 Organic molecules in the interstellar medium, comets and meteorites: A voyage from dark clouds to the early Earth. Annu. Rev. Astronomy and Astrophysics 38, 427–483.

Ehrenfreund P, Glavin DP, Botta O, Cooper G, Bada JL, 2001 Extraterrestrial amino acids in Orgueil and Ivuna: Tracing the parent body of CI type carbonaceous chondrites. Proc. Nat. Acad. Sci 98, 2138–2141. [PubMed: 11226205]

Floss C, Stadermann FJ, Bradley JP, Dai ZR, Bajt S, Graham G, 2004 Carbon and nitrogen isotopic anomalies in an anhydrous interplanetary dust particle. Science 303, 1355–1358. [PubMed: 14988560]

Floss C, Stadermann FJ, Bradley JP, Dai ZR, Bajt S, Graham GA, Lea AS, 2006 Identification of isotopically primitive interplanetary dust particles: A NanoSIMS isotopic imaging study. Geochim. Cosmochim. Acta 70, 2371–2399.

Floss C, Stadermann FJ, 2009 High abundances of circumstellar and interstellar C-anomalous phases in the primitive CR3 chondrites QUE 99177 and MET 00426. Astrophys. J 697, 1242–1255.

Floss C, Le Guillou C, Brearley A, 2014 Coordinated NanoSIMS and FIB-TEM analyses of organic matter and associated matrix materials in CR3 chondrites. Geochim. Cosmochim. Acta 139, 1–25.

Flynn GJ, Keller LP, Feser M, Wirick S, Jacobsen C, 2003 The origin of organic matter in the solar system: Evidence from interplanetary dust particles. Geochim. Cosmochim. Acta 67, 4791–4806.

Foustoukos DI, Houghton JL, Seyfried WE Jr, Sievert SM, Cody GD, 2011 Kinetics of H_2-O_2-H_2O redox equilibria and formation of metastable H_2O_2 under low temperature hydrothermal conditions. Geochim. Cosmochim. Acta 75, 1594–1607.

Fujiya W, Sugiura N, Sano Y, Hiyagon H, 2013 Mn-Cr ages of dolomites in CI chondrites and the Tagish Lake ungrouped carbonaceous chondrite. Earth Planet. Sci. Lett 362, 130–142.

Gail H-P, 2002 Radial mixing in protoplanetary accretion disks. III. Carbon dust oxidation and abundance of hydrocarbons in comets. Astron. Astrophys 390, 253–265.

Gardinier A, Derenne S, Robert F, Behar F, Largeau C, Maquet J, 2000 Solid state CP/MAS ^{13}C NMR of the insoluble matter of the Orgueil and Murchison meteorites: quantitative study. Earth Planet. Sci. Lett 184, 9–21.

Garvie LAJ, Buseck PR, 2004 Nanosized carbon-rich grains in carbonaceous chondrite meteorites. Earth Planet. Sci. Lett 224, 431–439.

Garvie LAJ, Buseck PR, 2005 Structure and bonding of carbon in clays from CI carbonaceous chondrites. Lunar Planet. Sci 36, #1515.

Garvie LAJ, Buseck PR, 2006 Carbonaceous materials in the acid residue from the Orgueil carbonaceous chondrite meteorite. Meteor. Planet. Sci 41, 633–642.

Garvie LAJ, Baumgardener G, Buseck PR, 2008 Scanning electron microscopical and cross sectional analysis of extraterrestrial carbonaceous nanoglobules. Meteor. Planet. Sci 43, 899–903.

Geiss J, Gloeckler G, 1998 Abundances of deuterium and helium-3 in the protosolar cloud. Space Sci. Rev 84, 239–250.

Gibb EL, Whittet DCB, Boogert ACA, Tielens AGGM, 2004 Interstellar Ice: The Infrared Space Observatory Legacy. Astrophysical Journal Supplement Series 151, 35–73.

Gilmour I, 2003 Structural and isotopic analysis of organic matter in carbonaceous chondrites, in: Davis AM (Ed.), Meteorites, Comets and Planets. Elsevier-Pergamon, Oxford, pp. 269–290.

Glavin DP, Callahan MP, Dworkin JP, Elsila JE, 2011 The effects of parent body processes on amino acids in carbonaceous chondrites. Meteor. Planet. Sci 45, 1948–1972.

Godard M, Féraud G, Chabot M, Carpentier Y, Pino T, Brunetto R, Duprat J, Engrand C, Bréchignac P, D'Hendecourt L, Dartois E, 2011 Ion irradiation of carbonaceous interstellar analogues. Effects of cosmic rays on the 3.4 μm interstellar absorption band. Astron. Astrophys 529, 146.

Gourier D, Robert F, Delpoux O, Binet L, Vezin H, Moissette A, Derenne S, 2008 Extreme deuterium enrichment of organic radicals in the Orgueil meteorite: Revisiting the interstellar interpretation? Geochim. Cosmochim. Acta 72, 1914–1923.

Gradie JC, Chapman CR, Tedesco EF, 1989 Distribution of taxonomic classes and the compositional structure of the asteroid belt, in: Binzel RP, Gehrels T, Matthews MS (Eds.), Asteroids II. Univ. Arizona Press, Tucson, pp. 316–335.

Grady MM, Wright IP, Carr LP, Pillinger CT, 1986 Compositional differences in enstatite chondrites based on carbon and nitrogen stable isotope measurements. Geochim. Cosmochim. Acta 50, 2799–2813.

Greenberg JM, Gillette JS, Muñoz Caro GM, Mahajan TB, Zare RN, Li A, Schutte WA, de Groot M, Mendoza-Gómez C, 2000 Ultraviolet photoprocessing of interstellar dust mantles as a source of polycyclic aromatic hydrocarbons and other conjugated molecules. Astrophys. J 531, L71–L73. [PubMed: 10673417]

Grossman JN, Alexander CM, Wang J, Brearley AJ, 2002 Zoned chondrules in Semarkona: Evidence for high- and low-temperature processing. Meteor. Planet. Sci 37, 49–73.

Halbout J, Robert F, Javoy M, 1990 Hydrogen and oxygen isotope compositions in kerogen from the Orgueil meteorite: Clues to a solar origin. Geochim. Cosmochim. Acta 54, 1453–1462.

Hanna RD, Ketcham RA, Zolensky M, Behr WM, 2015 Impact-induced brittle deformation, porosity loss, and aqueous alteration in the Murchison CM chondrite. Geochim. Cosmochim. Acta 171, 256–282.

Harju ER, Rubin AE, Ahn I, Choi B-G, Ziegler K, Wasson JT, 2014 Progressive aqueous alteration of CR carbonaceous chondrites. Geochim. Cosmochim. Acta 139, 267–292.

Hashiguchi M, Kobayashi S, Yurimoto H, 2013 In situ observation of D-rich carbonaceous globules embedded in NWA 801 CR2 chondrite. Geochim. Cosmochim. Acta 122, 306–323.

Hashiguchi M, Kobayashi S, Yurimoto H, 2015 Deuterium- and ^{15}N-signatures of organic globules in Murchison and Northwest Africa 801 meteorites. Geochem. J 49, 377–391.

Hayatsu R, Matsuoka S, Scott RG, Studier MH, Anders E, 1977 Origin of organic matter in the early solar system-VII. The organic polymer in carbonaceous chondrites. Geochim. Cosmochim. Acta 41, 1325–1339.

Hayatsu R, Winans RE, Scott RG, McBeth RL, Moore LP, Studier MH, 1980 Phenolic esters in the organic polymer of the Murchison meteorite. Science 207, 1202–1204. [PubMed: 17776856]

Herd CDK, Blinova A, Simkus DN, Huang Y, Tarozo R, Alexander CMO'D, Gyngard F, Nittler LR, Cody GD, Fogel ML, Kebukawa Y, Kilcoyne ALD, Hilts RW, Slater GF, Glavin DP, Dworkin JP, Callahan MP, Elsila JE, De Gregorio BT, Stroud RM, 2011 Origin and evolution of prebiotic organic matter as inferred from the Tagish Lake meteorite. Science 332, 1304–1307. [PubMed: 21659601]

Hilts RW, Herd CDK, Simkus DN, Slater GF, 2014 Soluble organic compounds in the Tagish Lake meteorite. Meteor. Planet. Sci 49, 526–549.

Howard KT, Alexander CMO'D, Schrader DL, Dyl KA, 2015 Classification of hydrous meteorites (CR, CM and C2 ungrouped) by phyllosilicate fraction: PSD-XRD modal mineralogy and planetesimal environments. Geochim. Cosmochim. Acta 149, 206–222.

Huang Y, Wang Y, Alexandre MR, Lee T, Rose-Petruck C, Fuller M, Pizzarello S, 2005 Molecular and compound-specific isotopic characterization of monocarboxylic acids in carbonaceous meteorites. Geochim. Cosmochim. Acta 69, 1073–1084.

Huang Y, Alexandre MR, Wang Y, 2007 Structure and isotopic ratios of aliphatic side chains in the insoluble organic matter of the Murchison carbonaceous chondrite. Earth Planet. Sci. Lett 259, 517–525.

Huss GR, Lewis RS, Hemkin S, 1996 The "normal planetary" noble gas component in primitive chondrites: Compositions, carrier, and metamorphic history. Geochim. Cosmochim. Acta 60, 3311–3340.

Huss GR, Meshik AP, Smith JB, Hohenberg CM, 2003 Presolar diamond, silicon carbide, and graphite in carbonaceous chondrites: Implications for thermal processing in the solar nebula. Geochim. Cosmochim. Acta 67, 4823–4848.

Huss GR, Rubin AE, Grossman JN, 2006 Thermal metamorphism in chondrites, in: Lauretta DS, McSween HY Jr. (Eds.), Meteorites and the Early Solar System II. University of Arizona Press, Houston, pp. 567–586.

Hutchison R, Alexander CMO, Barber DJ, 1987 The Semarkona meteorite: First recorded occurrence of smectite in an ordinary chondrite, and its implications. Geochim. Cosmochim. Acta 51, 1875–1882.

Iben I Jr., Renzini A, 1983 Asymptotic giant branch evolution and beyond. Annu. Rev. Astronomy and Astrophysics 21, 271–342.

Jones AP, Duley WW, Williams DA, 1990 The structure and evolution of hydrogenated amorphous carbon grains and mantles in the interstellar medium. Quart. J. Roy. Astron. Soc 31, 567–582.

Kebukawa Y, Nakashima S, Ishikawa M, Aizawa K, Inoue T, Nakamura-Messenger K, Zolensky ME, 2010 Spatial distribution of organic matter in the Bells CM2 chondrite using near-field infrared microspectroscopy. Meteor. Planet. Sci 45, 394–405.

Kebukawa Y, Alexander CMO'D, Cody GD, 2011 Compositional diversity in insoluble organic matter in type 1, 2 and 3 chondrites as detected by infrared spectroscopy. Geochim. Cosmochim. Acta 75, 3530–3541.

Kebukawa Y, Kilcoyne ALD, Cody GD, 2013 Exploring the potential formation of organic solids in chondrites and comets through polymerization of interstellar formaldehyde. Astrophys. J 771, 19.

Kebukawa Y, Kobayashi S, Kawasaki N, Cody GD, Yurimoto H, 2014 Isotope imaging and the kinetics of deuterium-hydrogen exchange between insoluble organic matter and water. Lunar Planet. Sci. Conf 45, #1308.

Kebukawa Y, Cody GD, 2015 A kinetic study of the formation of organic solids from formaldehyde: Implications for the origin of extraterrestrial organic solids in primitive Solar System objects. Icarus 248, 412–423.

Keller LP, Messenger S, Flynn GJ, Clemett S, Wirick S, Jacobsen C, 2004 The nature of molecular cloud material in interplanetary dust. Geochim. Cosmochim. Acta 68, 2577–2589.

Kemper F, Vriend WJ, Tielens AGGM, 2004 The absence of crystalline silicates in the diffuse interstellar medium. Astrophys. J 609, 826–837.

Kemper F, Vriend WJ, Tielens AGGM, 2005 Erratum: The absence of crystalline silicates in the diffuse interstellar medium (2004 ApJ 609, 826). Astrophys. J 633, 534–534.

Kerridge JF, 1983 Isotopic composition of carbonaceous-chondrite kerogen: evidence for an interstellar origin of organic matter in meteorites. Earth Planet. Sci. Lett 64, 186–200.

Kerridge JF, Chang S, Shipp R, 1987 Isotopic characterisation of kerogen-like material in the Murchison carbonaceous chondrite. Geochim. Cosmochim. Acta 51, 2527–2540. [PubMed: 11542082]

Kerridge JF, Chang S, Shipp R, 1988 Deuterium exchange during acid-demineralisation. Geochim. Cosmochim. Acta 52, 2251–2255. [PubMed: 11539748]

Kilcoyne ALD, Tyliszczak T, Steele WF, Fakra S, Hitchcock P, Franck K, Anderson E, Harteneck B, Rightor EG, Mitchell GE, Hitchcock AP, Yang L, Warwick T, Ade H, 2003 Interferometer controlled scanning transmission microscopes at the advanced light source. J. Synchrotron Radiation 10, 125–136.

Kissel J, Krueger FR, 1987 The organic component in dust from comet Halley as measured by the PUMA mass spectrometer on board Vega 1. Nature 326, 755–760.

Klöck W, Thomas KL, McKay DS, Palme H, 1989 Unusual olivine and pyroxene compositions in interplanetary dust and unequilibrated ordinary chondrites. Nature 339, 126–128.

Komiya M, Shimoyama A, Harada K, 1993 Examination of organic compounds from insoluble organic matter isolated from some Antarctic carbonaceous chondrites by heating experiments. Geochim. Cosmochim. Acta 57, 907–914.

Komiya M, Shimoyama A, 1996 Organic compounds from insoluble organic matter isolated from the Murchison carbonaceous chondrite by heating experiments. Bulletin of the Chemical Society of Japan 69, 53–58.

Kress ME, Tielens AGGM, 2001 The role of Fischer-Tropsch catalysis in solar nebula chemistry. Meteor. Planet. Sci 36, 75–92.

Krot AN, Petaev MI, Scott ERD, Choi B-G, Zolensky ME, Kiel K, 1998 Progressive alteration in CV3 chondrites: More evidence for asteroidal alteration. Meteor. Planet. Sci 33, 1065–1085.

Krot AN, Keil K, Scott ERD, Goodrich CA, Weisberg MK, 2014 Classification of meteorites and their genetic relationships, in: Davis AM (Ed.), Meteorites and cosmochemical processes. Elsevier-Pergamon, Oxford, pp. 1–63.

Kwok S, 2004 The synthesis of organic and inorganic compounds in evolved stars. Nature 430, 985–991. [PubMed: 15329712]

Kwok S, Zhang Y, 2011 Mixed aromatic-aliphatic organic nanoparticles as carriers of unidentified infrared emission features. Nature 479, 80–83. [PubMed: 22031328]

Lambert DL, Gustafsson B, Eriksson K, Hinkle KH, 1986 The chemical composition of carbon stars. I. Carbon, nitrogen, and oxygen in 30 cool carbon stars in the galactic disk. The Astrophysical Journal Supplemental Series 62, 373–425.

Laurent B, Roskosz M, Remusat L, Leroux H, Vezin H, Depecker C, 2014 Isotopic and structural signature of experimentally irradiated organic matter. Geochim. Cosmochim. Acta 142, 522–534.

Laurent B, Roskosz M, Remusat L, Robert F, Leroux H, Vezin H, Depecker C, Nuns N, Lefebvre J-M, 2015 The deuterium/hydrogen distribution in chondritic organic matter attests to early ionizing irradiation. Nat. Commun 6.

Le Guillou C, Rouzaud J-N, Bonal L, Quirico E, Derenne S, Remusat L, 2012 High resolution TEM of chondritic carbonaceous matter: Metamorphic evolution and heterogeneity. Meteor. Planet. Sci 47, 345–362.

Le Guillou C, Remusat L, Bernard S, Brearley AJ, Leroux H, 2013 Amorphization and D/H fractionation of kerogens during experimental electron irradiation: Comparison with chondritic organic matter. Icarus 226, 101–110.

Le Guillou C, Bernard S, Brearley AJ, Remusat L, 2014 Evolution of organic matter in Orgueil, Murchison and Renazzo during parent body aqueous alteration: In situ investigations. Geochim. Cosmochim. Acta 131, 368–392.

Le Guillou C, Brearley A, 2014 Relationships between organics, water and early stages of aqueous alteration in the pristine CR3.0 chondrite MET 00426. Geochim. Cosmochim. Acta 131, 344–367.

Lee J-E, Bergin EA, Nomura H, 2010 The solar nebula on fire: A solution to the carbon deficit in the inner Solar System. Astrophys. J. Lett 710, L21–L25.

Leroux H, Cuvillier P, Zanda B, Hewins RH, 2015 GEMS-like material in the matrix of the Paris meteorite and the early stages of alteration of CM chondrites. Geochim. Cosmochim. Acta 170, 247–265.

Levin EM, Bud'ko SL, Mao JD, Huang Y, Schmidt-Rohr K, 2007 Effect of magnetic particles on NMR spectra of Murchison meteorite organic matter and a polymer-based model system. Solid State Nuclear Magnetic Resonance 31, 63–71. [PubMed: 17324558]

Lindgren P, Hanna RD, Dobson KJ, Tomkinson T, Lee MR, 2015 The paradox between low shock-stage and evidence for compaction in CM carbonaceous chondrites explained by multiple low-intensity impacts. Geochim. Cosmochim. Acta 148, 159–178.

Llorca J, Casanova I, 2000 Reaction between H_2, CO, and H_2S over Fe,Ni metal in the solar nebula: Experimental evidence for the formation of sulfur-bearing organic molecules and sulfides. Meteor. Planet. Sci 35, 841–848.

Lodders K, 2003 Solar System abundances and condensation temperatures of the elements. Astrophys. J 591, 1220–1247.

Mahaffy PR, Donahue TM, Atreya SK, Owen TC, Niemann HB, 1998 Galileo probe measurements of D/H and ^{3}He/^{4}He in Jupiter's atmosphere. Space Sci. Rev 84, 251–263.

Martins Z, Alexander CMO'D, Orzechowska GE, Fogel ML, Ehrenfreund P, 2007 Indigenous amino acids in primitive CR meteorites. Meteor. Planet. Sci. 42, 2125–2136.

Marty B, 2012 The origins and concentrations of water, carbon, nitrogen and noble gases on Earth. Earth Planet. Sci. Lett 313–314, 56–66.

Matrajt G, Muñoz Caro GM, Dartois E, D'Hendecourt L, Deboffle D, Borg J, 2005 FTIR analysis of the organics in IDPs: Comparison with the IR spectra of the diffuse interstellar medium. Astron. Astrophys 433, 979–995.

Matrajt G, Ito M, Wirick S, Messenger S, Brownlee DE, Joswiak D, Flynn G, Sandford S, Snead C, Westphal A, 2008 Carbon investigation of two Stardust particles: A TEM, NanoSIMS, and XANES study. Meteor. Planet. Sci 43, 315–334.

Matsumoto T, Tsuchiyama A, Nakamura-Messenger K, Nakano T, Uesugi K, Takeuchi A, Zolensky ME, 2013 Three-dimensional observation and morphological analysis of organic nanoglobules in a carbonaceous chondrite using X-ray micro-tomography. Geochim. Cosmochim. Acta 116, 84–95.

McCanta MC, Treiman AH, Dyar MD, Alexander CMO'D, Rumble III D, Essene EJ, 2008 The LaPaz Icefield 04840 meteorite: Mineralogy, metamorphism, and origin of an amphibole- and biotite-bearing R chondrite. Geochim. Cosmochim. Acta 72, 5757–5780.

Mennella V, Muñoz Caro GM, Ruiterkamp R, Schutte WA, Greenberg JM, Brucato JR, Colangeli L, 2001 UV photodestruction of CH bonds and the evolution of the 3.4 mu m feature carrier. II. The case of hydrogenated carbon grains. Astron. Astrophys 367, 355–361.

Mennella V, Brucato JR, Colangeli L, Palumbo P, 2002 CH bond formation in carbon grains by exposure to atomic hydrogen: The evolution of the carrier of the interstellar 3.4 micron band. Astrophys. J 569, 531–540.

Messenger S, Walker RM, 1997 Evidence for molecular cloud material in meteorites and interplanetary dust, in: Bernatowicz T, Zinner E (Eds.), Astrophysical implications of the laboratory study of presolar materials. Amer. Inst. Phys., Woodbury, pp. 545–564.

Messenger S, 2000 Identification of molecular-cloud material in interplanetary dust particles. Nature 404, 968–971. [PubMed: 10801119]

Messenger S, Keller LP, Lauretta DS, 2005 Supernova olivine from cometary dust. Science 309, 737–741. [PubMed: 15994379]

Meyer JC, Eder F, Kurasch S, Skakalova V, Kotakoski J, Park HJ, Roth S, Chuvilin A, Eyhusen S, Benner G, Krasheninnikov AV, Kaiser U, 2012 Accurate measurement of electron beam induced displacement cross sections for single-layer graphene. Physical Review Letters 108, 196102. [PubMed: 23003063]

Mimura K, Okamoto M, Sugitani K, Hashimoto S, 2007 Selective release of D and ^{13}C from insoluble organic matter of the Murchison meteorite by impact shock. Meteor. Planet. Sci 42, 347–355.

Morbidelli A, Bottke WF Jr., Froeschle C, Michel P, 2002 Origin and evolution of near-Earth objects, in: Bottke WF Jr., Cellino A, Paolicchi P, Binzel RP (Eds.), Asteroids III. University of Arizona Press, Tucson, pp. 409–422.

Morgan WA Jr., Feigelson ED, Wang H, Frenklach M, 1991 A new mechanism for the formation of meteoritic kerogen-like material. Science 252, 109–112. [PubMed: 17739082]

Mumma MJ, Charnley SB, 2011 The chemical composition of comets - Emerging taxonomies and natal heritage. Ann. Rev. Astron. Astrophys 49, 471–524.

Muñoz Caro GM, Ruiterkamp R, Schutte WA, Greenberg JM, Mennella V, 2001 UV photodestruction of CH bonds and the evolution of the 3.4 mu m feature carrier. I. The case of aliphatic and aromatic molecular species. Astron. Astrophys 367, 347–354.

Muñoz Caro GM, Matrajt G, Dartois E, Nuevo M, D'Hendecourt L, Deboffle D, Montagnac G, Chauvin N, Boukari C, Le Du D, 2006 Nature and evolution of the dominant carbonaceous matter in interplanetary dust particles: effects of irradiation and identification with a type of amorphous carbon. Astron. Astrophys 459, 147–159.

Nakamura K, Zolensky ME, Tomita S, Nakashima S, Tomeoka K, 2002 Hollow organic globules in the Tagish Lake meteorite as possible products of primitive organic reactions. International Journal of Astrobiology 1, 179–189.

Nakamura-Messenger K, Messenger S, Keller LP, Clemett SJ, Zolensky ME, 2006 Organic globules in the Tagish Lake meteorite: Remnants of the protosolar disk. Science 314, 1439–1442. [PubMed: 17138898]

Nakamura-Messenger K, Clemett SJ, Messenger S, Keller LP, 2011 Experimental aqueous alteration of cometary dust. Meteor. Planet. Sci 46, 843–856.

Naraoka H, Shimoyama A, Komiya M, Yamamoto H, Harada K, 1988 Hydrocarbons in the Yamato-791198 carbonaceous chondrite from Antarctica. Chem. Lett 17, 831–834.

Naraoka H, Mita H, Komiya M, Yoneda S, Kojima H, Shimoyama A, 2004 A chemical sequence of macromolecular organic matter in the CM chondrites. Meteor. Planet. Sci 39, 401–406.

Nesvorný D, Jenniskens P, Levison HF, Bottke WF, Vokrouhlicky D, Gounelle M, 2010 Cometary origin of the Zodiacal Cloud and carbonaceous micrometeorites. Implications for hot debris disks. Astrophys. J 713, 816–836.

Nittler LR, 2003 Presolar stardust in meteorites: recent advances and scientific frontiers. Earth Planet. Sci. Lett 209, 259–273.

Nuevo M, Milam SN, Sandford SA, De Gregorio BT, Cody GD, Kilcoyne ALD, 2011 XANES analysis of organic residues produced from the UV irradiation of astrophysical ice analogs. Advances in Space Research 48, 1126–1135.

Nuth JA III, Johnson NM, Manning S, 2008 A self-perpetuating catalyst for the production of complex organic molecules in protostellar nebulae. Astrophys. J. Lett 673, L225–L228.

Oba Y, Naraoka H, 2009 Elemental and isotopic behavior of macromolecular organic matter from CM chondrites during hydrous pyrolysis. Meteor. Planet. Sci 44, 943–954.

Okumura F, Mimura K, 2011 Gradual and stepwise pyrolyses of insoluble organic matter from the Murchison meteorite revealing chemical structure and isotopic distribution. Geochim. Cosmochim. Acta 75, 7063–7080.

Orthous-Daunay F-R, Quirico E, Lemelle L, Beck P, Deandrade V, Simionovici A, Derenne S, 2010 Speciation of sulfur in the insoluble organic matter from carbonaceous chondrites by XANES spectroscopy. Earth Planet. Sci. Lett 300, 321–328.

Orthous-Daunay FR, Quirico E, Beck P, Brissaud O, Dartois E, Pino T, Schmitt B, 2013 Mid-infrared study of the molecular structure variability of insoluble organic matter from primitive chondrites. Icarus 223, 534–543.

Palguta J, Schubert G, Travis BJ, 2010 Fluid flow and chemical alteration in carbonaceous chondrite parent bodies. Earth Planet. Sci. Lett 296, 235–243.

Pearson VK, Sephton MA, Kearsley AT, Bland PA, Franchi IA, Gilmour I, 2002 Clay mineral-organic matter relationships in the early solar system. Meteor. Planet. Sci 37, 1829–1833.

Pearson VK, Kearsley AT, Sephton MA, Gilmour I, 2007 The labelling of meteoritic organic material using osmium tetroxide vapour impregnation. Planet. Space Sci 55, 1310–1318.

Peeters Z, Changela H, Stroud RM, Alexander CMO'D, Nittler LR, 2012 Coordinated analysis of in situ organic material in the CR chondrite QUE 99177. Lunar Planet. Sci 43, #2612.

Pendleton YJ, Sandford SA, Allamandola LJ, Tielens AGGM, Sellgren K, 1994 Near-infrared absorption spectroscopy of interstellar hydrocarbon grains. Astrophys. J 437, 683–696.

Pendleton YJ, Allamandola LJ, 2002 The organic refractory material in the diffuse interstellar medium: Mid-infrared spectroscopic constraints. Astrophys. J. Suppl 138, 75–98.

Piani L, Robert F, Beyssac O, Binet L, Bourot-Denise M, Derenne S, Le Guillou C, Marrocchi Y, Mostefaoui S, Rouzaud J-N, Thomen A, 2012 Structure, composition, and location of organic matter in the enstatite chondrite Sahara 97096 (EH3). Meteor. Planet. Sci 47, 8–29.

Piani L, Robert F, Remusat L, 2015 Micron-scale D/H heterogeneity in chondrite matrices: A signature of the pristine solar system water? Earth Planet. Sci. Lett 415, 154–164.

Pizzarello S, Cooper GW, Flynn GJ, 2006 The nature and distribution of the organic material in carbonaceous chondrites and interplanetary dust particles, in: Lauretta DS, McSween HY Jr. (Eds.), Meteorites and the Early Solar System II. University of Arizona Press, Tucson, pp. 625–651.

Pizzarello S, Huang Y, Alexandre MR, 2008 Molecular asymmetry in extraterrestrial chemistry: Insights from a pristine meteorite. Proc. Nat. Acad. Sci 105, 3700–3704. [PubMed: 18310323]

Quirico E, Raynal PI, Bourot-Denise M, 2003 Metamorphic grade of organic matter in six unequilibrated ordinary chondrites. Meteor. Planet. Sci 38, 795–811.

Quirico E, Rouzaud J-N, Bonal L, Montagnac G, 2005 Maturation grade of coals as revealed by Raman spectroscopy: Progress and problems. Spectrochimica Acta 61, 2368–2377. [PubMed: 16029859]

Quirico E, Montagnac G, Rouzaud JN, Bonal L, Bourot-Denise M, Duber S, Reynard B, 2009 Precursor and metamorphic condition effects on Raman spectra of poorly ordered carbonaceous matter in chondrites and coals. Earth Planet. Sci. Lett 287, 185–193.

Quirico E, Bourot-denise M, Robin C, Montagnac G, Beck P, 2011a A reappraisal of the metamorphic history of EH3 and EL3 enstatite chondrites. Geochim. Cosmochim. Acta 75, 3088–3102.

Quirico E, Orthous-Daunay F-R, Beck P, Bonal L, Briani G, Bourot-Denise M, Montagnac G, Dobrica E, Engrand C, Charon E, Rouzaud J-N, Gounelle M, 2011b Pre-accretion heterogeneity of organic matter in types 1 and 2 chondrites. Lunar Planet. Sci 42, #2372.

Quirico E, Orthous-Daunay F-R, Beck P, Bonal L, Brunetto R, Dartois E, Pino T, Montagnac G, Rouzaud J-N, Engrand C, Duprat J, 2014 Origin of insoluble organic matter in type 1 and 2 chondrites: New clues, new questions. Geochim. Cosmochim. Acta 136, 80–99.

Remusat L, Derenne S, Robert F, 2005a New insight on aliphatic linkages in the macromolecular organic fraction of Orgueil and Murchison meteorites through ruthenium tetroxide oxidation. Geochim. Cosmochim. Acta 69, 4377–4386.

Remusat L, Derenne S, Robert F, Knicker H, 2005b New pyrolytic and spectroscopic data on Orgueil and Murchison insoluble organic matter: A different origin than soluble? Geochim. Cosmochim. Acta 69, 3919–3932.

Remusat L, Palhol F, Robert F, Derenne S, France-Lanord C, 2006 Enrichment of deuterium in insoluble organic matter from primitive meteorites: A solar system origin? Earth Planet. Sci. Lett 243, 15–25.

Remusat L, Robert F, Meibom A, Mostefaoui S, Delpoux O, Binet L, Gourier D, Derenne S, 2009 Proto-planetary disk chemistry recorded by D-rich organic radicals in carbonaceous chondrites. Astrophys. J 698, 2087–2092.

Remusat L, Guan Y, Wang Y, Eiler JM, 2010 Accretion and preservation of D-rich organic particles in carbonaceous chondrites: Evidence for important transport in the early Solar System nebula. Astrophys. J 713, 1048–1058.

Remusat L, Rouzaud JN, Charon E, Le Guillou C, Guan Y, Eiler JM, 2012 D-depleted organic matter and graphite in the Abee enstatite chondrite. Geochim. Cosmochim. Acta 96, 319–335.

Remusat L, Piani L, Bernard S, 2016 Thermal recalcitrance of the organic D-rich component of ordinary chondrites. Earth Planet. Sci. Lett 435, 36–44.

Robert F, Epstein S, 1982 The concentration and isotopic composition of hydrogen, carbon and nitrogen in carbonaceous meteorites. Geochim. Cosmochim. Acta 46, 81–95.

Robert F, Javoy M, Halbout J, Dimon B, Merlivat L, 1987 Hydrogen isotope abundances in the solar system. Part 1: Unequilibrated chondrites. Geochim. Cosmochim. Acta 51, 1787–1805.

Rubin AE, Trigo-Rodriguez JM, Huber H, Wasson JT, 2007 Progressive aqueous alteration of CM carbonaceous chondrites. Geochim. Cosmochim. Acta 71, 2361–2382.

Rubin AE, 2012 Collisional facilitation of aqueous alteration of CM and CV carbonaceous chondrites. Geochim. Cosmochim. Acta 90, 181–194.

Sandford SA, Allamandola LJ, Tielens AGGM, Sellgren K, Tapia M, Pendleton YJ, 1991 The interstellar C-H stretching band near 3.4 microns - Constraints on the composition of organic material in the diffuse interstellar medium. Astrophys. J 371, 607–620. [PubMed: 11538103]

Sandford SA, Aléon J, Alexander CMO'D, Araki T, Bajt S, Baratta GA, Borg J, Bradley JP, Brownlee DE, Brucato JR, Burchell MJ, Busemann H, Butterworth A, Clemett SJ, Cody G, Colangeli L, Cooper G, d'Hendecourt L, Djouadi Z, Dworkin JP, Ferrini G, Fleckenstein H, Flynn GJ, Franchi IA, Fries M, Gilles MK, Glavin DP, Gounelle M, Grossemy F, Jacobsen C, Keller LP, Kilcoyne ALD, Leitner J, Matrajt G, Meibom A, Mennella V, Mostefaoui S, Nittler LR, Palumbo ME, Papanastassiou DA, Robert F, Rotundi A, Snead CJ, Spencer MK, Stadermann FJ, Steele A, Stephan T, Tsou P, Tyliszczak T, Westphal AJ, Wirick S, Wopenka B, Yabuta H, Zare RN, Zolensky ME, 2006 Organics captured from comet 81P/Wild 2 by the Stardust spacecraft. Science 314, 1720–1724. [PubMed: 17170291]

Schmitt-Kopplin P, Gabelica Z, Gougeon RD, Fekete A, Kanawati B, Harir M, Gebefuegi I, Eckel G, Hertkorn N, 2010 High molecular diversity of extraterrestrial organic matter in Murchison meteorite revealed 40 years after its fall. Proc. Nat. Acad. Sci 107, 2763–2768. [PubMed: 20160129]

Schramm LS, Brownlee DE, Wheelock MM, 1989 Major element composition of stratospheric micrometeorites. Meteoritics 24, 99–112.

Schulze H, Kissel J, Jessberger EK, 1997 Chemistry and mineralogy of comet Halley's dust, in: Pendleton YJ, Tielens AGGM (Eds.), From Stardust to Planetesimals. Astronomical Society of the Pacific, San Francisco, pp. 397–414.

Sekine K, Sugita S, Shido T, Yamamoto T, Iwasawa Y, Kadono T, Matsui T, 2006 An experimental study on Fischer-Tropsch catalysis: Implications for impact phenomena and nebular chemistry. Meteor. Planet. Sci 41, 715–730.

Sephton MA, Pillinger CT, Gilmour I, 1998 $\delta^{13}C$ of free and macromolecular aromatic structures in the Murchison meteorite. Geochim. Cosmochim. Acta 62, 1821–1828.

Sephton MA, Pillinger CT, Gilmour I, 2000 Aromatic moieties in meteoritic macromolecular materials: analyses by hydrous pyrolysis and $\delta^{13}C$ of individual compounds. Geochim. Cosmochim. Acta 64, 321–328.

Sephton MA, Gilmour I, 2001 Pyrolysis-gas chromatography-isotope ratio mass spectrometry of macromolecular material in meteorites. Planet. Space Sci 49, 465–471.

Sephton MA, 2002 Organic compounds in carbonaceous meteorites. Nat. Prod. Rep 19, 292–311. [PubMed: 12137279]

Sephton MA, Verchovsky AB, Bland PA, Gilmour I, Grady MM, Wright IP, 2003 Investigating the variations in carbon and nitrogen isotopes in carbonaceous chondrites. Geochim. Cosmochim. Acta 67, 2093–2108.

Sephton MA, Love GD, Watson JS, Verchovsky AB, Wright IP, Snape CE, Gilmour I, 2004 Hydropyrolysis of insoluble carbonaceous matter in the Murchison meteorite: New insights into its macromolecular structure. Geochim. Cosmochim. Acta 68, 1385–1393.

Sephton MA, 2005 Organic matter in carbonaceous meteorites: past, present and future research. Philosophical Transactions of the Royal Society A: Mathematical, Physical and Engineering Sciences 363, 2729–2742.

Sephton MA, Love GD, Meredith W, Snape CE, Sun C-G, Watson JS, 2005 Hydropyrolysis: A new technique for the analysis of macromolecular material in meteorites. Planet. Space Sci 53, 1280–1286.

Sephton MA, Watson JS, Meredith W, Love GD, Gilmour I, Snape CE, 2015 Multiple cosmic sources for meteorite macromolecules? Astrobiology 15, 779–786. [PubMed: 26418568]

Serra Díaz-Cano L, Jones AP, 2008 Carbonaceous dust in interstellar shock waves: hydrogenated amorphous carbon (a-C:H) vs. graphite. Astron. Astrophys 492, 127–133.

Smith JW, Kaplan IR, 1970 Endogenous carbon in carbonaceous meteorites. Science 167, 1367–1370. [PubMed: 17778772]

Strazzulla G, 1997 Ion irradiation: Its relevance to the evolution of complex organics in the outer Solar System. Adv. Space Res 19, 1077–1084. [PubMed: 11541336]

Stroud RM, Bernatowicz TJ, 2005 Surface and internal structure of pristine presolar silicon carbide. Lunar and Planetary Science Conference XXXVI, #2010 (abstr.).

Stroud RM, Chisholm MF, Heck PR, Alexander CMO'D, Nittler LR, 2011 Supernova shock-wave-induced CO-formation of glassy carbon and nanodiamond. Astrophys. J. Lett 738, L27.

Sugiura N, Fujiya W, 2014 Correlated accretion ages and $e^{54}Cr$ of meteorite parent bodies and the evolution of the solar nebula. Meteor. Planet. Sci 49, 772–787.

Tachibana S, Piani L, Dessimoulie L, Hama T, Kimura Y, Endo Y, Fujita K, Nakatsubo S, Fukushi H, Mori S, Chigai T, Yurimoto H, Kouchi A, 2015 Photochemistry in molecular clouds: Structure and physical properties of organic residues and ice and sublimation of volatile molecules. LPI Contributions 1856, #5248.

Thomas KL, Blanford GE, Keller LP, Klöck W, McKay DS, 1993 Carbon abundance and silicate mineralogy of anhydrous interplanetary dust particles. Geochim. Cosmochim. Acta 57, 1551–1566. [PubMed: 11539451]

Tonui E, Zolensky M, Hiroi T, Nakamura T, Lipschutz ME, Wang M-S, Okudaira K, 2014 Petrographic, chemical and spectroscopic evidence for thermal metamorphism in carbonaceous chondrites I: CI and CM chondrites. Geochim. Cosmochim. Acta 126, 284–306.

Vinogradoff V, Remusat L, Bernard S, Le Guillou C, 2015 The insoluble organic matter of the Paris CM chondrite. Meteoritics Planet. Sci. Suppl 50, #5032.

Vito M, 2010 H atom irradiation of carbon grains under simulated dense interstellar medium conditions: The evolution of organics from diffuse interstellar clouds to the Solar System. Astrophys. J 718, 867–875.

Vollmer C, Kepaptsoglou D, Leitner J, Busemann H, Spring NH, Ramasse QM, Hoppe P, Nittler LR, 2014 Fluid-induced organic synthesis in the solar nebula recorded in extraterrestrial dust from meteorites. Proc. Nat. Acad. Sci 111, 15338–15343. [PubMed: 25288736]

Wang Y, Huang Y, Alexander CMO'D, Fogel M, Cody G, 2005 Molecular and compound-specific hydrogen isotope analyses of insoluble organic matter from different carbonaceous chondrites groups. Geochim. Cosmochim. Acta 69, 3711–3721.

Watson DM, Leisenring JM, Furlan E, Bohac CJ, Sargent B, Forrest WJ, Calvet N, Hartmann L, Nordhaus JT, Green JD, Kim KH, Sloan GC, Chen CH, Keller LD, d'Alessio P, Najita J, Uchida KI, Houck JR, 2009 Crystalline silicates and dust processing in the protoplanetary disks of the Taurus young cluster. The Astrophysical Journal Supplement Series 180, 84–101.

Wdowiak TJ, Flickinger GC, Cronin JR, 1988 Insoluble organic material of the Orgueil carbonaceous chondrite and unidentified infrared bands. Astrophys. J 328, L75–L79. [PubMed: 11538467]

Yabuta H, Naraoka H, Sakanishi K, Kawashima H, 2005 The solid-state ^{13}C NMR characterization of insoluble organic matter from Antarctic CM2 chondrites: Evaluation of the meteoritic alteration level. Meteor. Planet. Sci 40, 779–788.

Yabuta H, Williams LB, Cody GD, Alexander CMO'D, Pizzarello S, 2007 The insoluble carbonaceous material of CM chondrites: A possible source of discrete organic compounds under hydrothermal conditions. Meteor. Planet. Sci 42, 37–48.

Yabuta H, Alexander CMO'D, Fogel ML, Kilcoyne ALD, Cody GD, 2010 A molecular and isotopic study of the macromolecular organic matter of the ungrouped C2 WIS 91600 and its relationship to Tagish Lake and PCA 91008. Meteor. Planet. Sci 45, 1446–1460.

Yang J, Epstein S, 1983 Interstellar organic matter in meteorites. Geochim. Cosmochim. Acta 47, 2199–2216.

Zasowski G, Kemper F, Watson DM, Furlan E, Bohac CJ, Hull C, Green JD, 2009 Spitzer Infrared Spectrograph observations of Class I/II objects in Taurus: Composition and thermal history of the circumstellar ices. Astrophys. J 694, 459–478.

Zega T, Alexander CMO'D, Busemann H, Nittler LR, Hoppe P, Stroud RM, Young AF, 2010 Mineral associations and character of isotopically anomalous organic material in the Tagish Lake carbonaceous chondrite. Geochim. Cosmochim. Acta 74, 5966–5983.

Zega TJ, Nittler LR, Busemann H, Hoppe P, Stroud RM, 2007 Coordinated isotopic and mineralogic analyses of planetary materials enabled by in situ lift-out with a focused ion beam scanning electron microscope. Meteor. Planet. Sci 42, 1373–1386.

Zolensky ME, Krot AN, Benedix G, 2008 Record of low-temperature alteration in asteroids. Reviews in Mineralogy and Geochemistry 68, 429–462.

Zolotov MY, Shock EL, 2001 Stability of condensed hydrocarbons in the solar nebula. Icarus 150, 323–337.

Zubko V, Dwek E, Arendt RG, 2004 Interstellar dust models consistent with extinction, emission, and abundance constraints. Astrophysical Journal Supplement 152, 211–249.

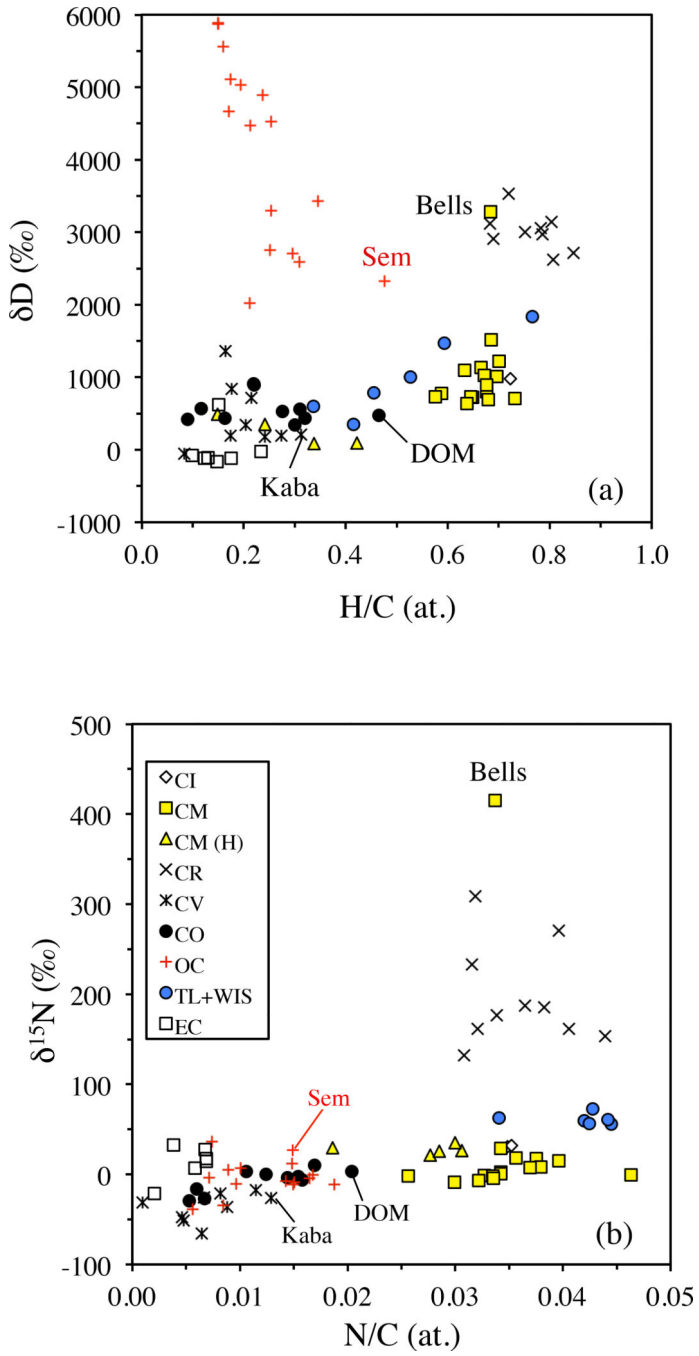

Figure 1.

The variations in bulk IOM H and N elemental and isotopic compositions within and between chondrite groups (updated from Alexander et al., 2010). TL is Tagish Lake, WIS is WIS 91600, Sem is Semarkona (LL3.0), DOM is DOM 08006 (CO3.0) and Kaba is a CV 3.1.

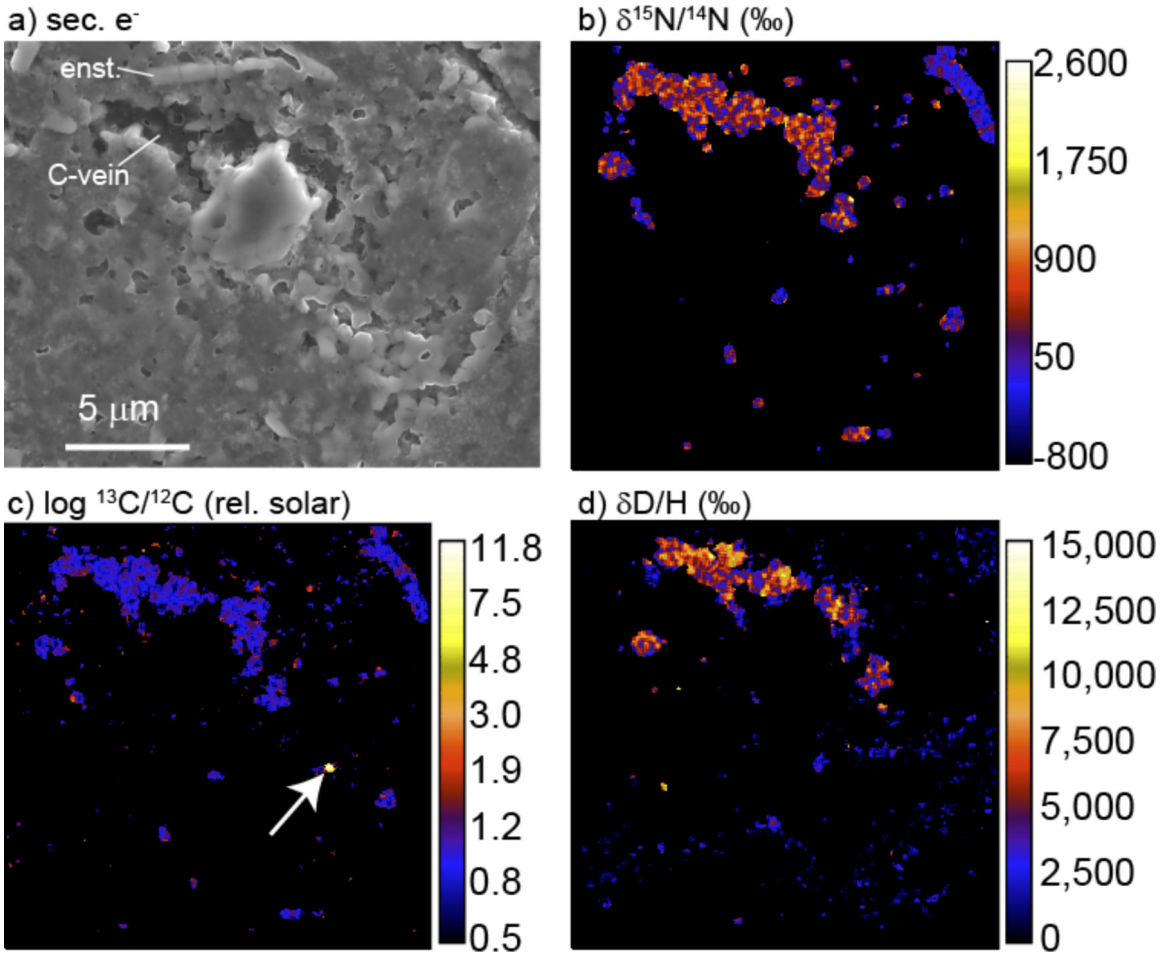

Figure 2.

Images of an area of QUE 99177 (CR2) matrix: (a) a secondary electron scanning electron micrograph, (b) a N isotope ratio map, (c) a C isotope ratio map, and (d) a H isotope ratio map. The isotopic maps were all measured by NanoSIMS. A relatively large ^{15}N- and D-rich "vein" of organic matter is visible. Arrow in (c) indicates a highly ^{13}C-enriched presolar SiC grain with no obvious spatial relationship to the organic matter.

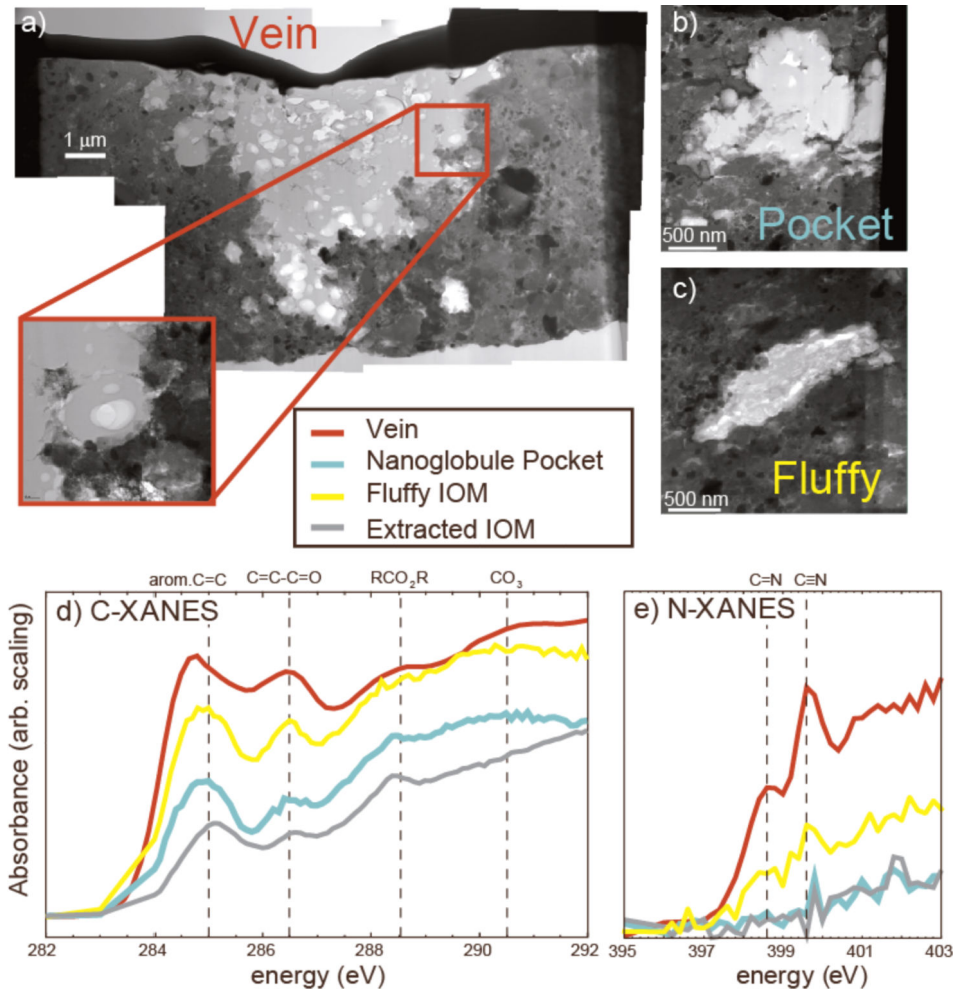

Figure 3.

Coordinated *in situ* microanalyses of organic matter in QUE 99177 (CR2). (a) A bright field STEM image mosaic of a FIB section cut through the organic-rich vein in Figure 2, which appears to be an aggregate of nanoglobules (see inset). Figures (b) and (c) are bright field STEM images of organic inclusions in another QUE 99177 FIB section, a small aggregate ("pocket") of nanoglobules and a carbonaceous particle with a fluffy texture, respectively. Figures d) and e) are C-XANES and N-XANES spectra, respectively, of organic features indicated in the STEM images compared to the average spectra of IOM extracted from the same meteorite. The XANES measurements reveal heterogeneity in functional-group chemistry on a μm scale. There is a much stronger nitrile peak associated with this vein than in the fluffy IOM and bulk extracted IOM.

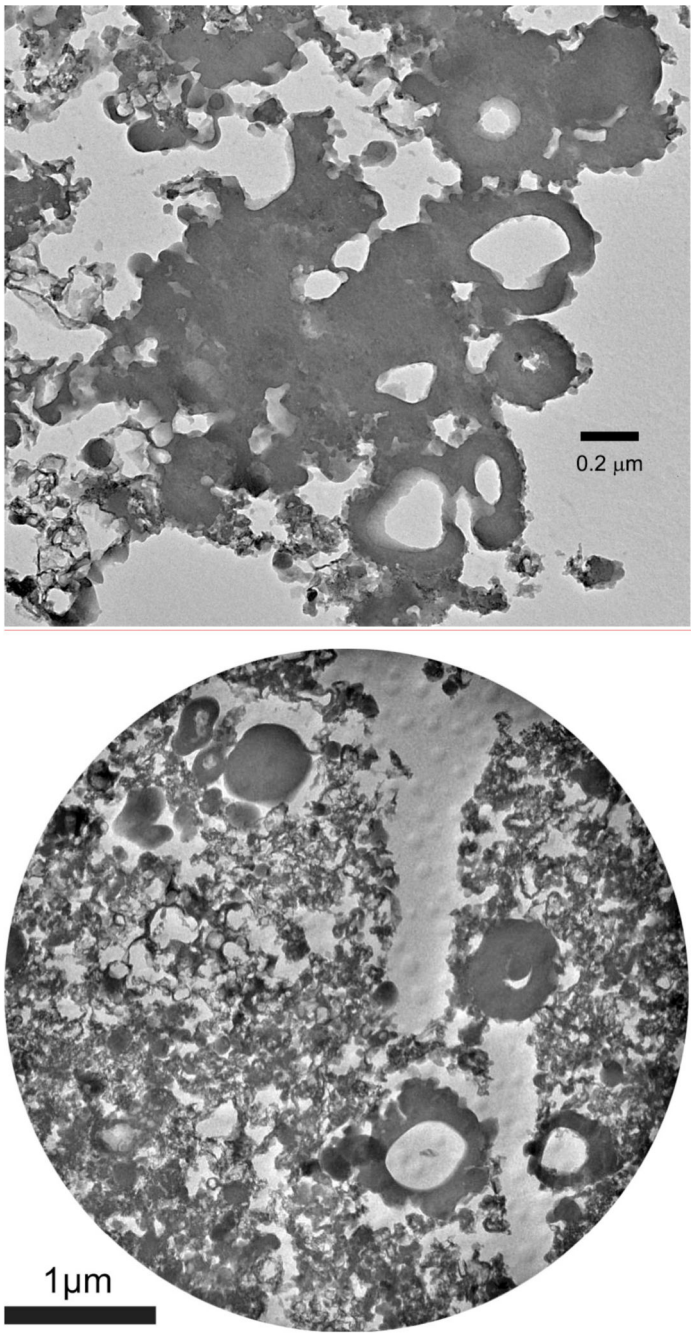

Figure 4.

Bright-field TEM images of microtomed sections of IOM residues from (a) Bells, and (b) the primitive 5b Tagish Lake lithology. The images include solid and hollow nanoglobules, and finer grained ‘fluffy’ material.

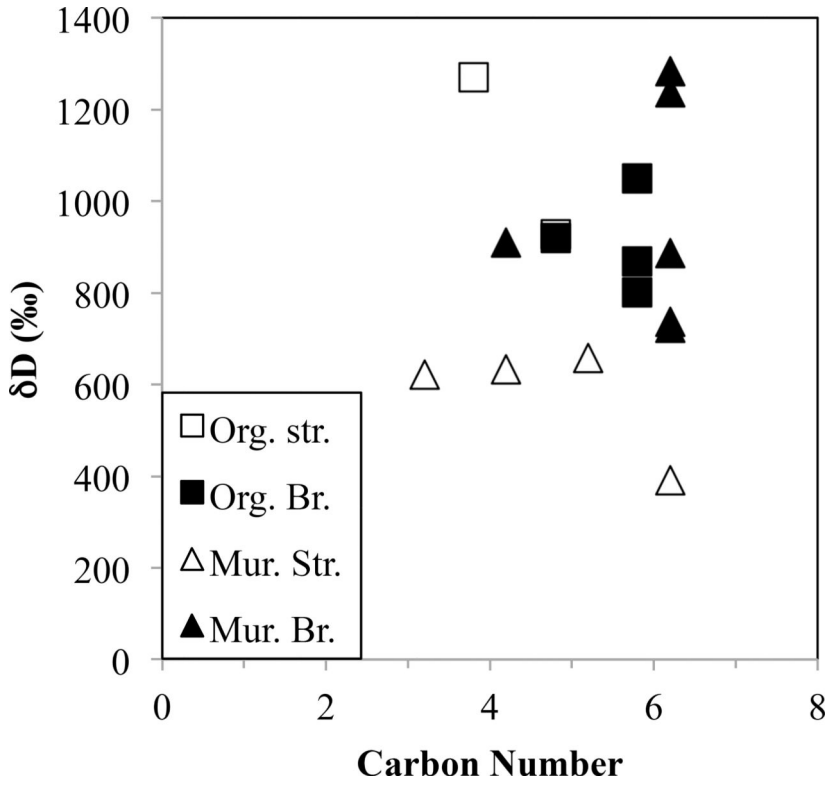

Figure 5.

The H isotopic compositions vs. C number for the products of RuO_4 oxidation degradation of Orgueil (Remusat et al., 2005a) and Murchison (Huang et al., 2007) IOM. The Murchison data are for straight (Str.) and branched (Br.) monocarboxylic acids, and the Orgueil data are for straight and branched dicarboxylic acids. The monocarboxylic acids are side chains to aromatic moieties, the dicarboxylic acids are linkages between aromatic moieties.

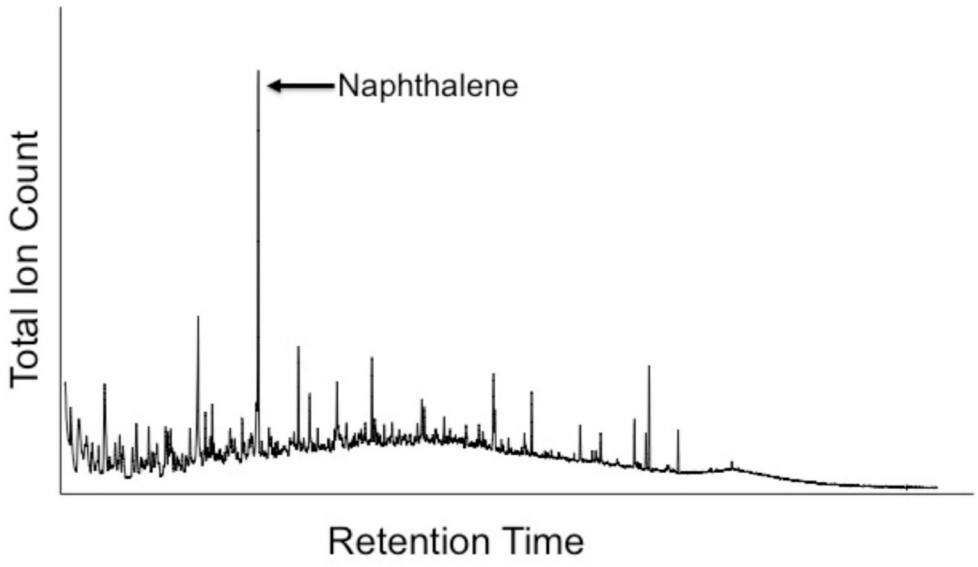

Figure 6.

A total ion chromatogram for pyrolysates with molecular weights of benzene and higher produced by flash pyrolysis GCMS of a Murchison IOM residue at 600°C. Roughly 25–30 wt.% of the sample was lost as volatile, low molecular weight material, much of this being CO, CO_2, H_2O, SO_2 and H_2S. The remainder of the sample formed a char. For the pyrolysates with molecular weights of benzene and higher shown here, the bulk (ca. 80 % of the ion intensity) are in an unresolved organic matter (UOM), sometimes also referred to as humpane, that produces the nearly continuous humped background. Superimposed on the UOM are many sharp peaks (totaling ca. 20 % of the ion intensity), but even the most intense of these, naphthalene, only accounts for ~1.5 % of the total ion intensity in this chromatogram and a much smaller fraction of the material in the IOM residue.

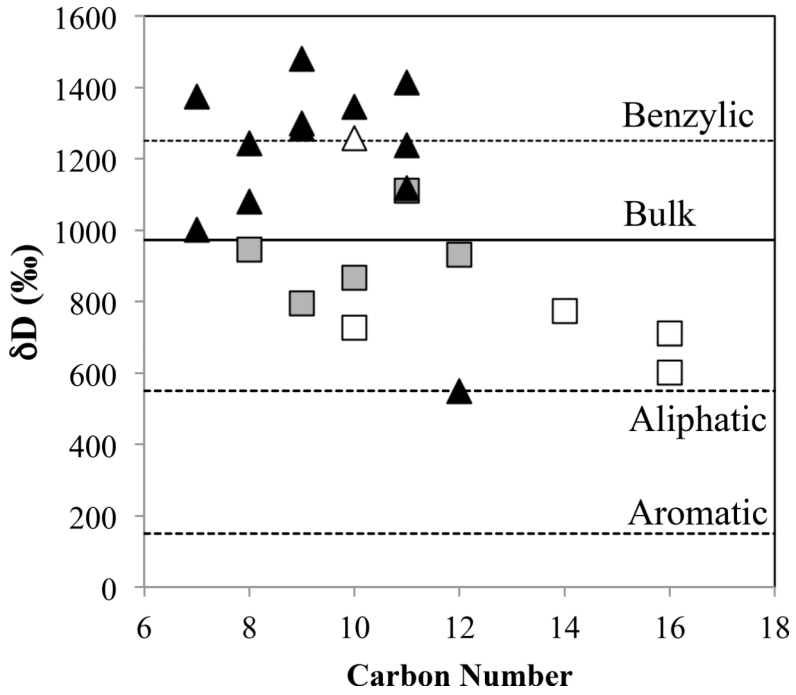

Fig. 7.

The isotopic compositions of individual aromatic molecules produced during pyrolysis of Orgueil IOM. Squares are from Remusat et al. (2006) and triangles are from Wang et al. (2005). Open symbols are for unsubstituted molecules, and filled symbols are for substituted molecules. The solid line is the bulk composition of Orgueil IOM (Alexander et al., 2007b), and the dashed lines are the isotopic compositions of the end-member components for Orgueil IOM proposed by Remusat et al. (2006).

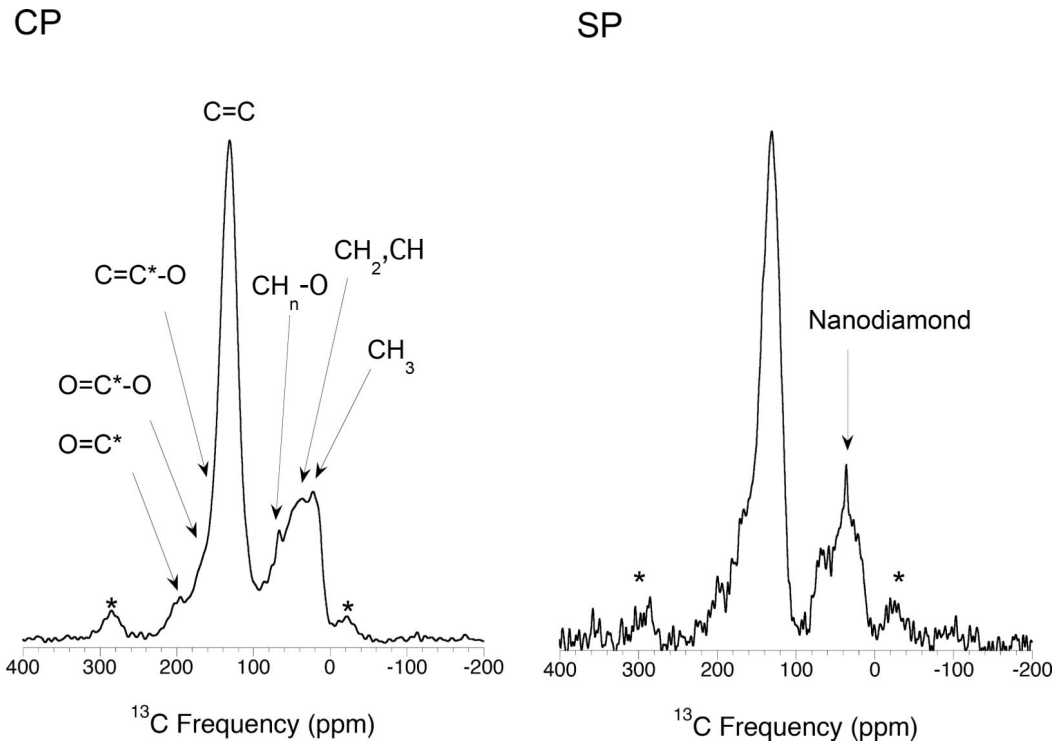

Fig. 8.

Comparison of CP and SP ^{13}C NMR spectra of Murchison IOM (Cody and Alexander, 2005). The signal-to-noise of the SP spectrum is lower than for the CP spectrum, but within the uncertainties they are the same. This shows that the CP spectrum was collected under conditions where all functional groups have similar detection efficiencies and that, except in the nanodiamonds, little of no C is so far from a H that it is not detected by the CP technique (i.e., there are no large PAHs present).

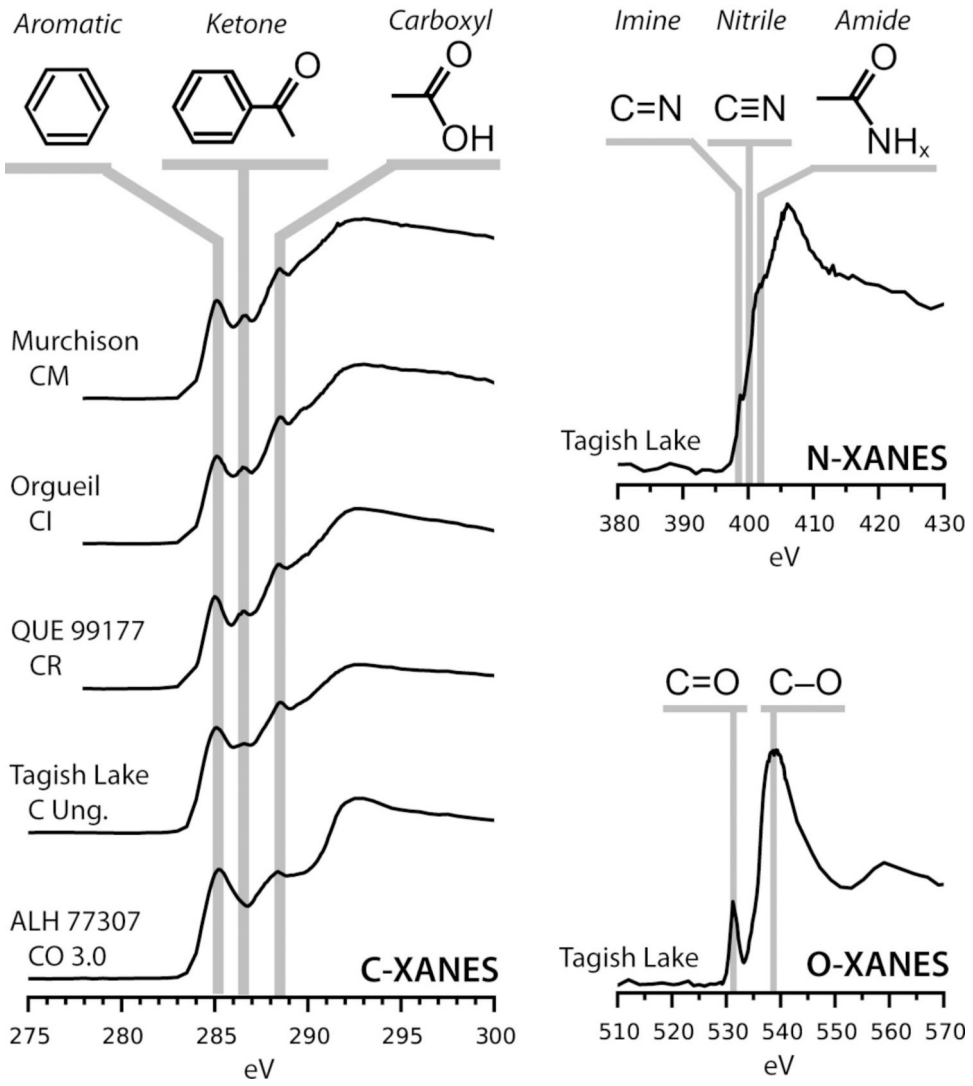

Figure 9.

Average bulk XANES spectra of IOM from several primitive carbonaceous chondrites: Murchison (CM2), Orgueil (CI1), QUE 99177 (CR2), Tagish Lake (C2, lithology 5b) and ALH 77307 (CO3.0). The C XANES spectra show the greatest variation in functional chemistries between different meteorite groups and petrologic types, but are still very similar. As shown in the representative spectrum from Tagish Lake, the N XANES spectra from primitive IOM are relatively featureless, only containing minor spectral “shoulders” on the main N absorption edge. In addition, IOM O XANES spectra rarely show spectral features other than the main π^* and σ^* peaks for C=O and C-O bonds, respectively. The C XANES data are taken from De Gregorio et al. (2013), while the data for Tagish Lake are unpublished.

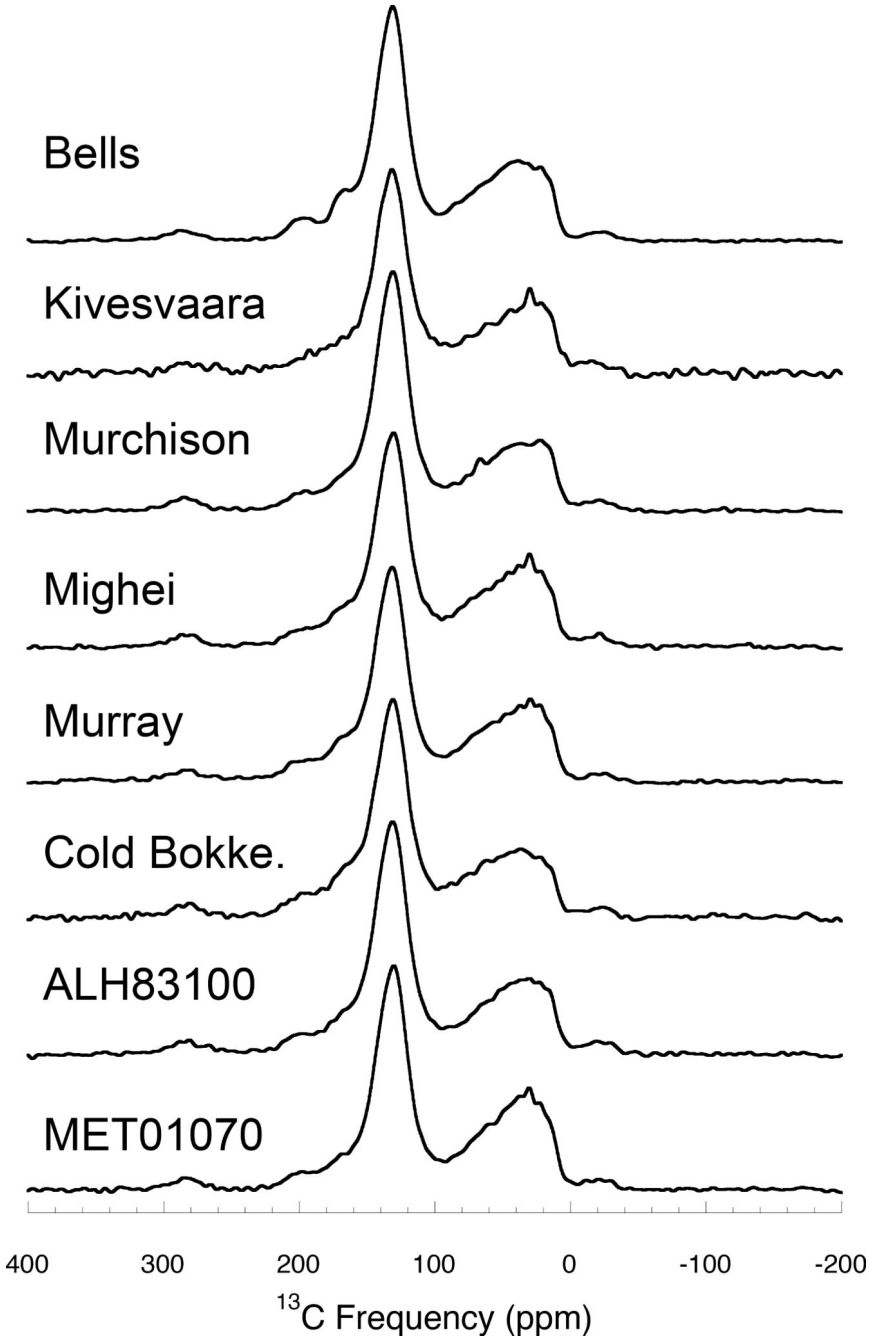

Figure 10.
The CP ^{13}C NMR spectra of IOM from a number CM chondrites that experienced a range of degrees of alteration (Cody et al., 2008d). The samples are stacked (top to bottom) in order of increasing degree of alteration (Alexander et al., 2013). As can be seen, there is very little variation in their functional group chemistries.

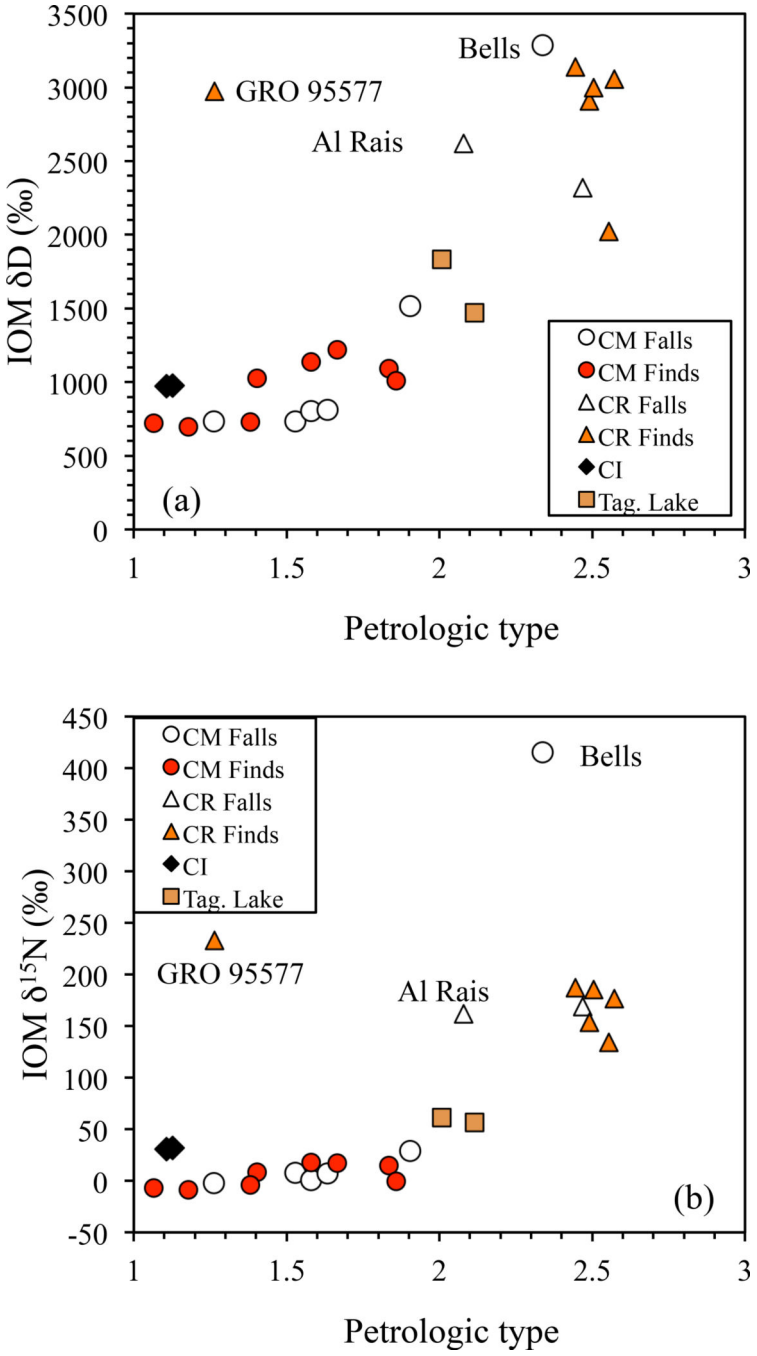

Figure 11.

The variations in bulk IOM H and N isotopic compositions with petrologic type for CIs, CMs, CRs and the two most primitive Tagish Lake (C2) lithologies (after Alexander et al., 2013). There seem to be general trends of bulk IOM isotopic compositions with petrologic type. However, there are notable exceptions in the highly altered CR GRO 95577 and the more heavily processed Tagish Lake lithologies (not shown), and there is little overlap in the petrologic types of the different chondrite groups.

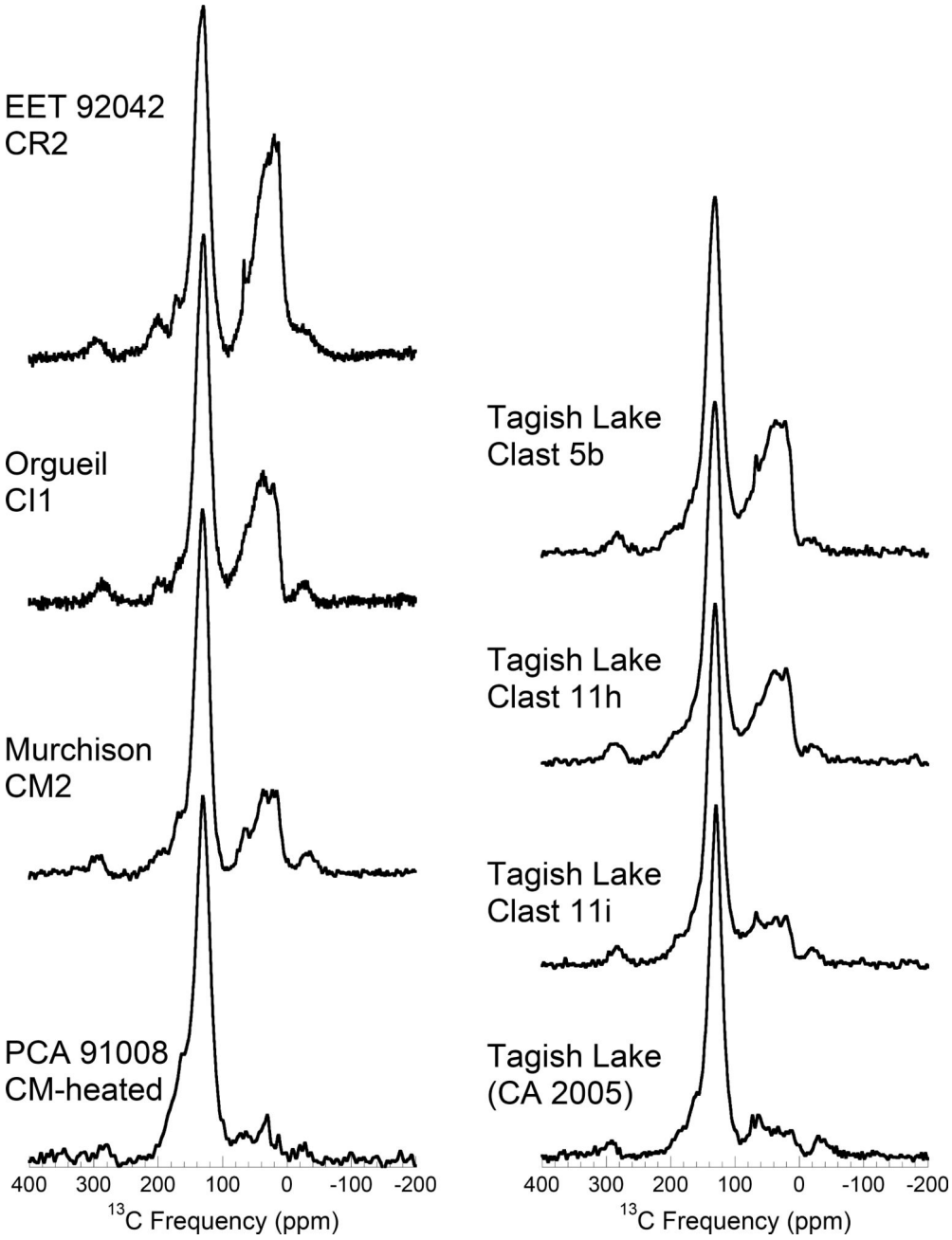

Figure 12.

Comparison of the NMR spectra of IOM from several Tagish Lake (C2) lithologies (Cody and Alexander, 2005; Herd et al., 2011; Alexander et al., 2014) with those for IOM from EET 92042 (CR2), Orgueil (CI1), Muchison (CM2) (Cody and Alexander, 2005) and the strongly heated CM PCA 91008 (Yabuta et al., 2010). The variation in IOM NMR spectra amongst the various Tagish Lake lithologies range from intermediate between CR and CI, to similar to the heated CM PCA 91008. This is consistent with the changes in H/C ratio of the Tagish Lake IOM samples (Figs. 1 and 13). The Tagish Lake samples demonstrate that parent body processes are capable of producing much of the range of IOM elemental compositions and functional group chemistries seen amongst chondrites.

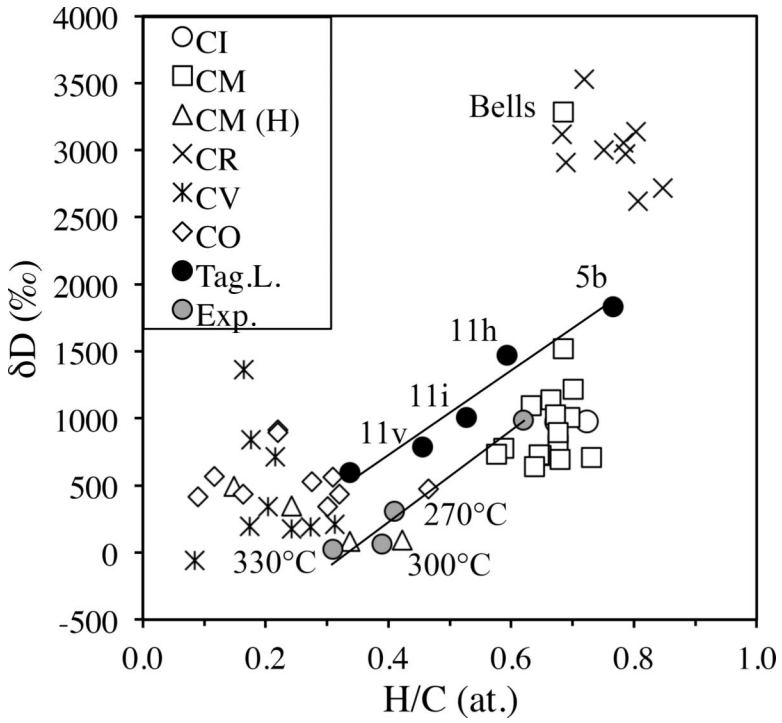

Figure 13.

Comparison of the IOM compositions from five Tagish Lake lithologies (Herd et al., 2011; Alexander et al., 2014) and the products of hydrothermal experiments on Murchison IOM conducted at three temperatures for 72 hours by Oba and Naraoka (2009). Also shown are the IOM compositions CI, CM, CR, CV and CO chondrites (Alexander et al., 2007b). The experiments parallel the Tagish Lake IOM samples. Both the Tagish Lake samples and experimental products cover wide ranges in H/C. In the case of the Tagish Lake samples, this range is from CR-like to H/C ratios that resemble heated CMs and the least metamorphosed CVs and COs. However, the Tagish Lake and experiment trends do not reproduce the full range of H/C and H isotopic compositions found in carbonaceous and ordinary (Fig. 1) chondrites. It seems likely that neither the experimental conditions nor the conditions experienced by the Tagish Lake lithologies cover the full range of parent body conditions experienced by the chondrites.

Table 1.

The abundances of insoluble (IOM) and soluble (SOM) organic components in the least metamorphosed carbonaceous chondrites, including the ungrouped C2 Tagish Lake. For the CMs, all data are from the Murchison CM2 meteorite (updated from Botta and Bada, 2002), unless otherwise noted. The abundances are in μg/g (ppm), except where indicated.

	CI	CM	CR	Tag. Lake
Matrix (vol.%)	100	~50	~30	~80
Bulk C (wt.%)[a]	3.7	2.0	1.2	4.1
C in IOM (wt.%)[b]	2.1	0.96	0.48	1.8
Amino acids	~5[c]	14–71[f]	~1–250[d]	1.9–4.9[e]
Aromatic hydrocarbons		3[f]	16[g]	
Aliphatic hydrocarbons		>35		
Monocarboxylic acids		>300	96[g]	359–656[e]
Hydroxy- and dicarboxylic acids		14–15	212[g]	
Purines and pyrimidines		1.3		
Basic N-heterocycles		7		
Amines	14[i]	5–7[i]	103[g]	
Alcohols		11		
Aldehydes and ketones		27		
Sulphonic acids		68		
Phosphonic acids		2		
Polyols		>8[h]		

[a] Averages from Alexander et al. (2012).

[b] Averages for recovered IOM from Alexander et al. (2007b) and Alexander et al. (2014).

[c] Average of the abundances in Orgueil and Ivuna (Ehrenfreund et al., 2001).

[d] Range of abundances in EET 92042, GRA 95229, and GRO 95577 (Martins et al., 2007).

[e] Range for different lithologies of Tagish Lake (Hilts et al., 2014).

[f] Abundance in Y-791198 (Naraoka et al., 1988).

[g] Abundances in GRA 95229 (Pizzarello et al., 2008).

[h] Lower limit for glyceric acid in Murchison (Cooper et al., 2001).

[i] From Aponte et al. (2014a, 2015).

Table 2.

The types, energies (eV) and strengths of transitions for major organic functional groups measured in XANES and EELS spectra.

Functional group	Formula	Transition	Strength	Energy
Carbon				
olefin	-C=C-	1s-π*	Strong	284.8
aromatic	C=C	1s-π*	Strong	285.0
ketones	R-CO-R	1s-π*	Strong	286.5–286.7
ene-ketones	AR-CO-R	1s-π*	Strong	286.5–286.7
nitrile	C≡N	1s-π*	Strong	286.6–286.7
phenols	AR-OH	1s-π*	Strong	287.2
aryl ethers	AR-O-R	1s-π*	Strong	287.8–287.9
aliphatic C	C-C	1s-3p/s	Weak	287.8–288.0
carboxyl	COOH	1s-π*	Strong	288.5
ester	COOR	1s-π*	Strong	288.7
alcohols	C-OH	1s-3p/s	Weak	289.5
ethers	C-O-C	1s-3p/s	Weak	289.5
Nitrogen				
imines	C=N-R	1s-π*	Strong	398.6–399.0
nitrile	C≡N	1s-π*	Strong	399.7–399.9
amine	$C\text{-}NH_2$	1s- σ*	Weak	401.2–401.4
amide	$\text{-}CO\text{-}NR_2$	1s-σ*	Strong	401.4–401.5
pyrroles	AR-NH-AR	1s-π*	Strong	402.3
nitro	$C\text{-}NO_2$	1s-π*	Strong	403.8
nitrate	NO_3^-	1s-π*	Strong	405.4
Oxygen				
carbonyl	C=O	1s-π*	Strong	531.3
ether/alcohol	C-O-R	1s-σ*	Weak	533.9–534.1
Sulfur				
disulfide	R-S-S-R	1s-3p	Weak	2472
thiols	R-S-R	1s-3p	Weak	2473
	AR-S-AR	1s-3p	Weak	2474
sulfoxides	$R_2\text{-}S{=}O$	1s-3p	Strong	2476
sulfones	$R\text{-}SO_2\text{-}R$	1s-3p	Strong	2480
sulfonates	$R\text{-}SO_2O\text{-}R$	1s-3p	Strong	2482